Drosophila MRP, a high turnover model of the long human Multidrug Resistance-associated Proteins

Ph.D. Doctoral Dissertation

Flóra Szeri

Semmelweis University, School of Molecular Medicine

Tutors: András Váradi, Ph.D., D.Sc.

Balázs Sarkadi, M.D., Ph.D., D.Sc.

Opponents: Tibor Vellai, Ph.D.

László Csanády M.D., Ph.D.

Head of Examination Commission:

Rajmund Machovich M.D., D.Sc., Prof.

Members of Examination Commission:

Krisztina Takács, Ph.D. and Miklós Csala, M.D., Ph.D.

Budapest

2009

Table of contents

1. List of Abbreviations

ABC, ATP-binding cassette

ATP, adenosine triphosphate

AlF_4, fluoroaluminate

BB, benzbromarone

cAMP, 3'-5'-cyclic adenosine mono-phosphate

cGMP, 3'-5'-cyclic guanosine mono-phosphate

CD, cyclodextrin

CDCF, carboxydichlorofluorescein

CFTR, cystic fibrosis transmembrane conductance regulator

DDT, dichlorodiphenyl trichloroethane

DHEAS, dehydroepiandrosterone 3-sulfate

DMRP, *Drosophila* multidrug resistance-associated protein

DTT, 1,4-dithiothreitol

DOC, deoxycholate

$\Delta H^{\ddagger}$, activation enthalpy

$\Delta G^{\ddagger}$, Gibbs free energy

$\Delta S^{\ddagger}$, activation entropy

E_a, activation energy

EC_{50}, half maximal effective concentration

$E_2$17ßG, ß-estradiol 17-ß-D-glucuronide

FACS, fluorescence activated cell sorter

FBS, foetal bovine serum

GSH/GSSG, reduced/oxidased glutathione

IC_{50}, half maximal inhibitory concentration

IM, indomethacin

K_m, Michaelis constant

LFER, linear free energy relationship

LTC_4, leukotriene C_4

MSD, membrane-spanning domain

MDR, multidrug resistance protein

MDR1, multidrug resistance protein1

MRP, multidrug resistance-associated protein

MRP1, 2 etc., multidrug resistance-associated protein1, 2 etc.

NBD, nucleotide-binding domain

NEM-GS, N-ethylmaleimide glutathione conjugate

PB, probenecid

Pgp, P-glycoprotein

PVDF, polyvinylidene difluoride

SDS, sodium dodecyl sulfate

SDS-PAGE, SDS-polyacrylamide gel electrophoresis

Sf9, Spodoptera frugiperda ovarian cells

S.E.M., standard error of mean

SUR, sulfonylurea receptor

TCA, trichloro acetic acid

TMD, transmembrane domain

V_i, orthovanadate

V_{max}, maximal value of initial velocity

2. Introduction

The ATP-binding cassette transporters (ABC transporters), constituting one of the major classes of membrane transporters, are present in all phyla of life and have been found ubiquitously in all of the species studied so far, constituting large protein families of 30-100 members (Holland and Blight, 1999). Most of the ABC proteins work as transporters and, in spite of their diversity, they all energise movement of compounds through membrane bilayers based on energy derived from binding and hydrolysis of adenosine triphosphate (ATP). In prokaryotes they mostly function as importers for a wide range of low molecular weight solutes (Higgins 2001 Res microbiol), whereas fewer function as parts of different secretory machineries. In contrast, in eukaryotes they function as exporters, transporting their substrates from the cytoplasm out of the cells or to cell organelles, such as the endoplasmic reticulum or the peroxisome, playing essential roles in various cellular processes. Besides their physiological relevance, ABC transporters have clinical and economical significance as well, since some of them can provide resistance to antibiotics, chemotherapeutic agents and herbicides, and their various dysfunctions underlie a number of human genetic diseases, such as cystic fibrosis and macular dystrophy (Dean and Annilo, 2005).

2.1. Structure and function of ABC transporters

ABC transporters are modular proteins harbouring the specific ABC domains, also called as nucleotide binding domains or NBDs, the globular cytoplasmic protein units of 200- to 250-amino acids, which can bind and hydrolyze ATP, and the polytropic membrane spanning domains (MSDs), also referred to as transmembrane domains (TMDs), consisting of six membrane spanning helices

for most of the cases (Higgins et al., 1986). The minimal functional unit of ABC transporters harbours two NBDs and two TMDs, often coded by separate genes within the same operon in archea and in prokaryotes, while in eukaryotes these four domains can be encoded by a single gene in different combinations (full transporters) or they can be present as dimers of two half transporters in the form of hetero or homodimers (Figure 2.1) (Higgins et al., 1986).

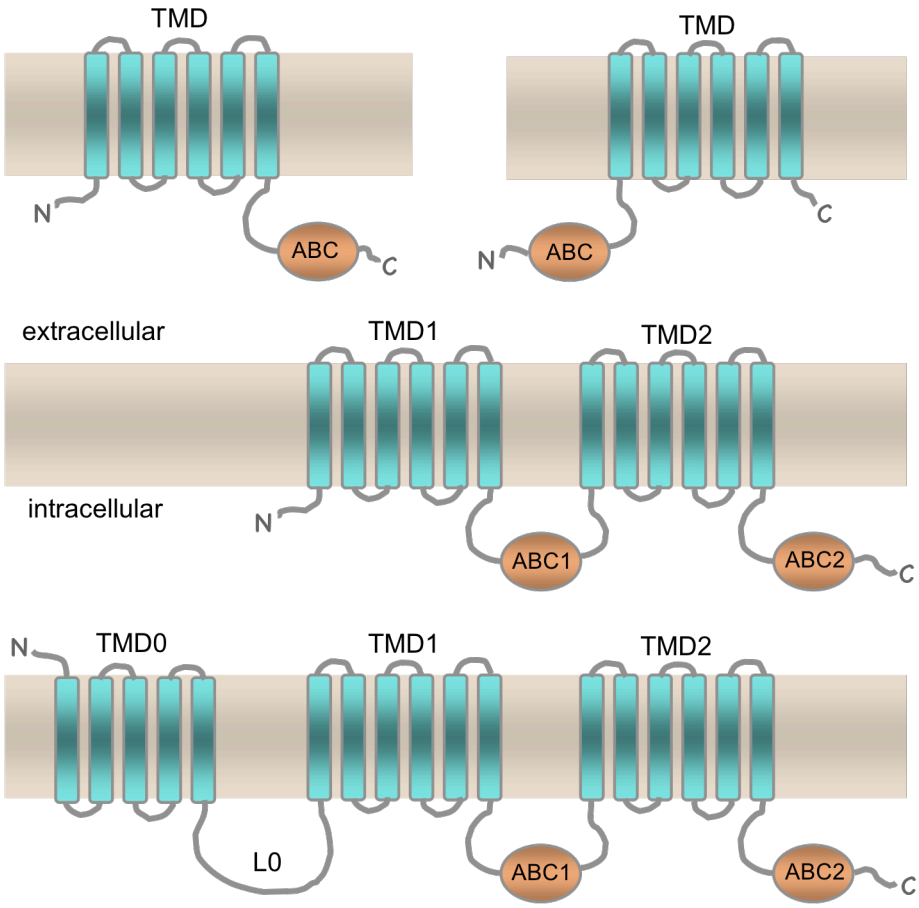

Figure 2.1 Domain arrangement prototypes of human and Drosophila ABC transporters. *Orange circles represent ABC domains, and vertical turquoise slabs represent transmembrane helices within transmembrane domains (TMD). Domains and transmembrane helices are connected via extra- and intracellular loops depicted as grey lines. The horizontal light areas represent the membrane bilayer, the upper side is extracellular while the lower side is intracellular, as indicated. The NH_2 and COOH terminal ends of the proteins are indicated as N and C, respectively. (Adapted from Klein et al. (Klein et al., 1999))*

The nucleotide binding domains (NBDs) are evolutionary highly conserved and comprise the above sequence motifs: the Walker A and B motifs, being present in many different proteins utilising the energy of ATP (Walker et al., 1982), the signature motif, also referred as the C-loop, the unique sequence motif ABC transporters were named after (Hyde et al., 1990), and the following ABC protein specific motives such as the conserved glutamine (Q-loop), His (His-switch) and the aromatic stacking A loop. The two functionally interacting NBDs can dimerise to form a "head to tail" oriented "sandwich" dimer. The dimer harbours two composite catalytic centres with the two bound nucleotides at the dimer interface coordinated by conserved amino acids from both NBDs (Hopfner et al., 2000; Lamers et al., 2000; Obmolova et al., 2000; Smith et al., 2002).

The transmembrane domains are evolutionary divergent and, in case of ABC transporters, they form the substrate translocation pathway, provide the binding site(s) for ligand(s) and ensure substrate specificity. The orchestrated cooperation of the NBDs and TMDs ensures close coupling of ATP hydrolysis and substrate transport of ABC transporters, by a mechanism, which is not well understood.

High-resolution structural data are only available for non-eukaryotic ABC transporters, mostly for cytoplasmic NBDs, with the exception of the complete crystal structure of three importers, the Vitamin B12 transporter BtuCD of *Escherichia coli* (Locher et al., 2002), the molybdate importer ModDC of *Archeoglobus fulgidus* (Hollenstein et al., 2007b), the putative metalchelate importer HI1470/71 of *Heamophilus influensae* (Pinkett et al., 2007) and the recently published crystal structures of the only exporter Sav1866 from *Staphyllococcus aureus* (Dawson and Locher, 2006; Dawson and Locher, 2007). The "switched" structure of the Sav1688, reflecting the ATP bound conformations in which the transmembrane domains are outward-facing, revealed unexpected interactions between TMDs and NBDs, as the two identical sub-domains of this protein were intricately interleaved (Figure 2.2). The

structure of Sav1866 allowed reliable homology modelling of full-length ABC transporters (DeGorter et al., 2008; Fulop et al., 2009; Mornon et al., 2008; Zolnerciks et al., 2007) and provided a structural basis for the understanding of the mechanism of actions.

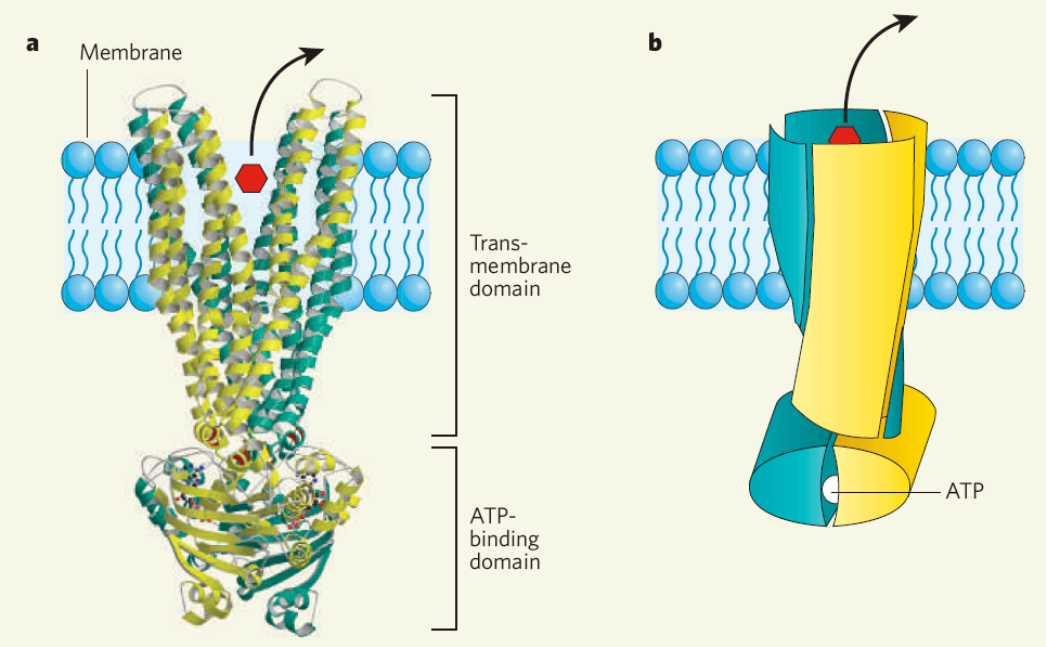

Figure 2.2 Structure of the Sav1866 transporter in the ATP-bound conformation. *Backbone of the Sav1866 transporter, in ribbon representation. The two subunits are shown in yellow and turquoise and the drug is designated as a red polygon* ***(panel a)****. The interaction between the membrane domains and the substrate translocation pathway reflect a switched structure* ***(panel b)****. (Adapted from Dawson et al. (Dawson and Locher, 2007))*

These current models suggest a common alternating access and release mechanism of action in which ATP binding to NBDs promotes conformational motions resulting in outward conformation of the TMDs, while the dissociation of the hydrolysis products releases the protein in inward-facing conformation of the TMDs. (Hollenstein et al., 2007a; Hollenstein et al., 2007b). These models seem to be more suitable for MDR-type proteins where the two NBDs are

identical than for ABC transporters harbouring asymmetric NBDs, the typical characteristics of MRP-type proteins.

Though ABC proteins function mostly as transporters, there are several exceptions to this rule. Among human ABC proteins there are proteins functioning as receptors and channels as well, such as ABCC7/CFTR, ABCC8/SUR1, and ABCC9/SUR2. CFTR is a chloride ion channel, well known as a protein underlying a frequent inherited disorder, cystic fibrosis, while the sulfonylurea receptors, ABCC8/SUR1 and ABCC9/SUR2, serve as the regulatory subunits of ATP-dependent potassium channels (K_{ATP}). Finally, several NBDs, lacking TMDs, have evolved to couple ATP hydrolysis to distinct biological functions, such as DNA repair (Rad50, MutS) and DNA binding (SMC proteins).

2.2. Human and *Drosophila* ABC transporter subfamilies

Based on phylogenetic analysis and amino acid sequence alignments of the NBD domains, the existing eukaryotic genes have been grouped into eight major subfamilies, termed from A to H, each characterized by typical and somewhat characteristic membrane topology patterns. The human genome encodes 48 ATP-binding cassette proteins, these proteins were grouped into the seven subfamilies, termed from A to G, while the 56 Drosophila ABC transporters were grouped into eight subfamilies, from A to H (Dean and Allikmets, 2001; Dean et al., 2001).

In the following we provide a brief description of the different ABC transporter subfamilies with respect to both human and *Drosophila* subfamily members.

2.2.1. ABCA subfamily

The human ATP-binding cassette subfamily A consists of 12 full transporters, arranged as TMD1-ABC1-TMD2-ABC2 (Figure 2.1), and comprise one of the most abundant subfamilies of the human ABC proteins. This family contains the largest ABC transporters known to date.

ABCA1 is the best characterised transporter in the A subfamily. Being a lipid translocator, it has been shown to take an essential role in generation of high-density lipoproteins (HDL) via promoting the efflux of cholesterol and membrane phospholipids, thus contributing to the reverse cholesterol transport from peripherial tissue to liver (Lee and Parks, 2005; Van Eck et al., 2005). Mutations affecting ABCA1 lead to a disorder in lipid metabolism, Tangier disease (Brooks-Wilson et al., 1999).

ABCA3 is hypothesised to play an active role in the excretion of the lipid components of the pulmonary surfactant and malfunction of ABCA3 causes fatal deficiencies of surfactant production in newborns (Nagata et al., 2004).

ABCR/ABCA4 is expressed exclusively in photoreceptors, where it transports retinol derivatives from the photoreceptor outer segment to the cytoplasm. Complete loss of ABCA4 function leads to retinitis pigmentosa while patients being compound heterozygotes for missence mutations of ABCA4 suffer from Stargardt macular dystrophy (Allikmets et al., 1997).

ABCA7 was suggested to play a role in lipid trafficking of defined microenvironments, such as apical brush border membrane of renal tubules of mice, keratinocytes, myelolymphatic tissues (Kaminski et al., 2000; Kielar et al., 2003; Linsel-Nitschke et al., 2005).

ABCA12 is proposed to play a role in skin lipid homeostasis, mutations of the gene lead to the severe hereditary disease Harlequin ichtyosis (Kelsell et al., 2005).

The genome of *Drosophila melanogaster* encodes ten ABCA genes (Dean M, 2003), their roles have not been investigated in details.

2.2.2. ABCB subfamily

The human ATP-binding cassette subfamily B comprises eleven functionally and structurally divergent ABC proteins. Three of them are full transporters, with the domain arrangement of TMD1-ABC1-TMD2-ABC2 (Figure 2.1), and are localised to the apical compartment of plasma membrane, such as ABCB1 (MDR/PgP), ABCB4 (MDR3) and ABCB11 (BSEP/sisterPgP). The other seven family members are half transporters, with the domain arrangement of TMD-ABC (Figure 2.1), and are localised to the endoplasmic reticulum, as ABCB2 (TAP1) and ABCB3 (TAP2), or reside in the mitochondrial membrane, as ABCB 6, 7, 8 and 10, while the ABCB9 (TAPL) half transporter has recently been reported to be localised to lysosomes.

ABCB1 (P-glycoprotein/Pgp/MDR/MDR1) is the archetype of ABC proteins, being the first ABC protein discovered in the 1970s (Chen et al., 1986; Gros et al., 1986) in certain tumours that inherited or developed the so-called "multidrug resistance" (MDR) phenotype. The hallmark of the multidrug resistance phenotype is the phenomenon that chemotherapeutic treatment of the cancer with one agent is potent at the beginning but results in a later resistance against this cytotoxic agent. Moreover, at the same time the tumour gains resistance against a wide range of structurally and functionally unrelated other cytotoxic agents as well, resulting in the failure of the chemotherapeutic treatment. Compelling evidence has proven that this phenomenon is the consequence of overexpression of a protein termed Pgp or Multidrug Resistance Protein1 (MDR1), a primarily active transporter that extrudes a wide range of substrates out of the cell, thus lowering cellular concentrations of the cytotoxic agents. In the past few decades, despite the discovery of a large number of human ABC proteins with some members also involved in multidrug resistance, MDR1 remained to be one of the most important ABC transporters due to its extremely wide substrate specificity and clinical relevance (for details see recent review by Szakacs and Sarkadi (Sarkadi et al., 2006; Szakacs et al., 2008)). The promiscuous character of MDR1 in substrate specificity raised the question of how such a large number of substrates could be transported by a single protein. The molecular basis of the recognition of such a wide variety of substrates still remains unsolved but extensive investigations revealed many aspects of MDR1 function and also resulted in the development of a large variety of experimental techniques to study ABC transporter function. The mechanism of action was extensively investigated in detail but, in the absence of high-resolution structures, basic questions including the coupling of ATPase activity to substrate transport and the way the four domains interact with each other in a concerted way still remain unsolved. The recently published high-resolution structure of the bacterial homodimer Sav1688 (Dawson and Locher, 2006) representing a "full transporter" complemented by biochemical approaches capable of dissecting the catalytic cycle of an ABC transporter might provide further insight into the intimates of the mechanism of action.

ABCB4/MDR3 is a lipid floppase translocating phosphatidylcoline (PC) from the inner leaflet to the outer leaflet of the plasma membranes in the canalicular membranes of the hepatocytes (Daleke, 2003; Smith et al., 1994), providing defence against harmful bile acid mediated injuries along the biliary tree. Mutations of ABCB4 cause various mild hepatic disorders and the severe progressive familiar intrahepatic cholestatis (PFIC) type 3, a chronic cholestatic syndrome of elevated gamma-glutamyltranspeptidase causing jaundice, pruritus, hepatosplenomegaly and biliary cirrhosis symptoms requiring liver transplantation (De Vree et al., 2000). Pregnant women with abnormal ABCB4 are affected with intrahepatic cholestasis of pregnancy.

ABCB11/BSEP has a narrow substrate specificity and is expressed predominantly in the liver, and is the key player of the bile flow formation due to its activity in canalicular secretion of bile salts. Malfunction of ABCB11 contributes to the heritable disorder progressive familiar intrahepatic cholestatis (PFIC) type 2 (Strautnieks et al., 1998).

ABCB-type half transporters are evolutionary related and, though having different compartmentalisations, display related functions of trafficking peptides across intracellular membranes. ABCB2 (TAP1) and ABCB3 (TAP2) form heterodimers (Kelly et al., 1992) and are crucial in the classical MHC class I-mediated immune response as TAPs transport peptides generated by proteasomal degradation in the cytosol into the ER lumen, where these peptides bind to MHC class I molecules and are shuttled in complex to the cell surface (Schrodt et al., 2006).

ABCB9 (TAPL) functions as a homodimer and is localised to lysosomes. It is a peptide transporter recognizing a very broad spectrum of peptides, ranging from 6- up to 59-mers (Wolters et al., 2005). TAPL was recently suggested to play a role in an alternative pathway of antigen presentation in professional antigen-presenting cells (Demirel et al., 2007).

There is a relatively little known about mitochondrial ABCB proteins. The localization of ABCB6 is unresolved with opposing observations localising ABCB6 to either the inner or outer membranes of mitochondria leading to

conflicting interpretation of the direction of ABCB6 mediated transport. Recent data based on laser scanning microscopic observations suggests that ABCB6 is localized in the ER-derived perinuclear compartments of the Golgi apparatus (Tsuchida et al., 2008). A recent report suggested the role of ABCB8 in the mitochondrial genome defence against doxorubicin in melanoma cells (Elliott and Al-Hajj, 2009). ABCB10 is located in the inner membrane of mitochondria and was suggested to play a role in erythroid differentiation (Shirihai et al., 2000).

Of the ten Drosophila ABCB genes (Dean M, 2003), Mdr49 and Mdr65 (Wu et al., 1991), and Mdr50 (Gerrard et al., 1993) have been studied in any detail. A fourth member of this group, CG10226, was found clustered with Mdr65. These genes are closely related to human ABCB1 and ABCB4, and disruption of Mdr49 resulted in sensitivity to colchicines (Wu et al., 1991). In wild-type third instar larvae mdr49 and mdr65 showed constitutive expression in different larval tissues. However, both of these genes were induced by tumorous shock, whereas heat shock and colchicine feeding induced the expression of only mdr49 significantly (Tapadia and Lakhotia, 2005).

2.2.3. ABCC subfamily

This subfamily is discussed in detail in section 2.3.

2.2.4. ABCD subfamily

This subfamily comprises four peroxisomal half-transporters with a TMD-ABC type of domain arrangement (Figure 2.1) and is suggested to play a role in the ß-oxidation of fatty acids mediated by peroxisomes. Among them there is the adrenoleukodystrophy protein (ALDP/ABCD1) mediating transport of coenzyme A esters of very-long-chain fatty acids. Mutations of the *ABCD1* gene lead to the severe X-linked progressive genetic disorder X-linked adrenoleukodystrophy affecting the adrenal glands and the white matter of the nervous system due to the accumulation of very-long-chain fatty acids in these tissues. The genome of

Drosophila melanogaster encodes two ABCD genes, their role have not yet been investigated (Dean M, 2003).

2.2.5. ABCE and ABCF subfamilies

ABCE and F subfamilies lack TMDs and are not involved in transport mechanisms, therefore they are out of scope of this introduction.

2.2.6. ABCG subfamily

The human ATP-binding cassette subfamily G consists of five half transporters, ABCG1/ABC8, ABCG2/BCRP/MXR, ABCG4, ABCG5 and ABCG8. They are composed of a single N terminal ABC domain followed by a TMD of six putative membrane-spanning helixes (Figure 2.1).

The physiological role of ABCG1 and G4 is basically unknown, while ABCG5 and ABCG8 are known to work as heterodimers (Graf et al., 2003; Muller et al., 2006) transporting cholesterol and various cholesterol derived sterols. ABCG5-G8 heterodimers provide resistance against sitosterols defending tissues from the accumulation of these toxic compounds of plant origin. The malfunction of ABCG5-G8 heterodimers causes a severe disease referred to as sitosterolemia (Berge et al., 2002).

ABCG2 is a highly active multidrug transporter present in various tissues serving as barriers, such as liver, intestine, colon, kidney, placenta, blood brain barrier and stem cells and is localised to the apical membrane in polarised cells (Cooray et al., 2002; Zhou et al., 2002). It harbours a wide substrate specificity encompassing large amphiphlic cytotoxic drugs, sulphated hormone metabolites, antibiotics, flavonoids etc. (Adachi et al., 2005; Merino et al., 2006; Schinkel and Jonker, 2003). ABCG2 is clinically relevant as a multidrug transporter as it can provide resistance against a wide variety of compounds, such as metotrexate, antifolate and their derivatives, topoisomerise I and tyrosine kinase inhibitors (Sarkadi et al., 2006). It also provides xenobiotic resistance against dietary toxins and modulates absorption of pharmaceutical agents and plays a major role in protecting the fetus, brain and stem cells against toxic compounds. Interestingly

it also actively concentrates drugs and carcinogen agents into milk (Jonker et al., 2005).

Surprisingly, in contrast to the 5 human and 6 mouse ABCG genes there are 15 ABCG genes in the fruit fly genome, making this the most abundant ABC subfamily (Dean M, 2003). The best-studied Drosophila ABC genes are white (w), scarlet (st), and brown (bw) forming heterodimers and playing essential roles in the cellular uptake of eye pigment precursors guanine and tryptophane (Dreesen et al., 1988; Ewart et al., 1994; Mackenzie et al., 1999; Tearle et al., 1989). Recent studies have shown that overexpression or mislocalisation of white lead to abnormal sexual behaviour (Anaka et al., 2008) and that these proteins play an essential role in regulation of monoamine levels such as dopamine, histamine and serotonin in the Drosophila brain (Borycz et al., 2008). The only Drosophila ABCG gene having a close orthologue in the human genome is Atet, being highly similar to human ABCG1 and ABCG4 (Dean M, 2003). Atet was designated as ABC Transporter Expressed in Trachea, because the transcript was localized to the respiratory system. (Kuwana et al., 1996). The Drosophila ABCG genes are very divergent phylogenetically and highly dispersed in the fly genome.

2.2.7. ABCH subfamily

Three *Drosophila melanogaster* genes, CG9990, CG6162, and CG11147, have been identified that did not fit into any of the known subfamilies and, in fact, were most closely related to ABC genes from bacteria (Dean M, 2003). These genes have been designated as subfamily H. The genes are within large contigs and have introns and therefore do not represent contamination from bacterial sequences. This group forms a distinct cluster on the Drosophila phylogenetic tree and is considered to be significantly different from all known families of ABC transporters. So far nothing is known about the possible functions of the members of this subfamily. The genome of the closely related *Anopheles gambiae* also contains a subgroup of ABCH genes (Roth et al., 2003).

2.3. The ABCC Subfamily of ABC transporters

The human ATP-binding cassette subfamily C consists of twelve members that share specific conserved structural features in their NBDs, distinguishing them from members of the other ABC transporter families. ABCC-type proteins are full transporters, and based on the presence or absence of an additional N-terminal TMD, the ABCC subfamily is divided into two sub-groups, "long" and "short" ABCC proteins. Short ABCC proteins show the domain organisation of TMD1-ABC1-TMD2-ABC2, while in the structure of the long ABCC proteins the above core domain, representing a full transporter, is preceded by an additional N-terminal 5 transmembrane helix domain (TMD0/MSD0), connected to the core domain via a large cytoplasmic loop (L0/CL3) (Figure 2.3) (Klein et al., 1999; Tusnady et al., 1997).

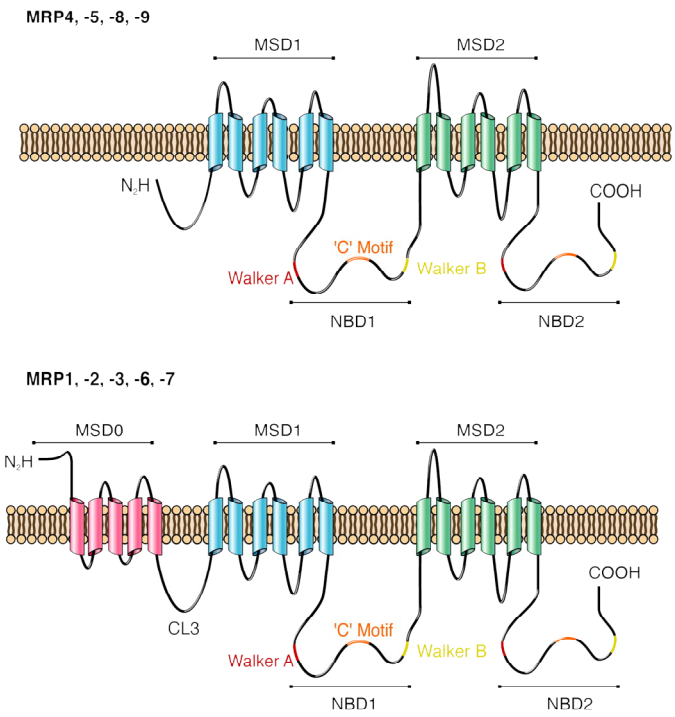

Figure 2.3 Domain arrangements of human short and long MRPs

Upper panel shows domain arrangements of short MRPs, lower panel shows those of the long MRPs. Transmembrane domains are indicated as MSDs and the three most important conserved regions of the NBDs are indicated as coloured lines (Adapted from Deeley et al (Deeley et al., 2006))

This domain organization is characteristic to seven proteins, ABCC1/MRP1, ABCC2/MRP2, ABCC3/MRP3, ABCC6/MRP6, ABCC8/SUR1, ABCC9/SUR2, and ABCC10/MRP7, designated as "long MRPs" (except for SURs). The remaining five proteins, ABCC4/MRP4, ABCC5/MRP5, ABCC7/CFTR, ABCC11/MRP8 and ABCC12/MRP9, belong to the short ABCC proteins, designated as "short MRPs" (except for CFTR).

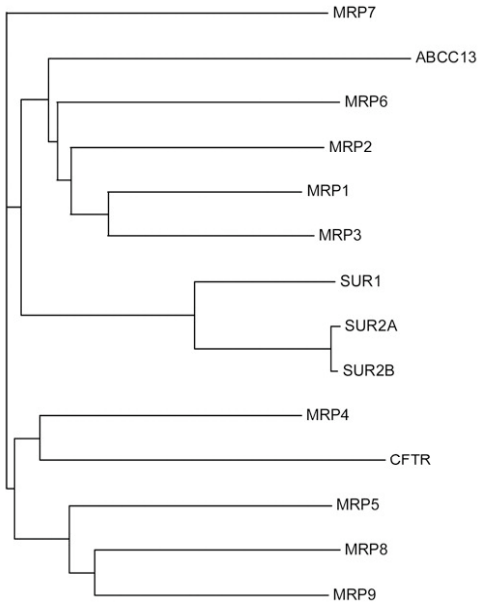

Figure 2.4 Evolutionary relationship of the human MRPs

The phylogenetic tree was generated by the entire sequences of the proteins by Deeley et al. (Deeley et al., 2006)

In *Drosophila*, among the 56 ABC genes, long ABCC proteins are only represented by two members, *dSUR and dMRP/CG6214* (Dean et al., 2001).

The groups of long and short MRPs share at some extent similar overlapping substrate specificities characteristic to their groups, reflecting their potential common evolutionary roles in the defence against xenobiotics and environmental toxins. Later they gained other functions in regulation of distribution of endogenous compounds. The members of both long and short MRPs are involved in multidrug resistance, and are characterised to some extent by overlapping substrate specificity against cytotoxic drugs. The key players among

long MRPs are MRP1 and MRP2, with wide substrate spectra, and MRP3 with a narrower one, but all long MRPs are able to confer resistance against at least some cytotoxic agents. Similarly, short MRPs characterised so far (MRP4, 5, 8) are all involved in multidrug resistance phenotype (Deeley et al., 2006).

ABCC proteins function as organic anion transporters with the exception of three family members, CFTR and SUR1/SUR2. These unique ABCC proteins are discussed first in the following.

ABCC7/CFTR

CFTR is an epithelial chloride ion channel identified by positional cloning in 1989 (Kerem et al., 1989; Riordan et al., 1989; Rommens et al., 1989). Mutations in the gene cause cystic fibrosis, the most common ABC protein related genetic disorder of Caucasians. Interestingly, among the more than 1400 different mutations detected so far in patients, one single deletion mutant ΔF508 is responsible for vast majority of the cases (up to ≈90% in certain populations) (Lewis et al., 2005). CFTR, being an ion channel, mediates the passive bidirectional movement of small anorganic anions. Unique feature of the protein is the presence of a regulatory subunit, called as CFTR R, which allows tight regulation of the channel via phosphorylation / dephosphorylation events as a result of changes in intracellular cAMP levels. This, together with ATP binding and subsequent slow rate of ATP hydrolysis of the N-terminal NBD, concerts the gating of the channel (Cheng et al., 1991; Csanady et al., 2000; Csanady et al., 2005). The intimates of the catalytic cycle of CFTR is the best investigated among ABC proteins, due to the application of high-sensitivity patch clamp techniques allowing detailed investigations of opening and closure of single channels (Gadsby et al., 2006).

ABCC8/SUR1and ABCC9/SUR2

The long ABCC proteins called sulfonylurea receptors, ABCC8/SUR1and ABCC9/SUR2, form the ATP-dependent potassium channel (K_{ATP}) together with

the inward rectifying selective K^+ channels, Kir6.1 or Kir6.2. K_{ATP} channels are obligate hetero-octamer complexes, formed by four ABCC protein/Kir6.x hetero-dimers (Shyng and Nichols, 1997). The SUR subunits of the K_{ATP} channels are ADP/ATP sensors, which connect the metabolic state of the cell to the membrane potential (Nichols, 2006). The binding of ATP or ADP to Kir6.x subunits reduces channel activity in a Mg^{2+} independent manner, while the Mg^{2+} dependent nucleotide binding and hydrolysis of the SUR subunit have a stimulatory role in channel open probabilities (Xie et al., 2007). The role of K_{ATP} channels has been studied most extensively in pancreatic ß-cells, where they link glucose metabolism to insulin secretion. Mutations of either K_{ATP} channel subunits, Kir6.2 and SUR1, cause neonatal diabetes or congenital hyperinsulinism (Ellard et al., 2007).

dSUR has been identified as the functional orthologue of the mammalian *SUR2* protein (Kim and Rulifson, 2004; Nasonkin et al., 1999). Recent data suggested that *dSUR* expression played a protective role against hypoxic stress and heart failure, and provided evidence about the relationship of *dSUR* expression and cardiac aging (Akasaka et al., 2006). A recent review detailed the applicability of the Drosophila heart model in the investigation of human cardiac development and heart function (Ocorr et al., 2007).

The following ABCC proteins are canonical transporters.

ABCC1/MRP1

MRP1 is an outstanding member of the ABCC subfamily, due to its remarkable broad substrate specificity, and importance in physiological and pathological mechanisms. It is ubiquitously expressed in the body with highest expression levels in the lung, kidney, testis, heart, placenta and with moderate levels in the colon, small intestine, brain, and blood mononuclear cells (Cole et al., 1992; Flens et al., 1996). In polarised cells MRP1 is predominantly expressed in the basolateral compartment of the plasma membrane (Hipfner et al., 1994),

however in some cells types apical trafficking of MRP1 had been observed, too. MRP1 is capable of transporting a vast variety of substrates, such as hydrophobic compounds, organic anions and their conjugates. The typical substrates are glutathione, glucuronide and sulfate conjugates such as leukotriene C_4 (LTC_4) (Bakos et al., 2000; Leier et al., 1994) and the artificial gluthatione conjugate of N-ethylmaleimide (NEM-GS) (Bakos et al., 2000) , ß-estradiol 17-ß-D-glucuronide ($E_2$17ßG) (Loe et al., 1996), estrone 3 sulfate (Qian et al., 2001) and xenobiotic conjugates such as the glutathione conjugate of the aflatoxin B6 carcinogen. MRP1 confers resistance against a broad spectrum of anticancer drugs, including anthracyclines (Cole et al., 1994), plant alkaloids, metotrexate and HIV protease inhibitors (Olson et al., 2002). MRP1 also transports metalloids and peptides, such as a sodium arsenite and gluthatione (GSH/GSSG) (Leier et al., 1994), and several fluorescent probes such as calcein and calcein-AM. Contrary to MDR1, the MRP1 mediated chemotherapeutic drug transport often requires the presence of GSH, and cross-stimulation of the drug-GSH transport was observed in many cases. It is supposed that the mechanism underlying the above phenomenon is the co-transport of the drugs and GSH. Many MRP1 substrates cross-inhibit the transport of the other substrate, while others do not interfere with each other. These observations suggest the existence of several non-overlapping and some partially overlapping cooperative substrate binding sites of MRP1. The exact substrate binding sites are not yet defined.

Since MRP1 is predominantly present in tissues, which are considered to constitute the major defence lines of the body, and harbours a wide substrate specificity involving endo and xenobiotics, it is considered to play an important role in the defence against the toxic compounds of endogenous and exogenous origin. In addition to its role in phase III detoxification reactions, MRP1 also functions in inflammatory responses as well, being responsible for the cellular release of the inflammatory mediator leukotriene C_4 (Robbiani et al., 2000; Wijnholds et al., 1997). Moreover, MRP1 was found to be important in oxidative stress response, when the GSH-GSSG mediated stress response is overwhelmed and MRP1 plays a role in the elimination of GSSG and GSH conjugated toxic

agents from the cells (Leier et al., 1996) thus contributing to the maintenance of the physiological redox potential.

The catalytic mechanism of MRP1 has been extensively studied. In contrast to MDR1 and the prokaryote ABC transporters, where the two NBDs are structurally and functionally identical (Beaudet and Gros, 1995) and ATP hydrolysis is an alternating process (Sauna and Ambudkar, 2000), MRP1 and its homologues harbour two structurally and functionally non-equivalent NBDs. The most obvious difference between the two NBDs of MRP-type proteins is the conservative deletion of a 13 amino acid sequence between the Walker A and Q loop in NBD1. Functional studies revealed that ATP binding occurs predominantly at NBD1 of MRP1 while trapping of ADP is shown predominantly at NBD2, indicating that NBD1 has a two-three fold higher affinity for ATP than NBD2, however NBD2 hydrolyse ATP at a much higher turnover than NBD1. The two NBDs of MRP1 function cooperatively in an asymmetric fashion, since hydrolysis at NBD2 is highly dependent on ATP binding to NBD1, while ATP binding of NBD1 is less dependent on the status of NBD2 (Deeley et al., 2006). The intimates of the catalytic cycle of MRP1 remain un-revealed, and there is a great need for a high-resolution 3D structure of an MRP-type asymmetric transporter.

ABCC2/MRP2

MRP2 is widely expressed in many organs, the highest expression level was detected in the villi of the proximal jejunum, but MRP2 is also expressed in the liver, kidney, small intestine, colon, gallbladder, placenta and lung. It is localised to the apical side of polarised cells, it is present in the canalicular (apical) membranes of hepatocytes, the apical membranes of intestinal epithelium, placental syncytiotrophoblasts and renal proximal tubules (Deeley et al., 2006). Similarly to MRP1, MRP2 can transport a vast array of gluthatione, glucuronide and sulphate conjugated endo and xenobiotics, playing essential role in the terminal elimination of metabolites of phase-II conjugation reactions. Defect of the close homologue in a naturally mutant rat strain (Eisai hyperbilirubinemic

/EHBR rats) with similar substrate specificity, was a useful tool for characterising the broad substrate specificity of the human MRP2. Among other compounds, MRP2 is able to transport conjugated leukotrienes, such as LTC_4, LTD_4 and LTE_4, steroid bile salt conjugates, such as estradiol 17-beta-D-glucuronide and bilirubin glucuronides (Bakos et al., 2000; Deeley et al., 2006; Nies and Keppler, 2007). MRP2, similarly to MRP1, also transports various unconjugated drugs, such as vincristine and doxorubicine, as a co-transport together with GSH. In a rare autosomal recessive disorder called Dubin-Johnson syndrome, canalicular efflux of bilirubin conjugates is impaired due to loss of MRP2 function, leading to mild jaundice observed in patients.

ABCC3/MRP3

MRP3 is expressed at high levels in the adrenal gland, pancreas, gut, gall bladder and placenta, and at lower levels in kidney distal tubules. MRP3 has an extremely wide substrate spectrum, resembling those of MRP1 and MRP2, with the below limitations: MRP3 does not transport GSH at all, while GSH-conjugates are poor substrates for MRP3, however, glucuronide conjugates are excellent MRP3 substrates. In addition, MRP3 transports conjugated bile salts and monovalent bile salts as well (Borst et al., 2007). MRP3 shows basolateral localisation and, in the liver, resides in the cholangiocytes or in the hepatocytes adjacent to bile ducts. In cholestatic conditions the expression of MRP3 is markedly elevated (Donner and Keppler, 2001), while MRP2 expression on the canalicular side is dramatically reduced (Trauner et al., 1997). These orchestrated changes in the level of the above transporters together with their functional complementarity is supposed to function as a defence mechanism of the liver to prevent the accumulation of biliary toxic compounds in cholestatic conditions (Bodo et al., 2003a). This hypothesis was supported by a recent study using knock out (KO) animal models (van de Wetering et al., 2007).

ABCC4/MRP4

The short MRP, ABCC4/MRP4, is expressed at high levels in prostate and at low to moderate levels in ovary, testis, adrenals lung and intestine (Lee et al., 1998). In polarized cells MRP4 is observed in the basolateral (Lee et al., 1998) and the apical compartment as well (Leggas et al., 2004; van Aubel et al., 2002). It functions as an organic anion transporter, and similarly to MRP5, it is capable of transporting nucleoside and nucleotide analogues (Sager, 2004). It provides resistance against a large number of base, nucleotide and nucleoside analogue chemotherapeutic or antiviral agents (Borst et al., 2007). The physiological role of MRP4 is yet unknown, though it has been suggested to play a role in the urinary excretion of cAMP and cGMP (van Aubel et al., 2002), and some organic anions (Smeets et al., 2004). MRP4 can also transport prostaglandins, PGE1 and PGE2, (Reid et al., 2003). A role for MRP4 in concert with MRP3 is also suggested in compensatory mechanisms when biliary excretion is impaired.

ABCC5/MRP5

MRP5 is a widely expressed short MRP with the highest expression levels in skeletal and cardiac/cardiovascular myocites (Dazert et al., 2003). It is localised in the apical side of capillary endothel cells and astrocytes (Hirrlinger et al., 2002) and to the basolateral compartment of polarised epithelial cells (Wijnholds et al., 2000). Similarly to MRP4 it is an organic anion transporter capable of transporting nucleoside and nucleotide analogues (Wijnholds et al., 2000) providing resistance against a wide spectrum of chemotherapeutic or antiviral agents (Borst et al., 2007). Its physiological function is unknown.

ABCC6/MRP6

The long MRP, ABCC6/MRP6, is highly expressed in the kidney and the liver, while the expression of the protein in other tissues is controversial. MRP6, and its mammalian orthologues, are established organic anion transporters for GS conjugated anions, such as LTC_4, NEM-GS, S92,4-dinitrophenyl gluthatione, and the cyclic peptide BQ-123 (Belinsky et al., 2002; Ilias et al., 2002; Madon et

al., 2000). Mutations of the ABCC6 gene were shown to cause a rare hereditable disease, called pseudoxanthoma elasticum (PXE), resulting in the calcification of soft connective tissues of different organs, such as skin, eye and arterial blood vessels (Neldner, 1988). Among the large numbers of mutations detected in MRP6 genes, three have been shown to be loss of function (Ilias et al., 2002). The expression pattern of MRP6 has high relevance, since the expression of the protein is practically missing from tissues affected by the disorder. This discrepancy had lead to the postulation of the so called "metabolic disease hypothesis" suggesting that ABCC6, which is located in the basolateral plasma membrane of the hepatocytes, might regulate the distribution of an unknown compound between the liver and the periphery, leading to the above symptoms at the periphery (Uitto et al., 2001). Recent compelling data underscores this possibility, but well-established data is needed to unravel the mechanism by which the malfunction of ABCC6 gene leads to PXE.

ABCC10/MRP7

MRP 7 is evolutionary divergent from the cluster of the other long MRPs (Figure 2.4). It had been detected in many tissues by RT-PCR (Kao et al., 2002) but expression levels of MRP7 protein was found to be low (Hopper et al., 2001). MRP7 was shown to be able to transport estradiol 17-beta-D-glucuronide and LTC_4 at relatively low transport rate (Chen et al., 2003), and was suggested to play a role in multidrug resistance, conferring resistance to docetaxel, paclitaxel, SN-38, daunorubicin, etoposide, vincristine and epothilone B (Hopper-Borge et al., 2009). A recent publication shows that MRP7 also confers resistance to nucleoside-based anticancer agents, cytarabine and gemcitabine, and the antiviral agent 2',3'-dideoxycytidine.

ABCC11/MRP8

The short MRP, ABCC11/MRP8, was found to be ubiquitously expressed in the body with the exception of kidney, spleen and colon at mRNA levels. MRP8

harbours the widest substrate specificity of any short MRPs, combining the substrate specificity of classical long MRP substrates, such as leukotriene C4, dehydroepiandrosterone 3-sulfate (DHEAS), estrone 3-sulfate, estradiol 17-beta-D-glucuronide, glycocholate, taurocholate and metotrexate and the typical short MRP substrates, cAMP and cGMP. These results suggest that MRP8 participates in physiological processes involving transport of bile acids, conjugated steroids, and cyclic nucleotides (Chen et al., 2005). The role of MRP8 in conferring resistance against nucleotide analogues was also demonstrated (Guo et al., 2003).

ABCC12/ MRP9

Only mRNA transcripts coding for truncated protein (the largest 100 kDa) were detected in testis and breast, and had been found at high level in the epithelial cells of breast cancer. The protein is predicted to have only 8 TMDs, lacking transmembrane domains 3, 4, 11, and 12 and the second nucleotide-binding domain (Bera et al., 2002).

2.4. Characteristics of Drosophila MRP (DMRP)

At the beginning of our investigations only very limited information was available on DMRP, and this knowledge focused only on the genomic and mRNA level of organisations.

Sequencing and initial annotation of the *Drosophila melanogaster* genome in 2000 (Adams et al., 2000; Myers et al., 2000) made it possible to investigate the evolutionary relationships between the human and fruit fly genomes. Based on the Celera and FlyBase databases Dean et al identified 56 fruit fly ABC genes and performed phylogenetic analyses (Figure 2.5). As it is shown on the phylogenetic tree CG6214/*dMRP* encoding DMRP (marked in red box) clustered with human MRP1 (marked in blue box) in respect to both NBD1 and NBD2 specific protein sequences (Dean et al., 2001).

The *dMRP/CG6214* gene, encoding Drosophila MRP, was cloned in 2003 (Grailles et al., 2003). Grailles et al. reported that the *CG6214* gene spanned more than 22kb and contained 19 exonic sequences and was localised to the long arm of 2L chromosome 33F3-33F4 cytogenic regions. They revealed two internally variable regions in the gene, the first containing 2 and the second 7 alternative exons. These alternative exons gave rise to different protein isoforms, presumably due to alternative splicing. The different mRNA isoforms harboured 12 exons and were all but one coding for proteins of the same size (1548 and 1549 amino acids, respectively). The 7 variants of exon 8 (a-g) were detected by nested PCR at different stages of life, from embryo to adult, suggesting that alternative splicing is not developmentally regulated. Though the temporal expression of the two exon 4 variants (a, b) was not investigated, there was a possibility that all fourteen splice variants could be present in the fly at the same time (Grailles et al., 2003).

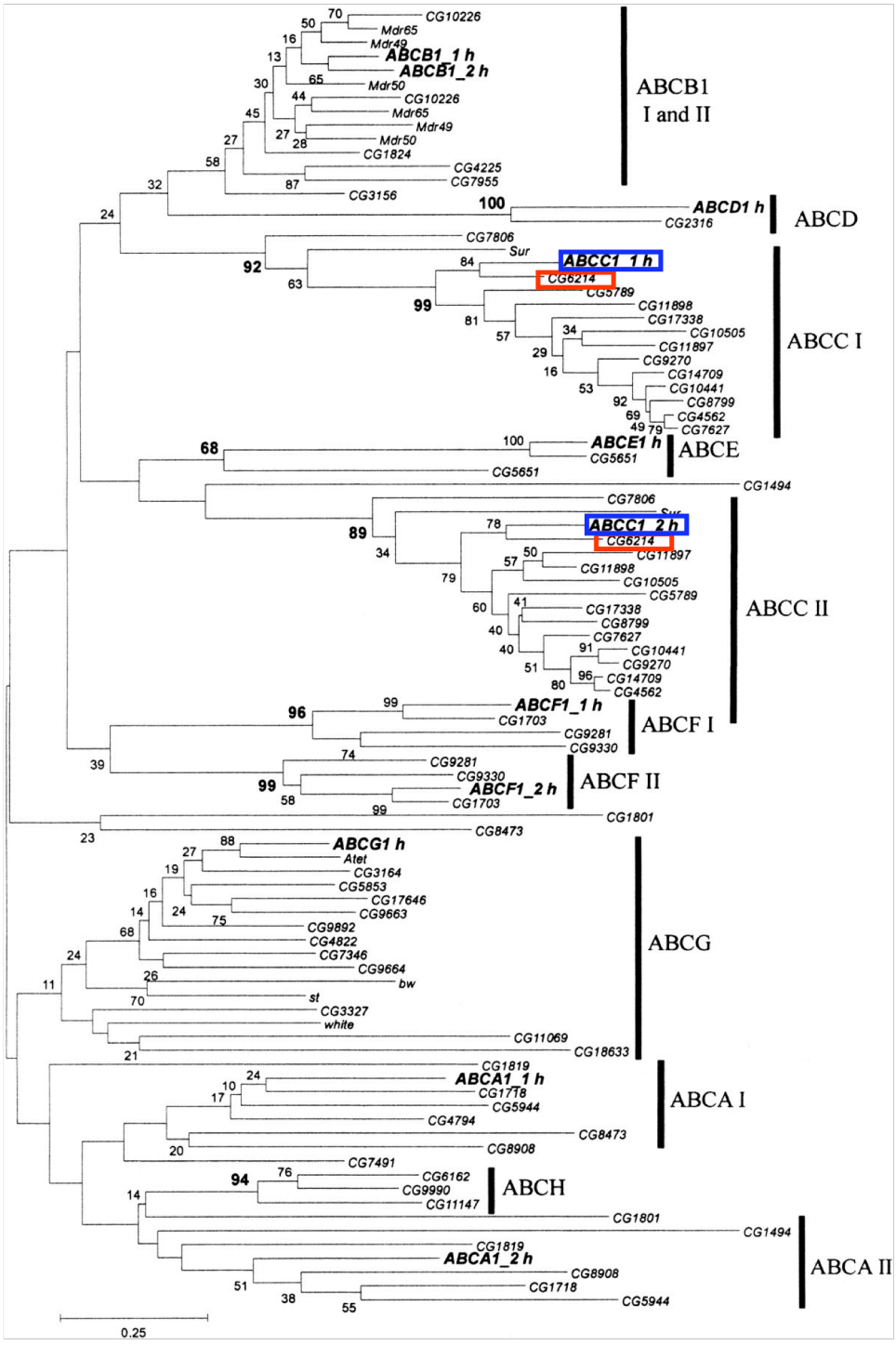

Figure 2.5.: Phylogenetic tree of the Drosophila ABC genes and representative human subfamily members. *Proteins containing two ATP-binding domains are denoted on the figures as I and II in respect to their NBDI (NBD1) and NBDII (NBD2) sequences (adapted from Dean et al. (Dean et al., 2001)) The CG6214/dMRP gene encoding DMRP is marked in a red box and clusters with hMRP1 (marked in a blue box) in respect to both NBD1 and NBD2.*

In the FlyBase database (www.flybase.org) there are currently 17 annotated mRNA transcripts (Figure 2.6). The only available dMRP cDNA clone is SD07655 coding for the 4b 8d isoform of DMRP is denoted as MRP-RB (FBtr0090014) and is indicated by a red arrow. It encodes a protein of 1548 amino acids with a calculated molecular mass of 173.4 kDa.

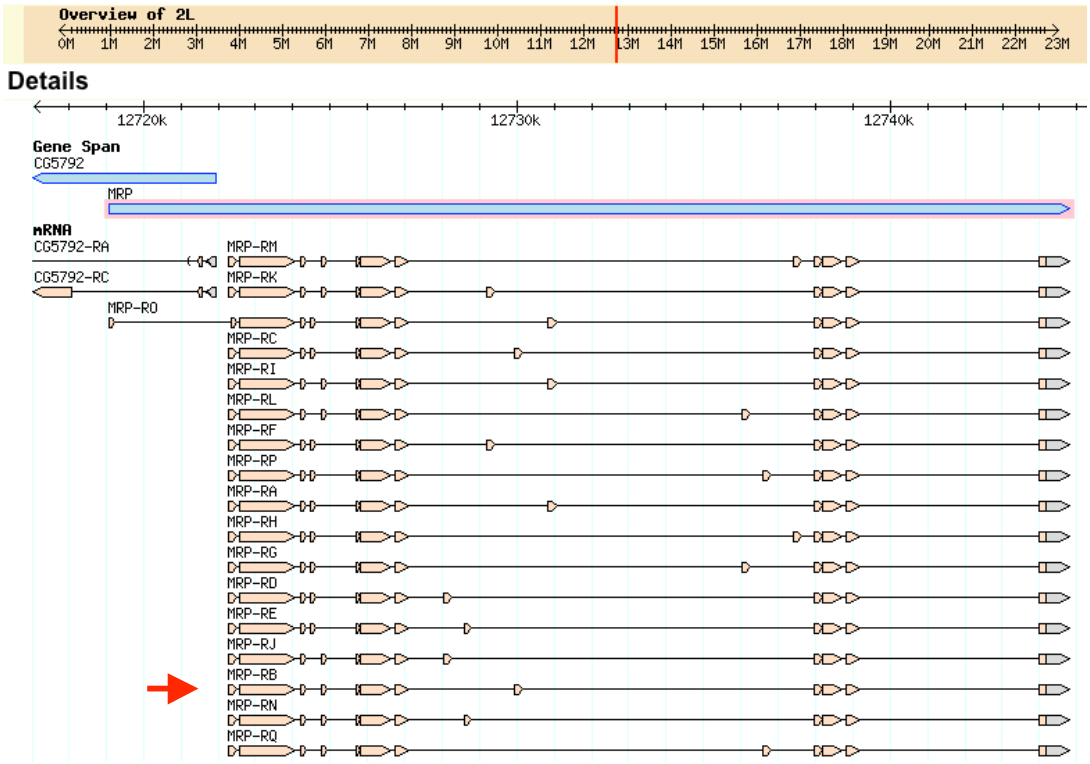

Figure 2.6.: Genetic map of Drosophila 2L chromosome region depicting dMRP/CG6214 gene (MRP) and its potential mRNA transcripts. *The transcript coding for DMRP isoform 4b8d is designated as MRP-RB and indicated by red arrow. (www.flybase.org)*

3. Aims/Objectives

The human multidrug resistance-associated proteins (hMRPs) have outstanding roles in either normal or pathological conditions of the body including chemo-resistance against endo and xenobiotics, regulated distribution of compounds of high physiological relevance and chemotherapy failure due to acquired multidrug resistance, therefore are in the focus of intensive investigations. Despite of their remarkable importance, substantial characteristics, including their structure, catalytic mechanism and physiological function, are not well understood. One of the several reasons concealing behind this is the moderate activity of human MRPs in functional assays.

In pilot experiments we studied the *Drosophila melanogaster* orthologue of the human long MRPs and our preliminary results indicated that this protein exhibited outstanding activity. Therefore we assumed that DMRP could be a useful model protein for its human counterparts and we decided to perform systematic comprehensive and comparative investigations aiming to reveal the characteristics of DMRP as a potential high turnover model of human MRPs.

At the beginning of our investigations only limited data were available on *dMRP* focusing exclusively on genetic and mRNA levels of organisations, while the functional and biochemical properties of the protein were un-revealed. To shed light on the characteristics of DMRP as a potential human MRP model we aimed to apply the following approaches.

1. We wanted to reveal the evolutionary relationship of *Drosophila* and human ABCC proteins and propose a correct membrane topology model for DMRP instead of the membrane topology arrangement previously published by Grailles et al.

2. We aimed to characterise the substrate and inhibitor profile of DMRP, in light of human MRPs showing the highest activity, in comparative functional assays towards well-established human MRP substrates and inhibitors.
3. We aimed to investigate the ATP hydrolytic cycle of DMRP studying nucleotide binding and trapping as well as the vanadate-sensitive ATPase activity of the protein.
4. In addition, we aimed to study the potential physiological role of DMRP by investigating endogenous DMRP expression and localisation in various cell cultures and tissues, and studying the potential role of DMRP in pesticide resistance.

In order to achieve the above general aims we needed the following tools; a suitable expression system and an antibody specifically recognising DMRP. To provide the basis for our investigations, we had the following specific aims.

a) We aimed to express DMRP in *Spodoptera frugiperda* Sf9 cells, in the expression system that had been previously used extensively in our laboratory to functionally characterise human MRP proteins. This well-established system seemed to be suitable for comparative analysis of the human and fruit fly MRPs.
b) We needed an antibody suitable for specifically recognising DMRP. Therefore we, in collaboration with a group from the University of Hawaii lead by Steven Robinow, ordered and validated a polyclonal antibody capable of recognising DMRP.

4. Methods

4.1. Materials

dMRP EST cDNA clone SD07655 was obtained from ResGen, Invitrogen Corporation. [^{3}H]leukotriene C_4 ([^{3}H]LTC_4; 148 Ci/mmol), and [^{3}H]ß-estradiol 17-ß-D-glucuronide ([^{3}H]$E_2$17ßG; 48 Ci/mmol) were purchased from PerkinElmer Life Sciences, [^{3}H] cAMP from American Radiolabelled Chemicals, Inc., and $^{45}CaCl_2$ (0.8 Ci/mmol) from Amersham. 8-N_3-[^{32}P]ATP (20 Ci/mmol) was obtained from ICN Pharmaceuticals, Inc. (Costa Mesa, CA). Calcein, fluo-4 AM, and CDCF were obtained from Invitrogen - Molecular Probes and ouabain was purchased from Fluka. DDT, bioallethrin, aldicarb and fenitrothion were purchased from Chem Service. Empty cyclodextrins were a kind gift of Cyclolab, Hungary. Nitrocellulose membrane filters (HAWP02500) were obtained from Millipore, and the scintillation fluid (Opti-fluor) from PerkinElmer. The anti-DMRP polyclonal antiserum pAB7655 was obtained from ZYMED Laboratories Inc., while the anti-MRP1 and anti-MRP2 monoclonal antibodies m6 and M_2I-4 were a kind gift of R. Scheper. Secondary HRP-conjugated anti-rabbit and anti-mouse antibodies were purchased from Jackson ImmunoResearch. Drosophila melanogaster flies and S2 cells were a kind gift of Beata Vertessy and Peter Friedrich (BRC-HAS, Hungary). All other compounds were obtained from Sigma.

4.2. Phylogenetic analysis, protein alignment and membrane topology prediction

Phylogenetic analyses were based upon alignments of full-length proteins of the ABCC (CFTR/MRP) subfamily. Sequences of the human proteins were downloaded from GenBank. *Anopheles* and *Drosophila* ABC transporters were identified using the Ensemble Genome Browser (http://www.ensembl.org). Protein sequences were aligned using CLUSTALW (1.83) software and

subjected to neighbour-joining tree producing algorithm in MEGA2 with the "exclude positions with gaps" option and 1000 bootstrap trials.

To obtain a suitable predicted membrane topology of DMRP we subjected the sequences of DMRP and hMRP1 to the online membrane topology prediction programme (http://www.enzim.hu/hmmtop/; (Tusnady and Simon, 1998).

4.3. Generation of pAcUW21L-*dMRP* vector construct

The *dMRP* open reading frame encoded within cDNA SD07655 was amplified by PCR using primers that incorporated a Not I restriction site at the 5'- end (5'-AGCGGCCGC ATTGCACGTGGAGGAGGTT-3') and a Sac I restriction site at the 3'- end (5'-AGAGCTC CCGTTTGAGTTTCGTGGAGT-3'). The amplified fragment was cloned into the Not I and Sac I sites of pACUW21L a modified version of baculovirus expression vector pAcUW21 (Invitrogen, San Diego, CA, USA), containing an additional linker sequence with a set of multiple cloning sites for the sake of better sub-cloning possibilities (Szakacs et al., 2001). The cloned segment was sequenced to verify the integrity and accuracy of the open reading frame.

4.4. Expression of proteins in Sf9 cells

To obtain recombinant baculovirus particles for the expression of DMRP in insect cells we used the BaculoGold Transfection kit (Pharmingen), following the manufacturer's protocol. Briefly, we co-transfected $1.5x10^5$ Sf9 cells with 250 ng of the pAcUW21L- *dMRP* vector construct, isolated from *E. coli* BMH strain (NEB), and 60 ng of the linearized BaculoGold DNA. We added 250µl buffer-A (Grace-medium, complemented with 10%FBS) and 250µl buffer-B (25mM Hepes, pH: 7.1; 125mM CaCl2; 140mM NaCl), and incubated the cells for 4 hours at 27˚C. We then removed the transfection buffer and incubated the cells in media for 4 days. We collected the supernatant containing recombinant

virus particles on the 4th day. The virus was than cloned by end-point dilution yielding virus clones providing suitable expression of the transgene. The expression levels gained by the different virus clones in the Sf9 cells were analysed by western blotting. Virus clones providing high expression levels were further amplified to high virus titer (10^8 pfu/ml).

For the expression of hMRP1 and hMRP2 and ß-galactosidase we used recombinant baculovirus particles previously generated in our laboratory (Bakos et al., 2000).

4.5. Membrane preparations

4.5.1. Membrane preparation of Sf9 cells

Spodoptera frugiperda (Sf9) cells were cultured and flasks containing $6*10^7$ cells in about 30 ml medium were infected with 3 ml of recombinant virus supernatant. After 72 hours of virus infection the Sf9 cells were harvested. The membranes were isolated following the protocol described previously (Sarkadi et al., 1992). Briefly, four flasks of $6*10^7$ cells expressing the protein of interest were harvested and washed twice with 15 ml ice-cold washing buffer (50 mM Tris (pH: 7.0), 300 mM mannitol and 50 µg/ml PMSF). Cells were disintegrated in 4 ml TMEP solution (50 mM Tris (pH: 7.0), 50 mM mannitol, 2 mM EGTA, 10 µg/ml leupeptin, 8 µg/ml aprotinin, 50 µg/ml PMSF and 2 mM DTT) and homogenized in a teflon-glass tissue potter for 10 min and subjected to 10 min centrifugation to remove cell and nuclear debris (4˚C, 13,000g). The homogenization-centrifugation step was repeated once again. The supernatant was subjected to ultracentrifugation (60,000g, 4˚C, 60 min, Beckman, LJ-7 ultracentrifuge). The pellet was dissolved and homogenized in ice-cold TMEP solution to gain membrane preparation of 7-12 mg/ml total protein content. Membrane preparations were stored at -70˚C.

4.5.2. Membrane preparation of S2 cells

Cultured wild type S2 cells were scraped and washed from their flasks in media containing 50 μg/ml PMSF and the cell numbers were determined for each flask. The membranes of the same amounts of cells were prepared using the protocol described above for Sf9 cell membrane preparation.

4.6. Cyclodextrin treatment of Sf9 membrane vesicles

50 μl of Sf9 membrane preparations overexpressing DMRP containing 5μg/μl total protein were incubated with 50μl of 10 mM empty cyclodextrins (dissolved in 40 mM MOPS-Tris, pH 7.0, 0.5 mM EGTA-TRIS, 2 mM DTT, 50 mM KCl) for 1 hour on ice. Subsequently membranes were washed twice in 300μl the above solution (40 mM MOPS-Tris, pH 7.0, 0.5 mM EGTA-TRIS, 2 mM DTT, 50 mM KCl) following centrifugation at 4˚C, 20,000g for 30 minutes. Pellet was re-suspended in 50μl TMEP, and the total protein content of the samples was determined with modified Lowry method. Samples were than diluted to the same 3μg/μl protein concentration, and freshly used for ATPase activity measurements. Control samples were treated similarly in the absence of cyclodextrin species.

4.7. Preparation of *Drosophila melanogaster* head, body and intact fly samples

The heads of 100 wild-type *Drosophila melanogaster* were separated from their bodies in CO_2 anesthety. Separated heads and bodies and another 100 intact flies killed by CO_2 administration were grained in glass-teflon tissue homogenisator in DB. Samples were filtered through a macroscopic filter in order to get rid of the corpuscular debris of the samples and sonicated and pottered again to relative homogeneity of the samples. The total protein content of the samples was

determined via modified Lowry method, and samples were sustained at -20˚C for further Laemmli-type SDS-polyacrylamide gel electrophoresis.

4.8. Determination of total protein content

4.8.1. Determination of total protein content of membrane preparations

Total membrane protein concentrations were determined by the modified Lowry method (Bensadoun and Weinstein, 1976). Briefly, 5 µl samples were dissolved in 1 ml Lowry solution (0,01 M NaOH - 2% Na-tartarate - 0,5% $CuSO_4$ in 100:1:1 ratio) than 100 ml Folin-Ciocalteu (Sigma) reagent was added, and the absorption of the samples were read in a Perkin Elmer spectrophotometer at 660nm following a 45 min incubation. The absolute value of the protein content was determined from the optical density (OD) of the samples of interest and the OD of BSA containing calibration samples.

4.8.2. Determination of total protein content of cell lysates and *Drosophila melanogaster* head, body and intact fly samples

5 µl aliquots of cell lysates or filtered fly samples dissolved in DB were diluted in 2 ml distilled water. 20 µl 2 % DOC (deoxycholate) was added to each sample, samples were mixed and incubated at room temperature for 15 minutes. Then, 0.75 ml 25 % trichloro acetic acid (TCA) was added and following a mixing step the samples were centrifuged at 4500 rpm for 40 min at room temperature. The resulting pellet was subjected to the modified Lowry-measurement (see above). The whole procedure was done in parallel with the BSA standard and a DB control.

4.9. Laemmli-type SDS-polyacrylamide gel electrophoresis (SDS-PAGE) and electro-blotting to polyvinylidene difluoride (PVDF) membrane

Gel electrophoresis and immunoblotting were performed as described previously (Sarkadi et al., 1992). Briefly total cell lysates or membrane preparations were suspended and sonicated in disaggregation buffer (DB; 50 mM Tris-PO_4 (pH: 6.8), 2 mM EDTA, 20% glycerin, 0,02% bromophenol blue, 2% β-mercaptoethanol, 2% sodium dodecyl sulfate (SDS)). Total cell lysates or membrane preparations containing 40μg total protein/sample or 5μg total membrane protein/sample, respectively, were than subjected to 7.5% SDS-polyacrylamide gels. Samples were separated by electrophoresis using Mini-Protean electrophoresis equipment (Bio-Rad) using 25mA and 35mA current in upper gel and lower gel, respectively. SDS-PAGE was carried out in ELFO buffer (25 mM Tris-OH pH: 7.7, 0.7 M glycine, 0,1% SDS) for 1,5-2 hours, and the separated proteins were electro-blotted to polyvinylidene difluoride (PVDF, Bio-Rad) membrane using Mini-Trans-Blot (Bio-Rad) equipment in transfer buffer (25 mM Tris pH: 8.3, 25 mM glycine, 20% methanol) at 200 mA current for 1.5 hours.

4.10. Immunoblotting

Following SDS-Page and electro-blotting of the proteins to PVDF membranes, the membranes were blocked in TBS-TWEEN buffer (50 mM Tris pH: 7.4, 200 mM NaCl and 0,1% (v/v) Tween 20) containing 5% (w/v) milk (diluted from nonfat dry milk powder) for 1-1.5 hours. Membranes were then incubated in anti-DMRP polyclonal antiserum pAB7655 (1:500) or anti hMRP1 monoclonal m6 and anti hMRP2 M_2I-4 monoclonal antibody (1:10,000) for 1 hour. Following a repeated washing step with 5% milk, 0.1% TBS-TWEEN, for 15 min, the membranes were incubated in anti-rabbit or anti-mouse horseradish

peroxidase-conjugated secondary antibodies (1:10,000, Jackson ImmunoResearch). To reduce the unspecific background of the detection membranes were washed three times in 5% milk, 0.1% TBS-TWEEN, for 20 minutes. The protein-antibody interaction was visualized by the enhanced chemiluminescence technique (ECL, Amersham Biosciences). The expression levels were determined by densitometry of the immunoblots, using Quantity One software (Bio-Rad).

4.11. Coomassie staining

For the detection of proteins by Coomassie-staining proteins of Sf9 membrane preparations (40µg total protein content/sample) were separated in 7.5% SDS-polyacrylamide gels and stained overnight in Coomassie Brillant Blue (Sigma) dye. The following day gels were incubated in 10% acetic acid 40% methanol, and later in 10% acetic acid. The quantitative measures of expression levels of Coomassie-stained gels were determined by densitometry using the Quantity One software (Bio-Rad).

4.12. Confocal microscopy

Cultured S2 cells were fixed and immunostained with the anti-DMRP polyclonal antiserum pAB7655 as a primer antibody (1:500) and Alexa fluor 488 labelled secondary anti-rabbit antibody (Molecular probes 1:10,000) and analysed using an Olympus FluoView500 Laser Scanning Microscope

4.13. Nucleotide binding and trapping

Nucleotide binding and trapping experiments were performed as described previously (Szabo et al., 1998) Briefly, isolated Sf9 cell membranes containing 150 µg membrane protein were incubated for 5 min at 0 or 37 °C for binding and trapping, respectively in a reaction buffer containing 50mM Tris-HCl (pH 7.0), 50 mM KCl, 0.1mM EGTA-TRIS (pH 7.0), 2mM $MgCl_2$, 1 mM sodium

orthovanadate or 2mM fluoro-aluminate in the presence of 5 μM 8-N_3[^{32}P]ATP either in the presence or in the absence of the indicated drugs. In case of binding experiments samples were irradiated for 5 min on ice with a UV lamp (λ_{max} ≈250 nm). In case of trapping experiments, the reaction on 37˚C was stopped by the addition of 500 μl of ice-cold washing buffer (50mM Tris-HCl, 50 mM KCl, 0.1 mM EGTA-TRIS (pH 7.0), 10 mM $MgCl_2$+10 mM ATP, 1 mM sodium orthovanadate or 2 mM fluoro-aluminate) followed by a 20 min 13.200 g centrifugation at 4 °C at. The washing step was repeated and the pellet was irradiated for 5 min on ice with a UV lamp (λ_{max} ≈250 nm). Thereafter the samples of binding and trapping experiments were suspended in disaggregation buffer and run on 6% Laemmli-type gels. The proteins were electroblotted onto polyvinylidene difluoride membranes and the blots were dried and subjected to autoradiography in a phosphorimager (Bio-Rad). The identity of the ^{32}P-azido nucleotide-labelled bands was confirmed by immunostaining of the same blot.

4.14. Vesicular transport measurements

Vesicular transport measurements with radio-labelled substrates were performed using a rapid filtration method (Bakos et al., 2000; Bakos et al., 1998). Briefly, isolated inside-out Sf9 membrane vesicles containing 100μg total membrane protein were incubated in the presence of 4 mM MgATP or 4 mM MgAMP in 150 μl of transport buffer (6 mM $MgCl_2$, 40 mM MOPS-Tris, pH 7.0, 40 mM KCl, 2mM DTT) at the indicated temperatures (0, 23˚C or 37°C). Incubation was stopped by the administration of 800 μl of ice-cold washing buffer (40 mM MOPS-TRIS, pH 7.0, 70 mM KCl) at the time points indicated and samples were filtered quickly through the 0.45 μm pore size nitrocellulose membrane filters (Millipore). The filters were washed twice with 5 ml of cold washing buffer and the filter-bound radioactivity was measured in scintillation fluid (Opti-fluor, PerkinElmer) with scintillation counter (Wallac 1409 DSA). ATP-dependent transport was calculated by subtracting the activity values obtained with AMP from those in the presence of ATP. For comparison of the uptakes, different

membrane preparations having similar proportion of inside-out vesicles were used. The relative amount of uptake-competent inside-out vesicles was determined from the rate of endogenous ATP-dependent $^{45}Ca^{2+}$ uptake of the membrane preparations using a rapid filtration method described previously (Bakos et al., 1998). Transport values were corrected for non-specific transport observed in the ß-galactosidase-expressing control membranes. The Michaelis-Menten kinetic parameters of transport have been determined either from the x-y intersections of the Lineweaver-Burk plots or from non-linear regressions of the concentration curves using KaleidaGraph (Synergy Software), as indicated. Data points depicted in the figures show the mean values of at least three independent experiments done in at least duplicates. The standard error of the estimate of mean value (S.E.M.) is depicted.

Vesicular transport measurements with fluorescent substrates were performed on uptake-competent inside-out Sf9 vesicles containing 100 µg membrane protein in the presence of 6 mM MgATP or MgAMP in 150 µl of transport buffer (6 mM $MgCl_2$, 40 mM MOPS-Tris, pH 7.0, 40 mM KCl) at 37 °C for the indicated incubation time and drug concentration. Reactions were stopped in ice-cold PBS (137 mM NaCl, 2.7 mM KCl, 8 mM Na_2HPO_4, 2 mM KH_2PO_4). Fluorescent intensity values of the vesicles were subsequently determined in a FACSCalibur flow cytometer (Becton-Dickinson, San Jose, CA, USA), using a 488 nm argon-ion laser excitation and a 525±10 nm bandpass filter. A total of 10,000 vesicles were counted in each experiment, and the FSC-SSC plot was detected as well. All data were collected and evaluated by CellQuest software (Becton-Dickinson, San Jose, CA, USA). Figures either show representative histograms of three independent experiments or the average of the ATP dependent difference of geometric mean values of the histograms. These figures depict experiments representing the average of at least three independent determinations. The corresponding standard error of mean value (S.E.M.) is shown.

4.15. ATPase activity measurements

The vanadate-sensitive ATPase activity was measured by colorimetric detection of inorganic phosphate liberation (Bakos et al., 2000; Sarkadi et al., 1992). In brief, membrane suspensions containing 30 µg of membrane protein were incubated at the indicated temperature for the indicated time in 150 µl of a buffer containing 40 mM MOPS-Tris, pH 7.0, 0.5 mM EGTA-TRIS, 2 mM DTT, 50 mM KCl, 5 mM sodium azide, and 1 mM ouabain. The ATPase reaction was started by the addition of 3.3 mM MgATP. The indicated drugs were added in DMSO, except for LTC_4 that was diluted in the above assay mix. The final concentration of DMSO in the assay buffer was less than 1%. The reactions were stopped by the addition of 0.1 ml of 5% SDS, and the amount of inorganic phosphate was determined based on a colorimetric reaction. 300 µl Pi reagent (2,5 M H_2SO_4, 1 % ammonium-molibdenate, 0,014 % K-Sb-tartarate) and 750 µl 20% (v/v) acidic acid was added to each sample and the colorimetric reaction was started by the administration of 150 µl 1% (g/v) ascorbic acid. The optical density of each sample was read at 700 nm after 20 min incubation. ATPase activity was calculated by the difference obtained in P_i levels between 0-min reaction (stopped immediately with SDS) and reactions after the indicated incubation periods. Since ATPase activity of the ABC transporters is inhibited by vanadate, to determine ABC transporter dependent ATPase activities the differences between the ATPase activities measured in the absence and presence of 1.33 mM vanadate were taken. This vanadate-sensitive ATPase activity was than corrected for non-specific activity observed in the ß-galactosidase-expressing control membranes. Data points in the figures depict the mean values of at least three independent experiments done in at least duplicates. The standard error of the estimate of mean value (S.E.M.) is depicted. As an exception only two independent experiments were done in duplicates for experiments documented in Figure 5.40. and this figure depicted the standard deviation of the estimate of mean values.

4.16. Transition-state thermodynamic analysis of the ATP hydrolysis

4.16.1. Determination of the steady-state thermodynamic parameters of the transition state complex formation

The apparent activation energies of ATP hydrolysis in the presence or the absence of modulator compounds were calculated from ATPase activity measurements performed as a function of temperature. The vanadate-sensitive ATPase activity was measured as described above, either in the absence of any external modulator (basal activity) or in the presence of 600 nM LTC_4 or 5 mM NEM-GS. The initial rate of the ATPase activity was determined in the 17˚C to 37˚C temperature range with 4˚C increments. Incubation times for the reaction at different temperatures were the following: 30, 20, 10, 7, 5, and 3 minutes for 17, 21, 25, 29, 31, and 37˚C, respectively. Data points in the figures depict the mean values of at least three independent experiments done in duplicates. The standard error of the estimate of mean value (S.E.M.) is depicted.

According to the transition-state theory, chemical reactions (in our case ATP hydrolysis) proceed through an unstable high-energy transition-state from the initial to the final state of the reaction. The thermodynamic parameters of this transition-state can be obtained from the linearized Eyring equation: $\ln (k/T) = -\Delta H^{\ddagger}/R*1/T + \ln (k_B/h) + \Delta S^{\ddagger}/R$, where k is the reaction rate, k_B is the Boltzmann constant, h is the Planck's constant, T is the absolute temperature, R is the universal gas constant, $\Delta G^{\ddagger}$ is the Gibbs free energy (activation free energy), $\Delta S^{\ddagger}$ is the activation entropy, and $\Delta H^{\ddagger}$ is the activation enthalpy.

A plot of ln (k/T) versus 1/T is referred to as the Eyring plot (Eyring, 1935). Theoretically it gives a straight line, that can also be described as: y = m*x + b, and the slope (m) of this line can be used to calculate the activation enthalpy, as follows: $\Delta H^{\ddagger} = -m*R$. From the y-intercept (b) of the line the value of $\Delta S^{\ddagger}$ can be calculated: $\Delta S^{\ddagger} = R*(b-\ln (k_B/h))$. The calculated value of $\Delta H^{\ddagger}$ and $\Delta S^{\ddagger}$ allows the determination of the Gibbs free energy as follow: $\Delta G^{\ddagger} = \Delta H^{\ddagger} - T*\Delta S^{\ddagger}$. The

activation energy E_a was calculated applying the following equation: $Ea=\Delta H^{\ddagger}+R*T$.

To estimate the real initial velocity of the ATP hydrolysis we determined the DMRP protein ratio to the total protein content of the membrane preparations via quantification of bands detected on Coomassie stained gels using PhosphoImager (Bio-Rad) and the Quantity One densitometry software (Bio-Rad). We corrected the ATPase activity values to DMRP protein amount. Though the value of the reaction rate must be considered as an apparent value, consisting of the intrinsic reaction rate of DMRP multiplied by a constant scale-factor, the value of which depends on the ratio of the active DMRP proteins to the inactive DMRP proteins present in the Sf9 membrane preparation. Thus, the thermodynamic parameters $\Delta H^{\ddagger}$, $\Delta S^{\ddagger}$ and $\Delta G^{\ddagger}$ determined from the Eyring analysis are also apparent values, referring to the given membrane preparation. Since we collected data from the same membrane preparations the calculated $\Delta H^{\ddagger}$, $\Delta S^{\ddagger}$ and $\Delta G^{\ddagger}$ values remained directly comparable.

The slope and intercept values in the Eyring plot were determined by nonlinear regression (KaleidaGraph v4, Synergy Software), yielding the estimated parameter values and their standard errors as well. The estimated standard error values were then used to calculate the errors of the thermodynamic parameters $\Delta H^{\ddagger}$ and $\Delta S^{\ddagger}$, as well as the related Ea and $\Delta G^{\ddagger}$ values as follows:

∂ (slope) = ∂ ($\Delta H^{\ddagger}$) = ∂ (ΔEa),

∂ (intercept) = ∂ ($\Delta S^{\ddagger}$) = ∂ ($T\Delta S^{\ddagger}$),

where the "∂" symbol refers to the relative error of the given parameter, and

D ($\Delta G^{\ddagger}$) = D ($\Delta H^{\ddagger}$) + D ($T\Delta S^{\ddagger}$),

where the "D" symbol refers to the absolute error value.

For statistical comparison of the $\Delta G^{\ddagger}$ values a one-way analysis of variance (ANOVA) was done with InStat 3 for Macintosh (GraphPad Inc). As the ANOVA assumes that the data are sampled from populations with variances, this

assumption was tested using the method of Bartlett (included in the software package). Generally, a difference would be considered statistically significant if the calculated p value is equal or less than 0.05.

4.16.2. Linear Free Energy Relationship (LFER)

We detected the initial velocity of the vanadate-sensitive ATPase activity of DMRP overexpressing Sf9 vesicles in parallel at two different temperatures, at 25 and 37˚C, in the presence or in the absence of 100, 200, 400 nM of LTC_4 and 100, 200, 400 μM of $E_2$17ßDG. We plotted log turnover numbers of ATPase activities measured at 37˚C as a function of the corresponding data for log turnover numbers at 25˚C. We determined the straight lines for the different concentration sets of LTC_4 and $E_2$17ßDG by nonlinear regression with KaleidaGraph v4 (Synergy Software), yielding the estimated slope and intercept values and their standard errors. These parameters were then compared by Student's t-test, looking for statistically significant differences at 95% probability level.

5. Results

5.1. *In-silico* analysis of DMRP

5.1.1. Phylogenetic analysis of DMRP

To resolve the evolutionary relationship between the human and *Drosophila* ABCC (MRP/CFTR) subfamily proteins we have subjected the entire protein sequences of the *Homo sapiens (Hsa)*, *Drosophila melanogaster (Dme)* and the evolutionary close relative *Anopheles gambiae (Aga)* to a phylogenetic analysis (Figure 5.1.). In the dendrogram DMRP clustered with human MRP1/ABCC1, MRP2/ABCC2, MRP3/ABCC3 and MRP6/ABCC6 proteins, while Dsur clustered with human SUR1/ABCC8 and SUR2/ABCC9. The remaining *Drosophila* genes clustered with a single human gene, *MRP4*/*ABCC4*. This remarkable expansion of the *ABCC4* proteins was also present in *Anopheles gambiae*.

Previously *dMRP* had been classified as an orthologue of human *MRP1 (Grailles et al., 2003)*, our phylogenetic analyses suggested that *dMRP*, in addition to being orthologous to *MRP1*, is also orthologous to *MRP2*, *MRP3* and *MRP6*. While comparison of the entire protein sequences indicated that MRP1 and MRP3 are most closely related to DMRP, comparison of the ATP-binding domains of DMRP to that of human MRPs revealed that the first NBD (N-ABC) is most closely related to that of hMRP2 while the second NBD (C-ABC) is most closely related to that of hMRP1 (data not shown). In spite of this minor difference both phylogenies were in line reflecting the same general relationships, relating DMRP to “long” human MRPs.

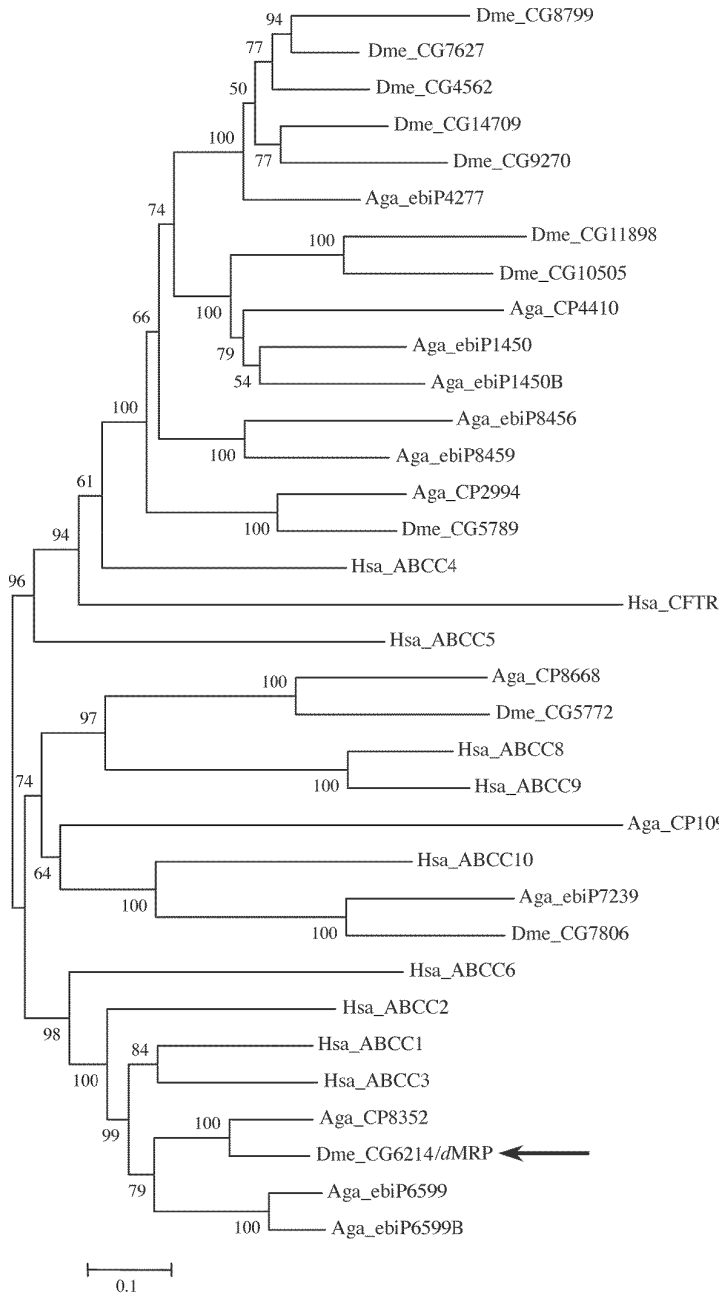

Figure 5. 1.: Phylogenetic analysis of the ABCC (CFTR/MRP) subfamily

Phylogenetic tree based on entire protein sequences of the ABCC subfamily members from human (Hsa), Drosophila melanogaster *(Dme) and* Anopheles gambiae *(Aga). DMRP/CG6214 is indicated by an arrow and is the only* Drosophila *sequence that clusters with human MRP1, MRP2, MRP3 and MRP6. Bootstrap values based on 1000 replications are shown at the nodes. The distance bar shows 10% difference based on Poisson correction distance.*

5.1.2. Predicted membrane topology of DMRP

All long MRPs share the unique feature of an additional N-terminal domain, TMD_0, consisting of five membrane spanning α-helices, (Tusnady et al., 1997) connected to the to the typical "core domain" (consisting of two TMDs and two ABCs) via the cytoplasmic loop called L_0 (Figure 2.3.). This 5+6+6 transmembrane topology has been experimentally confirmed for human MRP1 through site directed mutagenesis (Hipfner et al., 1997; Kast and Gros, 1997), hydrophobicity analysis (Tusnady et al., 1997), and glycosylation and proteolysis experiments (Bakos et al., 1996; Hipfner et al., 1997). In contrast to the 3+4+4 transmembrane topology model previously proposed by Grailles et al. for DMRP, based on our sequence alignments and phylogenetic analysis we propose the 5+6+6 transmembrane arrangement for DMRP (Figure 5.2.). According to this topology model DMRP has an extracellular N-terminus and a TMD0-L0-TMD1-ABC1-L1-TMD2-ABC2 domain arrangement consisting of five transmembrane helices in TMD0, and six transmembrane helices in both TMD1 and TMD2.

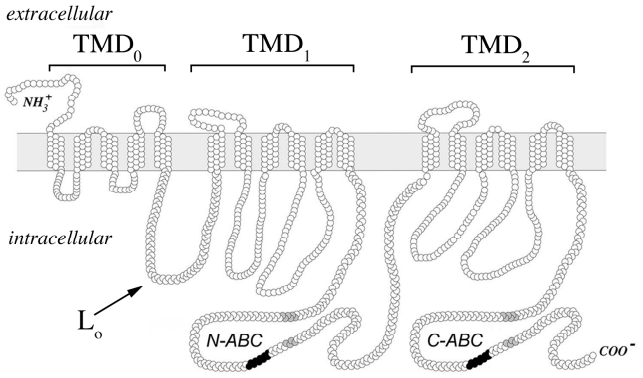

Figure 5. 2.:

Proposed membrane topology of DMRP

The membrane topology model of DMRP shown is based on the model experimentally confirmed for human MRP1. The three proposed transmembrane domains are indicated as TMD_0, TMD_1 and TMD_2. TMD_0 contains five, while TMD_1 and TMD_2 six membrane-spanning alpha helices. L_0, the intracellular linker region between TMD_0 and TMD_1, is identified by an arrow. The polypeptide segment that was used to generate polyclonal rabbit antiserum to DMRP (residues 209-222) resides in L_0. Lightly shaded regions of the polypeptide chain indicate Walker A and Walker B motifs, while darkly shaded areas correspond to the ABC-signature segments.

5.1.3. Sequence alignments

The full protein sequences of *Drosophila* MRP and the related human MRPs were aligned using ClustalW (1.83) program. In pairwise analysis we found that DMRP exhibited 50, 49, 44 and 39% amino acid identity with MRP1, 3, 2 and 6, respectively.

The protein sequence alignment of DMRP and hMRP1 is shown in Figure 5.3. Transmembrane helixes of hMRP1 determined by the online membrane topology prediction programme (http://www.enzim.hu/hmmtop/; (Tusnady and Simon, 1998) are highlighted in yellow. The following conserved regions are indicated in red boxes: Walker A (WA), signature (C) and Walker B motifs. The variable regions of the different *dMRP* isoforms published by Grailles et al. are indicated in highlighted red boxes and are designed as WR1 and WR2. The pan DMRP epitope residing in L_0 is indicated between red arrows.

```
dMRP            MADDTSSPMDRFCGSTFWNATETWYTNDPDFTPCFEQTALVWTPCAFYWAFVIFDFYYLK 60
MRP1            MALRGFCSAD--GSDPLWDWNVTWNTSNPDFTKCFQNTVLVWVPCFYLWACFPFYFLYLS 58
                **    .. * : ...:*: . ** *.:**** **::*.***.** : ** . * * **.

dMRP            ASLDRNIPWNKLNVSKALVNLGLLVITALDLIMALVKKGGDSELPLYDLDVWGPIIKFAT 120
MRP1            RHDRGYIQMTPLNKTKTALGFLLWIVCWADLFYSFWERSRG--IFLAPVFLVSPTLLGIT 116
                      *  . ** :*: :.: * ::   **: :: ::. .  : *  : : .* :   *

dMRP            FLLLFIFIPLNRKYGVQTTGCQFIFWFLLTVLSIPRCRTEVRLDAERQKILNSQQPSEQD 180
MRP1            TLLATFLIQLERRKGVQSSGIMLTFWLVALVCALAILR---------SKIMTALK---ED 164
                 **  ::* *:*: ***::*  : **::  * ::.  *  : :    .**:.: :   :*

                                          epitope
dMRP            FSWEEYQFVSFFIFFTFTSIMLILNCFADGMPRQTKYQRGENEIPELSASFLSRITYQWF 240
MRP1            AQVDLFRDITFYVYFSLLLIQLVLSCFSDRSPLFSETIHDPNPCPESSASFLSRITFWWI 224
                 . : :: ::*:::*::  * *:*.**:*  *  ::  :. *  ** *********: *:

dMRP            DKMALKGYRNPLEEKDLWDLRPQDSCSEVMPIFAHHWNQNVRKN--------YKNKARVE 292
MRP1            TGLIVRGYRQPLEGSDLWSLNKEDTSEQVVPVLVKNWKKECAKTRKQPVKVVYSSKDPAQ 284
                  : ::***:*** .***.*. :*:..:*:*::.::*:::  *.        *..*  .:

dMRP            PKAQFSNGNVTFENPHGEKNGRKKGMASIMPPIYKSFGGVFLFGALMKLFTDTLTFAQPQ 352
MRP1            PKESSKVDANEEVEALIVKSPQKEWNPSLFKVLYKTFGPYFLMSFFFKAIHDLMMFSGPQ 344
                ** . . .     :.   *. :*:  .*::  :**:**  **:. ::* : * : *: **

dMRP            VLSLIISFVEAQDAEPEWKGILYAVLLFVLAAAQTFILGQYFHRMFIVGLRIRTALINAI 412
MRP1            ILKLLIKFVN-DTKAPDWQGYFYTVLLFVTACLQTLVLHQYFHICFVSGMRIKTAVIGAV 403
                :*.*:*.**: :   *:*:* :*:***** *. **::* ****  *: *:**:**:*.*:

dMRP            YRKALRISNSTKKESTVGEIVNLMAVDAQRFMELTTYLNMIWSAPLQIGLALYFLWQQLG 472
MRP1            YRKALVITNSARKSSTVGEIVNLMSVDAQRFMDLATYINMIWSAPLQVILALYLLWLNLG 463
                ***** *:**::*.**********:*******:*:**:*********: ****:** :**
```

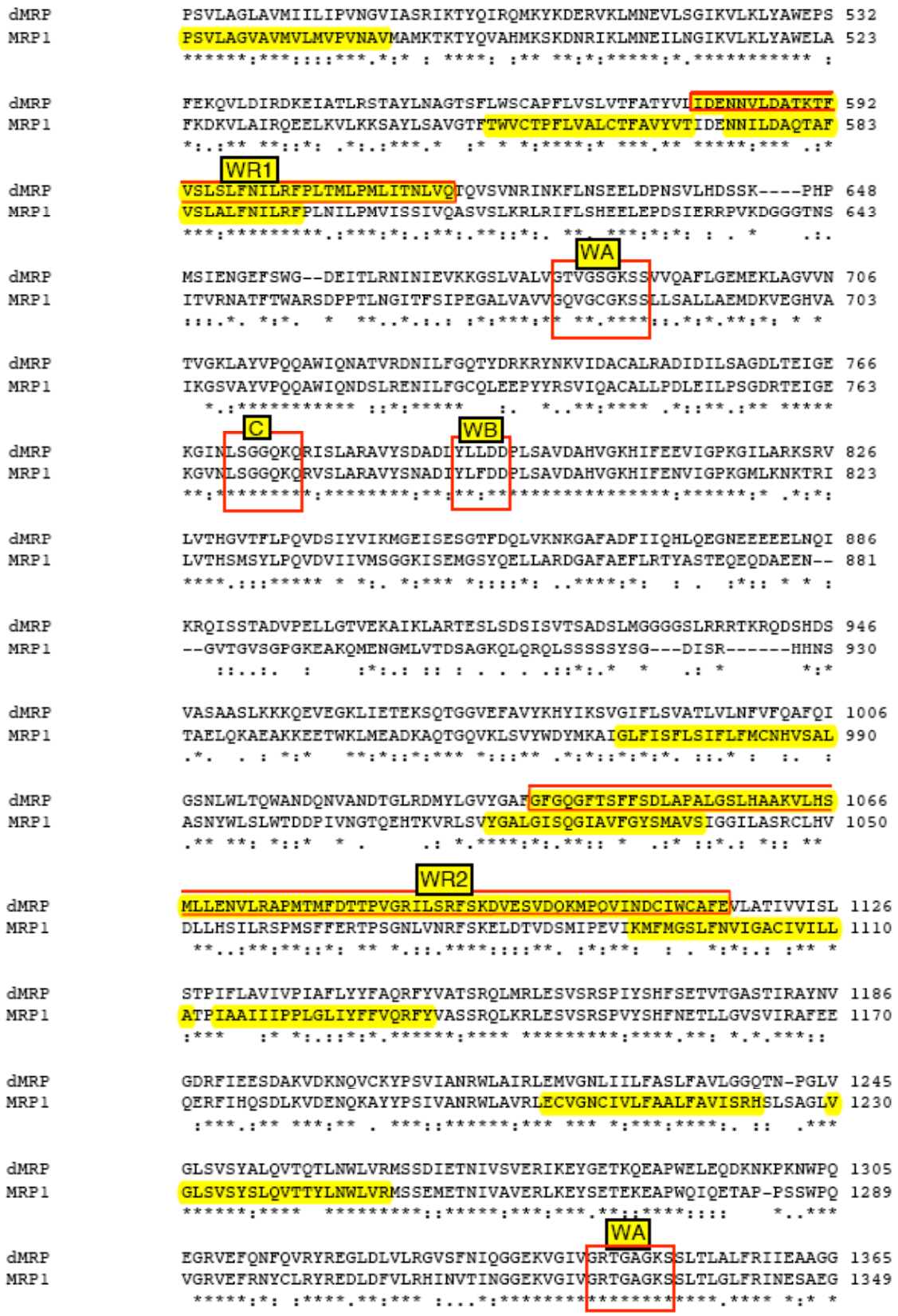
dMRP PSVLAGLAVMIILIPVNGVIASRIKTYQIRQMKYKDERVKLMNEVLSGIKVLKLYAWEPS 532
MRP1 PSVLAGVAVMVLMVPVNAVMAMKTKTYQVAHMKSKDNRIKLMNEILNGIKVLKLYAWELA 523
dMRP FEKQVLDIRDKEIATLRSTAYLNAGTSFLWSCAPFLVSLVTFATYVLIDENNVLDATKTF 592
MRP1 FKDKVLAIRQEELKVLKKSAYLSAVGTFTWVCTPFLVALCTFAVYVTIDENNILDAQTAF 583
WR1
dMRP VSLSLFNILRFPLTMLPMLITNLVQTQVSVNRINKFLNSEELDPNSVLHDSSK----PHP 648
MRP1 VSLALFNILRFPLNILPMVISSIVQASVSLKRLRIFLSHEELEPDSIERRPVKDGGGTNS 643
WA
dMRP MSIENGEFSWG--DEITLRNINIEVKKGSLVALVGTVGSGKSSVVQAFLGEMEKLAGVVN 706
MRP1 ITVRNATFTWARSDPPTLNGITFSIPEGALVAVVGQVGCGKSSLLSALLAEMDKVEGHVA 703
C
WB
dMRP KGINLSGGQKQRISLARAVYSDADIYLLDDPLSAVDAHVGKHIFEEVIGPKGILARKSRV 826
MRP1 KGVNLSGGQKQRVSLARAVYSNADIYLFDDPLSAVDAHVGKHIFENVIGPKGMLKNKTRI 823
dMRP LVTHGVTFLPQVDSIYVIKMGEISESGTFDQLVKNKGAFADFIIQHLQEGNEEEEELNQI 886
MRP1 LVTHSMSYLPQVDVIIVMSGGKISEMGSYQELLARDGAFAEFLRTYASTEQEQDAEEN-- 881
dMRP KRQISSTADVPELLGTVEKAIKLARTESLSDSISVTSADSLMGGGGSLRRRTKRQDSHDS 946
MRP1 --GVTGVSGPGKEAKQMENGMLVTDSAGKQLQRQLSSSSSYSG---DISR------HHNS 930
dMRP VASAASLKKKQEVEGKLIETEKSQTGGVEFAVYKHYIKSVGIFLSVATLVLNFVFQAFQI 1006
MRP1 TAELQKAEAKKEETWKLMEADKAQTGQVKLSVYWDYMKAIGLFISFLSIFLFMCNHVSAL 990
dMRP GSNLWLTQWANDQNVANDTGLRDMYLGVYGAFGFGQGFTSFFSDLAPALGSLHAAKVLHS 1066
MRP1 ASNYWLSLWTDDPIVNGTQEHTKVRLSVYGALGISQGIAVFGYSMAVSIGGILASRCLHV 1050
WR2
dMRP MLLENVLRAPMTMFDTTPVGRILSRFSKDVESVDQKMPQVINDCIWCAFEVLATIVVISL 1126
MRP1 DLLHSILRSPMSFFERTPSGNLVNRFSKELDTVDSMIPEVIKMFMGSLFNVIGACIVILL 1110
dMRP STPIFLAVIVPIAFLYYFAQRFYVATSRQLMRLESVSRSPIYSHFSETVTGASTIRAYNV 1186
MRP1 ATPIAAIIIPPLGLIYFFVQRFYVASSRQLKRLESVSRSPVYSHFNETLLGVSVIRAFEE 1170
dMRP GDRFIEESDAKVDKNQVCKYPSVIANRWLAIRLEMVGNLIILFASLFAVLGGQTN-PGLV 1245
MRP1 QERFIHQSDLKVDENQKAYYPSIVANRWLAVRLECVGNCIVLFAALFAVISRHSLSAGLV 1230
WA
dMRP EGRVEFQNFQVRYREGLDLVLRGVSFNIQGGEKVGIVGRTGAGKSSLTLALFRIIEAAGG 1365
MRP1 VGRVEFRNYCLRYREDLDFVLRHINVTINGGEKVGIVGRTGAGKSSLTLGLFRINESAEG 1349

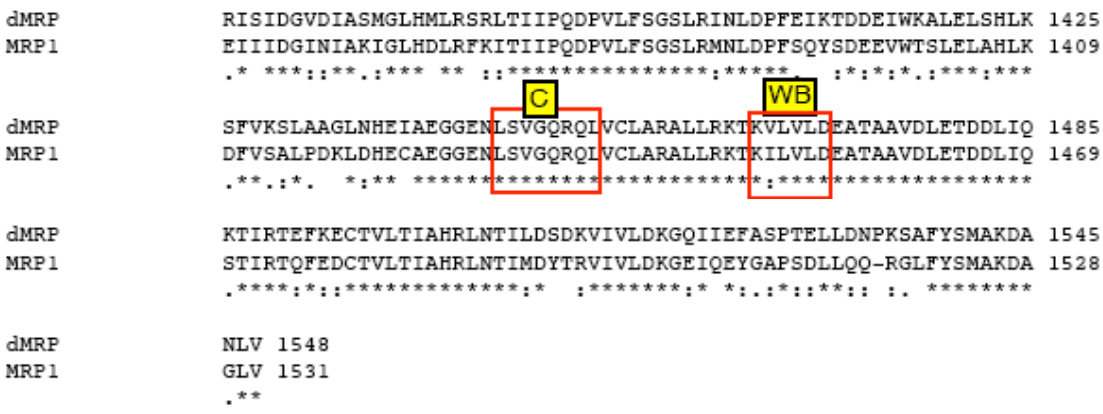

Figure 5.3. Protein sequence alignment of DMRP and hMRP1

Sequences were aligned using the online programme ClustalW. Transmembrane helixes of hMRP1 were determined by the online membrane topology prediction programme (http://www.enzim.hu/hmmtop/); (Tusnady and Simon, 1998) and are highlighted in yellow. Conserved sequence motifs are indicated in red boxes: Walker A (WA), signature (C) and Walker B motifs. The variable regions of the dMRP *isoforms published by Grailles et al. are indicated in highlighted red boxes and are designed as WR1 and WR2. The pan DMRP epitope residing in L_0 is indicated between red arrows.*

5.2. Generation of Polyclonal Antibody pAb7655

The polyclonal rabbit antibody against DMRP peptide residues 209-222 (Asp-Gly-Met-Pro-Arg-Gln-Thr-Lys-Tyr-Gln-Arg-Gly-Glu-Asn) was generated by ZYMED Laboratories Inc. (South San Francisco, Ca, USA). (The peptide corresponding to this epitope is referred to as anti-peptide in the following). This peptide was conjugated to the carrier protein keyhole limpet hemocyanin. Antibody titers were checked by ELISA assays using an IgG conjugated peptide. We confirmed the specificity of the pAb7655 antibody using Sf9 cells overexpressing DMRP, hMRP1, hMRP2, hMRP3, hMRP6 and ß-galactosidase in Western blot experiments not documented here.

5.3. Expression of DMRP in Sf9 cells

In order to elucidate the characteristics of DMRP we expressed the protein in the Sf9 baculovirus heterologous expression system. Due to its numerous advantages, this expression system is used widespread for functional characterisation of ABC proteins. Beyond that we have chosen the Sf9 expression system for our comprehensive study, since there was already an array of ABC transporters expressed in our laboratory, e.g. human MRP1 and MRP2, and the bacterial protein ß-galactosidase, commonly used as a control protein. For our investigations we used these previously generated baculovirus particles for the expression of hMRP1, MRP2 and ß-galactosidase in Sf9 cells (Bakos et al., 2000). In order to generate a baculovirus expression vector suitable for the expression of DMRP, the only available *dMRP* EST cDNA clone SD07655 (ResGen, Invitrogen Corporation) encoding the *dMRP* 4b 8d isoform was amplified by PCR using primers incorporating a Not I restriction site at the 5'-end and a Sac I restriction site at the 3'- end of the cDNA. The amplified 4.6 kb fragment was cloned into the Not I and Sac I sites of the modified baculovirus expression vector pAcUW21L (Invitrogen, San Diego, CA, USA) The cloned segment was sequenced to verify the integrity and accuracy of the open reading frame. Cultured Sf9 cells were than co-transfected with the above *dMRP*-pAcUW21L construct and the linearized BaculoGold DNA yielding virus particles, which were further cloned by end-point dilution to obtain suitable expression of the transgene. The expression levels gained by the different virus clones in the Sf9 cells were analysed by Western blotting. Virus clones providing high expression levels of the DMRP protein with the calculated mass of 173kDa were further amplified to high virus titer (10^8 pfu/ml). Sf9 cells were transfected with the high-titer virus and the transfected cells expressed a ~170 kDa protein that was detected by the anti-DMRP polyclonal antibody pAb7655 (Figure 5.4. panel A).

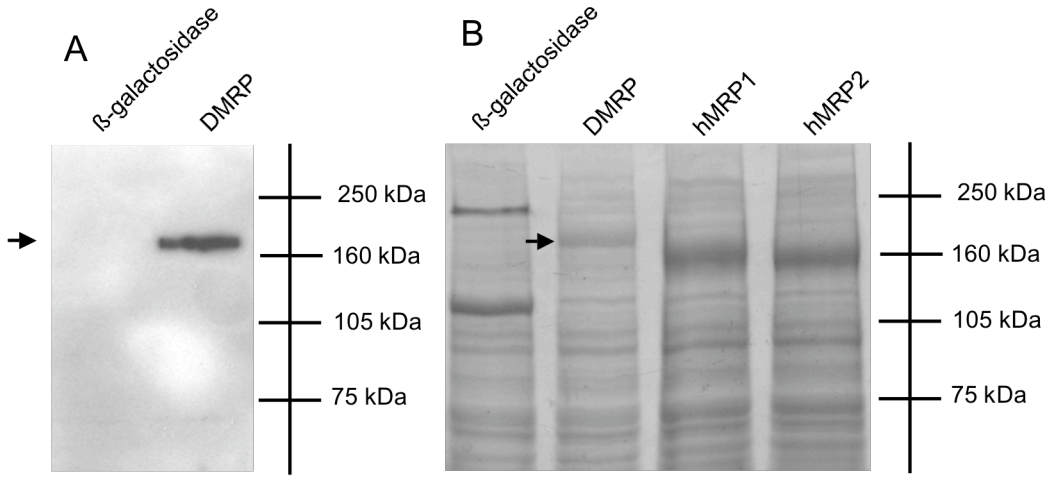

Figure 5.4. Expression of DMRP in Sf9 cells

Immunoblot of Sf9 membrane preparations overexpressing ß-galactosidase and DMRP. *Sf9 membrane preparations of 5µg total membrane protein content were separated by 7.5% SDS-PAGE, and incubated in the presence of anti-DMRP polyclonal antibody pAb76559 (1:500, ZYMED Laboratories Inc.) and anti-rabbit horseradish peroxidase-conjugated secondary antibodies (1:10,000, Jackson ImmunoResearch)* ***(Panel A)****.* ***Coomassie staining of Sf9 membrane preparations overexpressing ß-galactosidase, DMRP, hMRP1 and hMRP2.*** *Sf9 membrane preparations of 40µg total membrane protein content were separated by 7.5% SDS-PAGE, proteins were stained with Coomassie Brillant Blue* ***(Panel B)****.*

Anti-DMRP polyclonal antibody labelling was specific to DMRP, since the antibody did not show cross-reactivity either with any of the investigated hMRPs or with ß-galactosidase expressing membrane preparations, and this labelling was eliminated in the presence of 10μM anti-peptide, the peptide that is analogous to a part of the DMRP sequence from amino acid 209th to amino acid 222nd that was used as an epitope to generate the polyclonal antibody pAb7655 (Data not shown). Expression of DMRP was detectable on Coomassie stained gels as well, while this ~170kDa band was not present in either ß-gal or other MRP expressing membranes (Figure 5.4. panel B). The level of DMRP expression was comparable to the expression level of the human orthologues MRP1, and MRP2.

5.4. Detection of endogenous DMRP

5.4.1. Detection of DMRP in S2 cells and fruit fly

We investigated the presence of endogenous DMRP in *Drosophila* S2 cells. DMRP was not detectable on total cell lysates (Figure 5.5. panel A), while there was a faint but clear band in case of the S2 membrane preparations (S2 m.f.) at the expected molecular mass (indicated by an arrow) compared to DMRP overexpressing Sf9 membrane preparation (Sf9 m.p.). The cytosolic fraction of S2 membrane preparations (S2 c.f.) did not show labelling with the anti-DMRP polyclonal antibody pAb7655.

A B

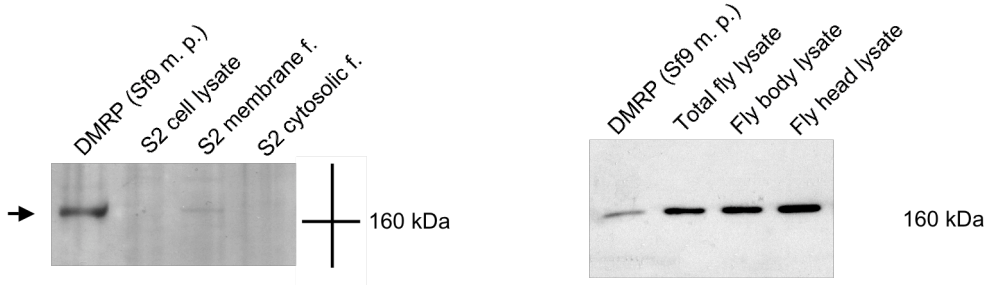

Figure 5.5. Immunoblot detection of endogenous DMRP in S2 cells and flies

Immunoblot of native S2 cells. *S2 cell preparations were labelled with the anti-DMRP polyclonal antibody pAb7655 (1:500, ZYMED Laboratories Inc.) and anti-rabbit horseradish peroxidase-conjugated secondary antibody (1:10,000, Jackson ImmunoResearch) after separation of the samples by 7.5% SDS-PAGE. Abbreviations: S2 total cell lysate of 80µg total protein content (S2 cell lysate.); membrane fraction of S2 cell membrane preparations of 30µg total protein content (S2 membrane f.); cytosolic fraction of S2 cell membrane preparations of 30µg total protein content (S2 cytosolic f.); and membrane preparation of DMRP overexpressing Sf9 cells of 5µg total protein content (DMRP Sf9 m.p.). The molecular mass of DMRP is indicated by an arrow. The negative control Sf9 membrane preparation overexpressing ß-galactosidase is not depicted on the figure* ***(panel A)****.*

Immunoblot of fruit fly samples. *Immunoblot of samples prepared from intact flies, separated heads and bodies (60µgof total protein / sample) and membrane preparation of DMRP overexpressing Sf9 cells as a positive control (4 µg of total protein / sample). Immunoblot labelled with anti-DMRP polyclonal antibody pAb7655 (1:500, ZYMED Laboratories Inc.) and anti-rabbit horseradish peroxidase-conjugated secondary antibody (1:10,000, Jackson ImmunoResearch) after separation of the samples by 7.5% SDS-PAGE. The negative control Sf9 membrane preparation overexpressing ß-galactosidase is not depicted on the figure* ***(panel B).***

Labelling of the membrane fraction of S2 membrane preparations was eliminated in the presence of 10µM anti-peptide (data not shown). Membrane preparation samples prepared from S2 cells incubated in the presence of 1nM -1µM of the insect moulting hormone 20-OH ecdysone for 0.5-3 days did not show alteration of the endogenous DMRP content (data not shown).

To study the localization of endogenous DMRP on fixed S2 cells we used confocal microscopy. After labelling with pAb7655 as a primary and Alexa488-labelled anti-rabbit as a secondary antibody we obtained diffused labelling of the cytoplasm of the S2 cells (data not shown). Labelling was pAb7655 dependent, since in the presence of the secondary antibody but in the absence of the primary antibody, pAb7655, we did not obtain significant labelling of the S2 cells. However, the presence of 10µM anti-peptide did not eliminate this labelling in our control experiments, suggesting that antigen-pAb7655 antibody interaction in case of confocal experiments was presumably not specific to DMRP. In conclusion, pAb7655 polyclonal antibody seems not to be suitable for localisation studies.

5.4.2. Detection of endogenous DMRP in wt fruit fly

The heads of 100 wild-type *Drosophila melanogaster* flies were separated from the body in CO_2 anaesthesia. Separated heads, remaining bodies and 100 intact flies were homogenised, filtered and sonicated in DB and subjected to gel

electrophoresis. Endogenous DMRP was detected via immunoblotting (Figure 5.5. panel B, section5.4.1.).

5.5. Functional studies

5.5.1. Nucleotide binding and trapping

In order to investigate the ATPase cycle of dMRP, we first studied the ability of DMRP to bind the commonly used nucleotide analogue Mg-8-N_3-[α-^{32}P]ATP (azido-ATP).

We incubated DMRP and MRP1 containing Sf9 membrane preparations at 0˚C in the presence of 5 μM Mg-8-N_3-[α-^{32}P]ATP for 5 min and irradiated samples with UV light. Both DMRP and the positive control hMRP1 was photo-chemically labelled by Mg-8-N_3-[α-^{32}P]ATP demonstrating that both proteins are able to bind ATP (Figure 5.6 Panel A). This labelling was specific, since the presence of access 1mM of Mg^{2+} eliminated the signal. At physiological temperatures ABC transporters are capable of hydrolysing azido-ATP due to their inherent catalytic activity. In the presence of so called “trapping anions”, such as orthovanadate (V_i) or fluoroaluminate (AlF_4), labelled azido-ADP generated by ATP hydrolysis can be trapped in the catalytic centre of the protein, mimicking the post-hydrolytic transition state formation of the catalytic cycle (Urbatsch et al., 1995).

Among ABC transporters, substrate transport and ATP hydrolysis are tightly coupled. Therefore administration of substrates might influence the trapping of azido-ATP in such experiments mostly by stimulating this activity. This approach is only suitable for the detection of interactions where substrates stimulate the ATP hydrolysis at high extent, for example in the case of MDR1.

To characterise the formation of the post-hydrolytic transition state intermediate of DMRP we investigated the ability of dMRP and MRP1 of trapping azido-ATP in Sf9 membrane preparations.

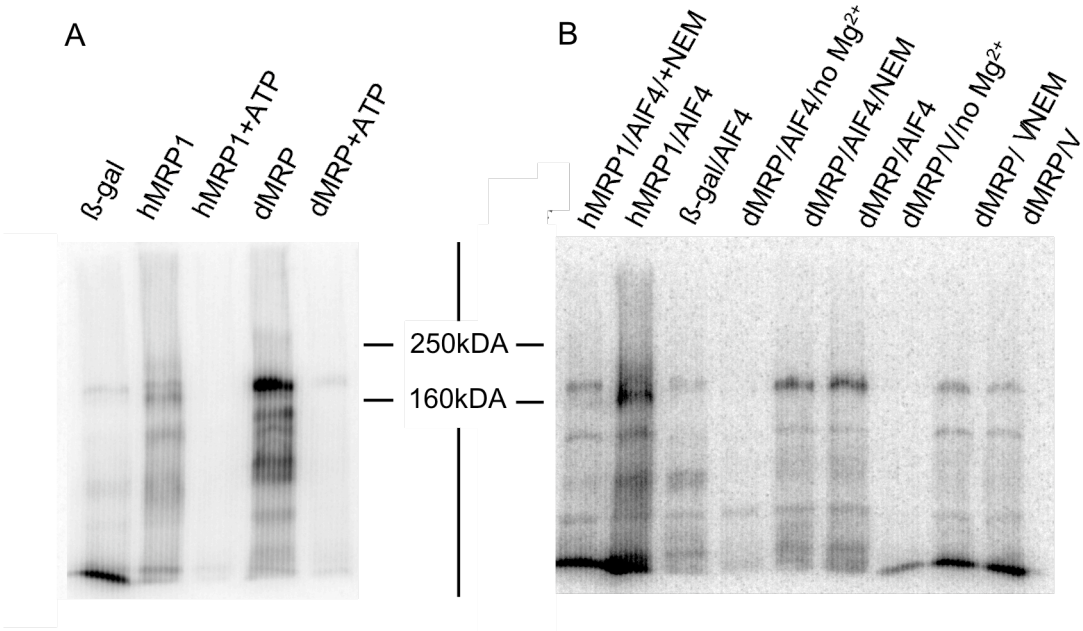

Figure 5.6.: Nucleotide binding and trapping of DMRP and hMRP1

Azido-ATP binding. *Autoradiogram showing azido-ATP (8-N_3-[α-^{32}P]ATP) binding of DMRP and hMRP1. Samples were incubated for 5 minutes in the presence of 5µM 8-N_3-[α-^{32}P]ATP in the presence or in the absence of 1mM ATP at 0˚C followed by 5 min UV illumination. Samples were separated by SDS PAGE (6% acrylamide) and were blotted to PVDF membranes. The identity of the corresponding bands was confirmed by immunoblot. Excess 1mM cold ATP eliminated the signal reflecting specificity.* ***(A)****.* ***Azido-ATP trapping in the presence of trapping anions****. Autoradiogram showing nucleotide trapping of DMRP and hMRP1 in the presence of orthovanadate (V) and fluoroaluminate (AlF_4) and cross-reacting agent NEM. Isolated membrane vesicles were incubated for 5 minutes at 37˚C with 5µM 8-N_3-[α-^{32}P]ATP in the presence of 2mM AlF_4 or 1mM orthovanadate. Thereafter samples were washed and then illuminated with UV light for 5 minutes. Membrane proteins were separated by SDS PAGE (6% acrylamide) and blotted to PVDF membranes. The identity of the corresponding bands was confirmed by immunoblot. The presence of 4mM EDTA (no Mg^{2+}) eliminated the labelling showing the specificity of the signal. The presence of NEM did not influence trapping properties of DMRP, in contrast to that of hMRP1.* ***(B)****.*

Samples were incubated in the presence of 5 µM Mg-8-N_3-[α-^{32}P]ATP and the trapping anions either orthovanadate or AlF_4 at 37˚C for 5 min. Incubation

followed by extensive washing with 10 mM Mg^{2+}ATP and then samples were irradiated with UV light. Under these conditions DMRP and the positive control hMRP1 was photo-chemically labelled by Mg-8-N_3-[α-^{32}P]ATP demonstrating that - similarly to other ABC transporters - the formation of the trapped nucleotide transition complex could be detected (Fig 5.6. Panel B). The labelling was specific, since the absence of Mg ions eliminated the signal. In trapping experiments we tested the effect of several established human MRP substrates, such as the inflammatory mediator leukotriene C_4 (LTC_4), the major metabolite of the estrogen metabolism ß-estradiol 17-ß-D-glucuronide ($E_2$17ßDG), the intracellular calcium indicator free-calcein and the artificial glutathione conjugate of N-ethylmaleimide (NEM-GS). The ability of the insect moulting hormone 20-OH ecdysone to modulate ATPase activity of DMRP was also tested in trapping experiments. We found that these compounds did not alter the DMRP specific Mg-8-N_3-[α-^{32}P]ATP labelling significantly (data not shown).

5.5.2. Transport properties of DMRP

In order to investigate the transport characteristics of DMRP we studied the ATP-dependent uptake of radiolabelled or fluorescent human MRP substrates in inside-out Sf9 membrane vesicles expressing DMRP and its human orthologues. We tested the following established human MRP substrates in comparative transport assays: the major metabolite of the estrogen metabolism ß-estradiol 17-ß-D-glucuronide ($E_2$17ßDG), the inflammatory mediator leukotriene C_4 (LTC_4), the secondary messenger cyclic AMP, the intracellular calcium indicator free calcein and the fluorescent dies Fluo3, and carboxydichlorofluorescein (CDCF). The isotope labelled [^{3}H]ß-estradiol 17-ß-D-glucuronide, [^{3}H]leukotriene C_4 and [^{3}H]cyclic AMP transport of the isolated Sf9 membrane vesicles was detected in a ß-counter, while the transport of the fluorescent compounds, calcein, Fluo4-AM, Fluo3, and carboxydichlorofluorescein, were detected by flow cytometry (FACS) using a FACSCalibur flow cytometer (Becton-Dickinson, San Jose, CA, USA). Measuring transport activities within the linear range of the incubation

times, we determined the transport kinetic parameters of the different substrates. Due to the lack of calibration, the apparent V_{max} values in FACS measurements were only arbitrary units, suitable for reflecting the turnover differences of the investigated transporters measured in the same experiment. To obtain transport activity values specific to the transporters of interest, the ATP-dependent transport activity values were corrected with the uptake measured in ß-galactosidase expressing control Sf9 membrane vesicles. The transport activity of the above substrates was determined in the presence of various established MRP inhibitors, such as the commonly used MRP specific inhibitor, the LTD_4 analogue MK571, and the organic anions, probenecide (PB), benzbromarone (BB), and indomethacin (IM).

5.5.2.1. ß-estradiol 17-ß-D-glucuronide (E217ßDG) transport

We measured the DMRP dependent transport activity at 37˚C as a function of incubation time in the presence of 1 µM $E_2$17ßDG. As it is shown on Figure 5.7 panel A., DMRP-dependent $E_2$17ßDG transport showed saturation kinetics and provided a good approximation of the initial transport rate at 30 seconds. Therefore, these conditions were used to study the concentration dependent uptake of $E_2$17ßDG (Figure 5.7 panel B). Tracer uptake showed significant DMRP dependent transport activity as a function of $E_2$17ßDG, and was mostly saturated in the applied concentration range. To determine transport kinetic parameters, transport activity values were depicted on a double reciprocal Lineweaver-Burk plot (Figure 5.8). The apparent K_m value was found to be 344 ± 182 µM and the maximum rate of transport was 50 ± 25 nmol/mg of membrane protein/min. Due to aspecific effect of the compound on the transport assay, the concentration dependence at higher concentrations could not be measured. Therefore these kinetic parameters have to be considered as best estimates. The expression level of DMRP in vesicles used for determination of $E_2$17ßDG transport kinetic parameters was approximately one-fourth of the expression of MRP2, while in experiments not demonstrated here we detected approximately 11 nmol/mg of membrane protein/min turnover rate for hMRP2.

We investigated the effect of known human MRP inhibitors on the $E_2$17ßDG transport. 2mM probenecid (PB), 50µM benzbromarone (BB), 300µM indomethacin (IM), and 30µM MK571 inhibited $E_2$17ßDG transport of DMRP effectively (Figure 5.9.).

A B

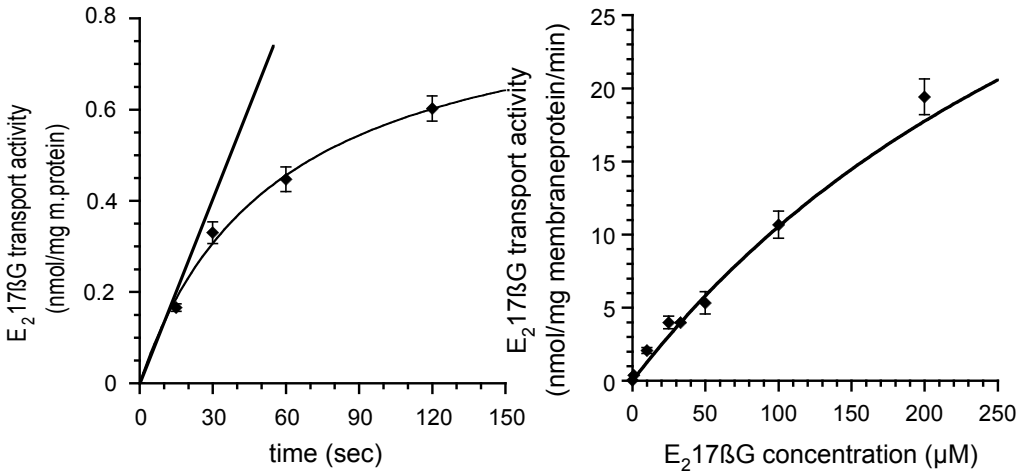

Figure 5.7.: Time-course and concentration dependence of $E_2$17ßDG uptake of DMRP

ATP dependent DMRP specific tracer uptake of isolated SF9 inside-out vesicles as a function of time at 37˚C, 1 µM of $E_2$17ßDG concentration ***(panel A)****. ATP dependent DMRP specific $E_2$17ßDG uptake of isolated SF9 inside-out vesicles as a function of $E_2$17ßDG concentration at 37˚C for 0.5 min* ***(panel B)****.*

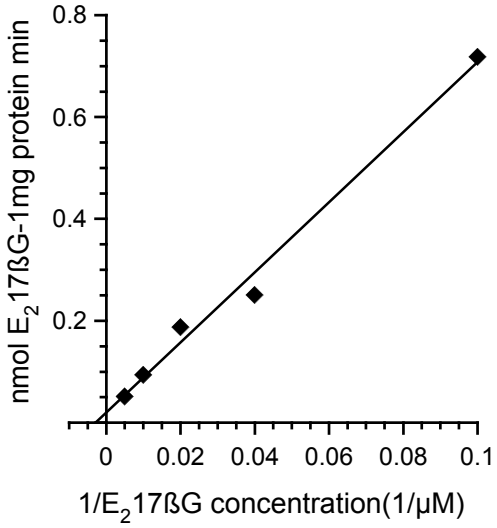

Figure 5.8.: Lineweaver-Burk representation of the DMRP mediated $E_2$17ßDG transport

Double reciprocal representation of data depicted on Figure 5.7 panel B.

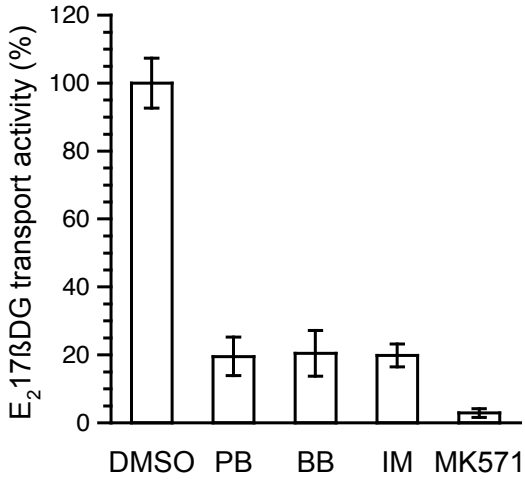

Figure 5.9.: Inhibition of E217ßDG uptake of DMRP

Inhibition of the $E_2$17ßDG transport measured for 0.5 min at 37˚C and 10 µM of $E_2$17ßDG concentration in the absence or presence 2 mM probenecid (PB), 50 µM benzbromarone (BB), 300 µM indomethacin (IM) and 30 µM MK571.

5.5.2.2. Leukotriene C_4 (LTC_4) transport

In case of LTC_4 due to the extremely high turnover rate of DMRP to the substrate the kinetic parameters could not be measured under the conditions formerly used in literature for the human MRPs. When we used the canonical 100µg protein, 23˚C circumstances to study time-course of LTC_4 we found substrate transport to be saturated even at 15 sec, at the time-scale limit of such measurements. To be able to determine the initial velocity for this substrate we applied two different alternative approaches. First, as enzyme activity is dependent on temperature, we reduced the incubation temperature and in parallel the expression level of DMRP in inside out vesicles. The expression level of DMRP was reduced to approximately 1/4 with co-expression of DMRP and ß-galactosidase at a virus-ratio of 1 to 9 (see Western blot at Figure 5.10.). The LTC_4 transport activity of decreased expression vesicles was monitored at various decreased temperatures, such as at 16, at 12 and at 6 ˚C and on ice, as a function of incubation time. The time-course of LTC_4 uptake only showed saturation kinetics at 0˚C (Figure 5.10.), showing approximate linearity up to 30 seconds. Therefore the kinetic parameters for LTC_4 transport were determined using reduced expression vesicles with 30 seconds incubation at 0˚C. As documented in Figure.5.11., the uptake was a saturable function of the LTC_4 concentration with a calculated maximum uptake rate of 52 ± 3 pmol/mg of membrane protein/min and an apparent K_m value of 58 ± 11nM.

The DMRP specific ATP dependent LTC_4 labelling at 0˚C was dramatically reduced after shrinking the vesicles by the addition of 2 M sucrose to the medium (Figure 5.12.), while the same osmotic shock totally eliminated hMRP1 dependent labelling at 37˚C. This experiment suggest that LTC_4 labelling of the vesicles overexpressing DMRP at 0˚C is dominantly due to active transport and the determined parameters refer to the real vesicular transport activity even at such a low temperature.

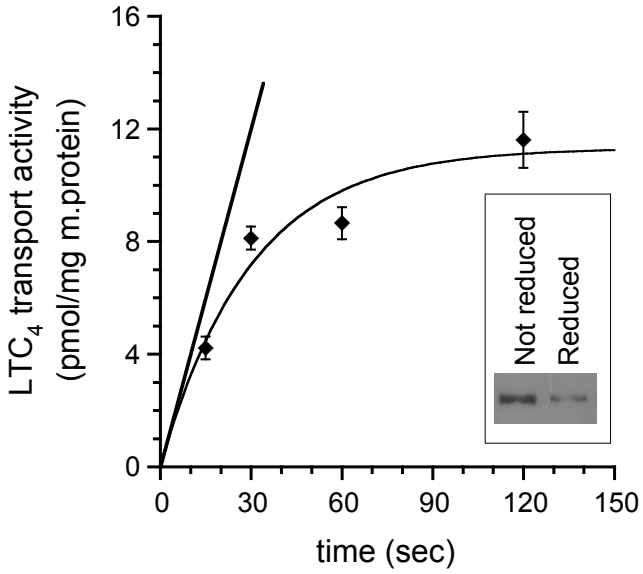

Figure 5.10.: Time-course of DMRP mediated LTC_4 uptake of reduced expression vesicles at 0˚C *LTC_4 uptake of reduced expression vesicles prepared from Sf9 cells co-transfected with DMRP and ß-galactosidase at a ratio of 1:9 (referred to as reduced expression vesicles) at 10 nM LTC_4 concentration at 0˚C. Inset shows immunoblot of DMRP in Sf9 vesicles expressing DMRP alone (Not reduced) or DMRP expressed along with ß-galactosidase (Reduced).*

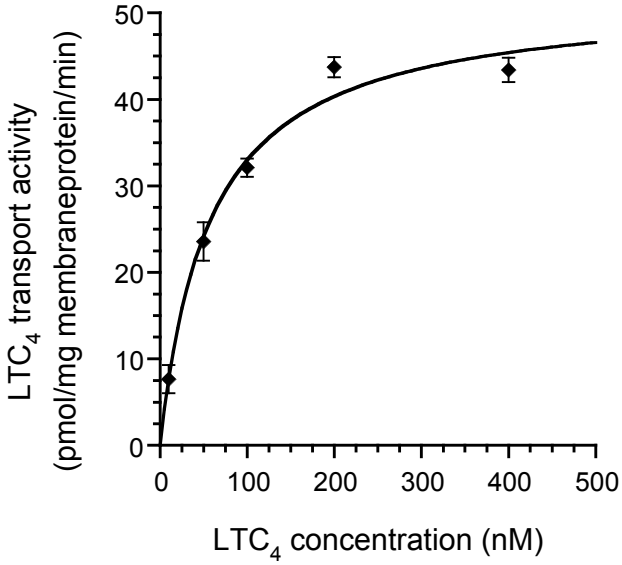

Figure 5.11.: Concentration dependence of DMRP mediated LTC_4 uptake of reduced expression vesicles at 0˚C *LTC_4 transport of reduced expression vesicles were measured as a function of LTC_4 concentration at 0˚C for 0.5 min.*

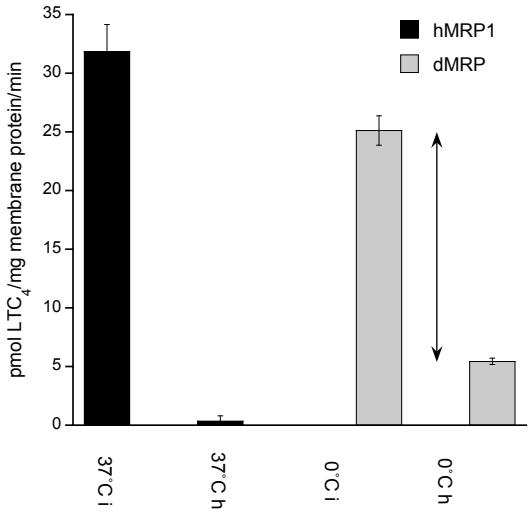

Figure 5.11.: Osmotic sensitivity of DMRP and hMRP1 mediated LTC_4 labelling

Labelling of hMRP1 vesicles or reduced expression DMRP vesicles measured in the presence of 50 nM LTC_4 at iso-osmotic conditions (i) or at hyper-osmotic conditions (+2M sucrose) (h). Measurements were performed for 0.5 min at 37 or 0˚C, as indicated. Arrow indicates osmotic shock sensitive labelling of reduced DMRP dependent vesicles.

As DMRP had an unusually high turnover rate for LTC_4, a comparison of the initial transport rates of DMRP and MRP1 were estimated as follows. The initial transport rate for DMRP was found to be about 52 pmol/mg of membrane protein/min measured at 0˚C with vesicles whose DMRP expression level was reduced to 1/4, while it was 50 pmol/mg of membrane protein/min at 23˚C for MRP1 determined in our laboratory previously (Bakos et al., 1998). Comparing the amount of the expressed proteins by quantification of Coomassie stained gels revealed that the amount of DMRP protein present in the original Sf9 membrane preparation was about 1/4 of the amount of MRP1, thus the 4-times reduced expression DMRP vesicles contained about 16-fold less transporter molecules than those containing MRP1. It was therefore necessary to take into account this factor of 16 to estimate the initial rate of DMRP. Another factor to consider was the effect of temperature. The factor of temperature could be estimated from ATPase activity values as a function of temperature depicted in Figure 5.36.,

which showed that the basal ATPase activity rose approximately 2.7 times for every 10˚C elevation of the temperature. Applying this temperature dependence for transport activity to compensate for the 23˚C temperature difference we used a correction factor of 6.2. Together with the 16-fold expression factor this makes an approximately 100-fold overall correction factor for DMRP activity. Thus, for not reduced expression DMRP vesicles at 23˚C one should theoretically detect approximately a 5.2 nmol/mg of membrane protein/min initial rate, that is about two orders of magnitude higher transport capacity compared to the human orthologues expressed and measured in the same system before by Bakos et al. Taking into consideration that it is only a roughly estimated value, and that ABC transporters are considered to be mostly unable to hydrolyze ATP at 0˚C we decided to apply a different approach, too.

To compare transport activities of DMRP and its human orthologues, we measured transport activity of DMRP and hMRP1 at the same temperature at 23˚C. In order to be able to measure initial velocity at such a high temperature, we reduced the amount of vesicles applied in the experiments dramatically from 100µg to 1 or 2µg total membrane protein/sample in case of DMRP. In control experiments not documented here we measured the transport activity values of mixed vesicle preparations (using 10µg DMRP, and 90µg ß-galactosidase or 1µg DMRP and 9µg ß-galactosidase vesicles), in parallel with 10µg or 1µg vesicles exclusively overexpressing DMRP. Since we obtained similar results for the mixed vesicle controls and the vesicles expressing DMRP alone (results not shown), we concluded that the dramatic reduction of the vesicular content from 100 to 1 µg did not result in any unspecific changes of the LTC_4 measurement conditions. Therefore, we performed the following experiments at 23˚C on 2 and 100 µg total membrane protein containing vesicles obtained from DMRP and hMRP1 over-expressing Sf9 cells, respectively. We measured LTC_4 uptake of DMRP and hMRP1 at 50 nM LTC_4 as a function of temperature. The time-course showed quasi linearity at 30 seconds for both proteins (Figure 5.12.), so that we used a 30 second incubation time in the following experiments. In concentration dependence experiments, transport activity values were saturated

for both proteins at the applied concentration range (Figure 5.13.). We determined the kinetic parameters of DMRP and hMRP1-mediated LTC_4 transport from the Lineweaver-Burk plots based on the concentration dependence experiments (Figure 5.14.). The maximum LTC_4 uptake rates were 3038±660 pmol/mg of membrane protein/min and 73± 10 pmol/mg of membrane protein/min; and the apparent K_m values were 231 ± 60 nM and 187 ± 50 nM for DMRP and MRP1, respectively. The vesicles contained similar amounts of over-expressed proteins as detected by Coomassie staining (data not shown). The investigated human MRP inhibitors 2mM of probenecid (PB), 50µM of benzbromarone (BB), 300µM of indomethacin (IM), and 30µM of MK571 effectively eliminated the DMRP dependent LTC_4 transport activity (Fig 5.15.).

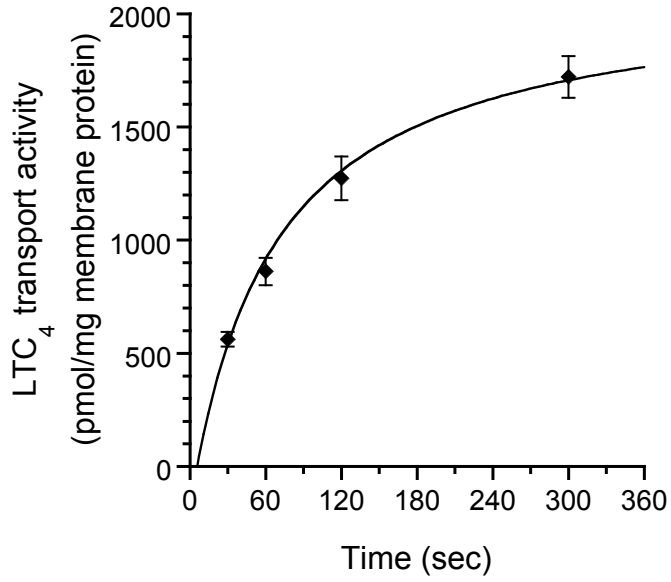

Figure 5.12.: time-course of the DMRP dependent LTC_4 uptake

ATP dependent LTC_4 uptake of 2 µg total protein containing inside-out membrane vesicles prepared from DMRP overexpressing Sf9 cells,. Transport activity measurements were performed at 23˚C 50 nM LTC_4 concentration.

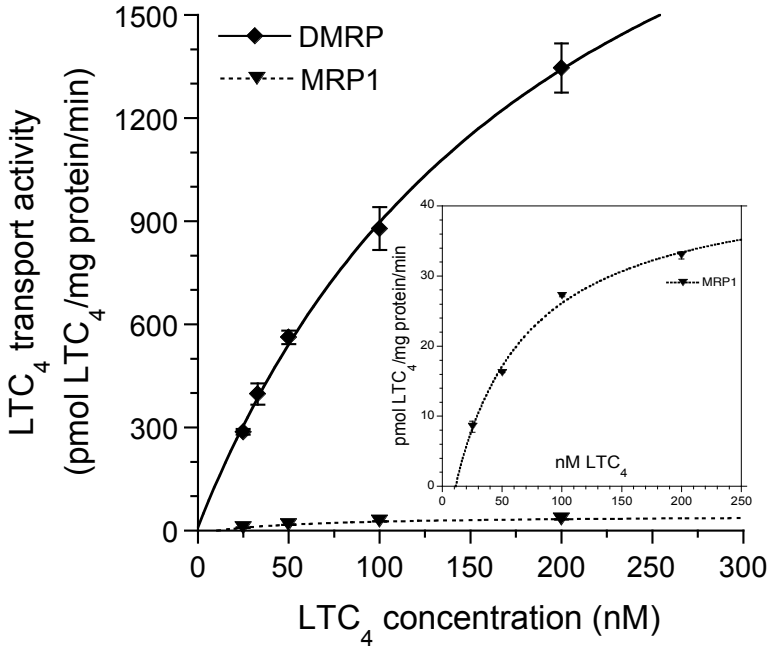

Figure 5.13.: Concentration dependence of DMRP and hMRP1 mediated LTC_4 transport *Experiments were performed at 23˚C for 0.5 min on either 2 or 100 µg of total protein containing inside-out membrane prepared from DMRP or MRP1 overexpressing Sf9 cells, respectively. Inset shows the re-plot of the MRP1-dependent LTC_4 uptake depicted on the main figure with a different scale.*

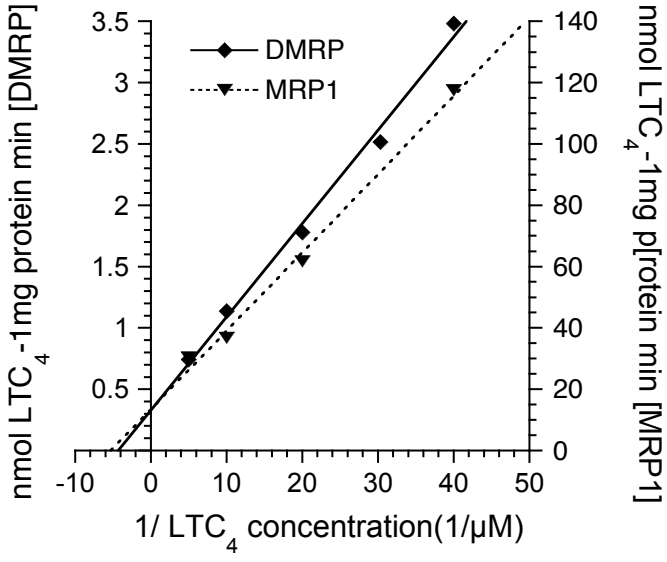

Figure 5.14.: Lineweaver-Burk plot of the DMRP and MRP1 mediated LTC_4 transport *Double reciprocal representation of data depicted on Figure 5.13.*

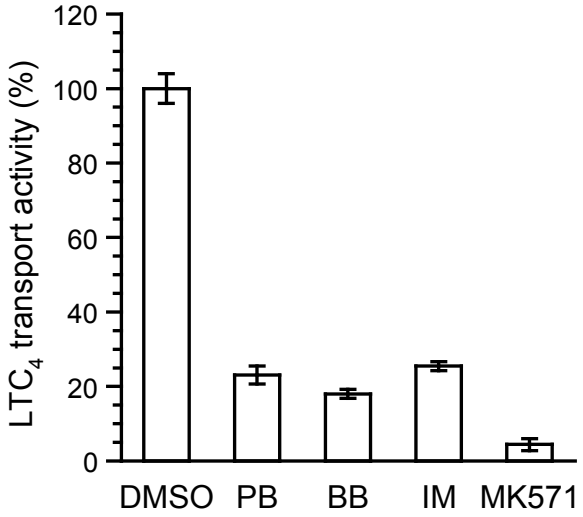

Figure 5.15.: Inhibition of the DMRP dependent LTC_4 uptake

Inhibition of DMRP dependent LTC_4 transport in the absence or presence of 2 mM probenecid (PB), 50 µM benzbromarone (BB), 300 µM indomethacin (IM) and 30 µM MK571. The experiments were performed at 10 nM of LTC_4 concentration at 23˚C for 0.5 min.

5.5.2.3. 3'-5'-cyclic adenosine mono-phosphate transport

We investigated the ability of DMRP to transport [3H] 3'-5'-cyclic adenosine mono-phosphate (cAMP), a substrate of the short MRPs, MRP4 (Chen et al., 2001) and MRP5 (Jedlitschky et al., 2000). We used 100 µg transport competent vesicles at 37˚C at the concentration of 1-100 µM cAMP for 10 minutes incubation. In parallel we tested the LTC_4 transport activity of DMRP to monitor DMRP-function. We didn't detect any ATP dependent accumulation of cAMP, suggesting that cAMP is not a substrate for DMRP (data not shown).

5.5.2.4. Calcein transport

We investigated the DMRP, MRP1 and MRP2 dependent uptake of calcein using flow cytometry of isolated inside out vesicles at 37˚C in the presence of 6 mM MgATP or MgAMP. A representative histogram is shown in Figure 5.16.,

illustrating that the ATP-dependent calcein uptake of the ß-galactosidase control membranes showed negligible background transport activity. In contrast, DMRP showed a high level ATP dependent transport activity as concluded from the remarkable right shift of the histogram of DMRP in the presence of ATP. The specific inhibitor MK571 effectively inhibited the accumulation of calcein in DMRP over-expressing Sf9 vesicles at a concentration of 30 µM.

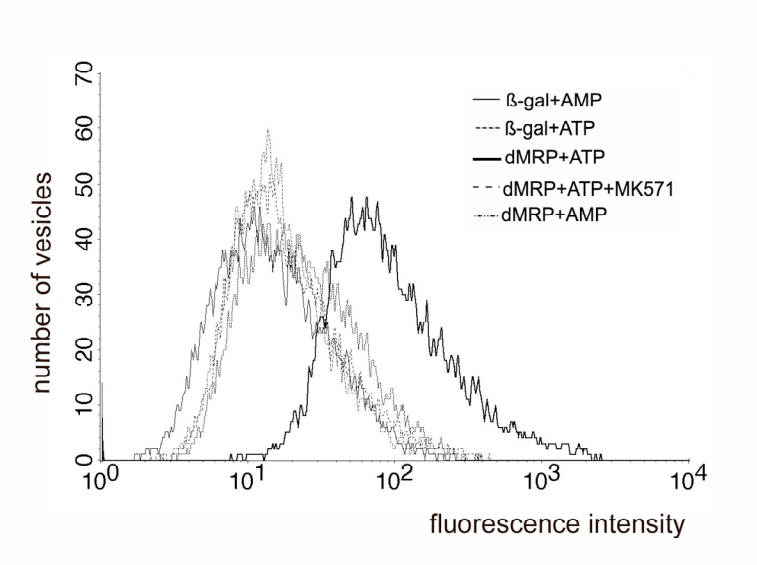

Figure 5.16.: ATP-dependent uptake of calcein into inside-out Sf9 vesicles

Histograms representing calcein accumulation of 10.000 Sf9 inside–out vesicles expressing ß-galactosidase, or DMRP incubated in the presence of 1 µM calcein at 37˚C for 20 minutes. in the presence of 6 mM MgAMP and 6 mM MgATP or 6 mM MgATP + 30 µM MK571 as indicated.

To further characterise DMRP dependent calcein transport activity we measured the uptake of calcein as a function of the incubation time in the presence of 1µm calcein, and detected a remarkable tracer accumulation showing approximate linearity up to 30 seconds for DMRP (Figure 5.17.), while transport activity was not detectable for hMRP1 and hMRP2 (data not shown). We measured DMRP dependent calcein accumulation as a function of tracer concentration at 37˚C in the linear time range using 0.5 min incubation time (Figure 5.18.).

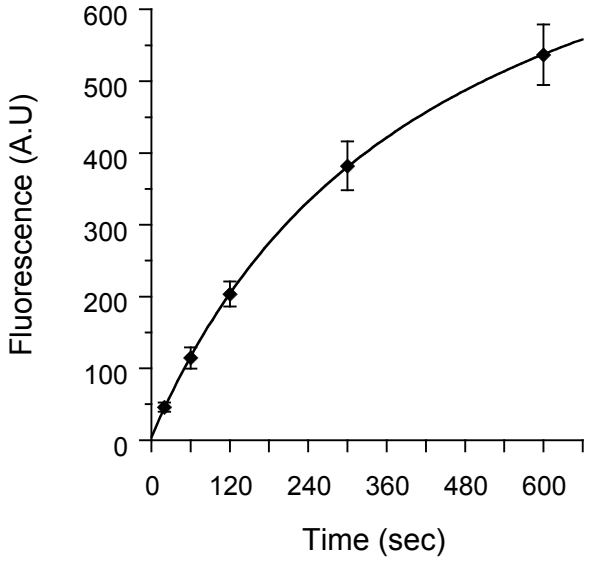

Figure 5.17: Time-course of DMRP mediated ATP-dependent calcein uptake

Geometric mean values of fluorescence intensity of 10,000 inside-out Sf9 vesicles as a function of incubation time measured at 37˚C at 1µM of calcein concentration.

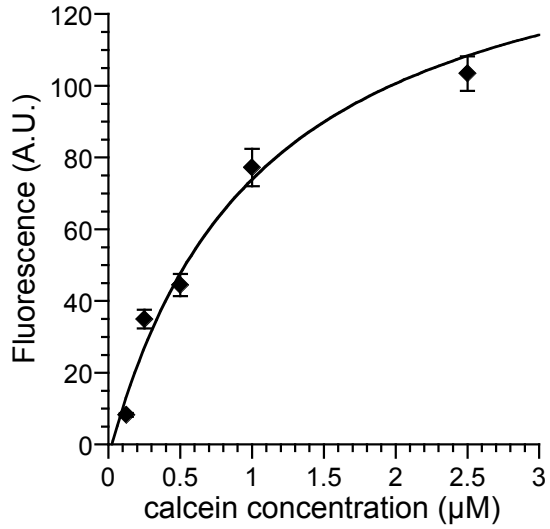

Figure 5.18: Concentration dependence of DMRP mediated ATP-dependent calcein uptake

Geometric mean values of the DMRP mediated ATP dependent fluorescence intensity values of 10,000 inside-out Sf9 vesicles as a function of calcein concentration measured at 37˚C for 0.5 minutes.

We depicted the DMRP dependent activity values on a Lineweaver-Burk plot and determined the apparent K_m of the calcein transport as 1.15 ± 0.17 µM (Figure 5.19.).

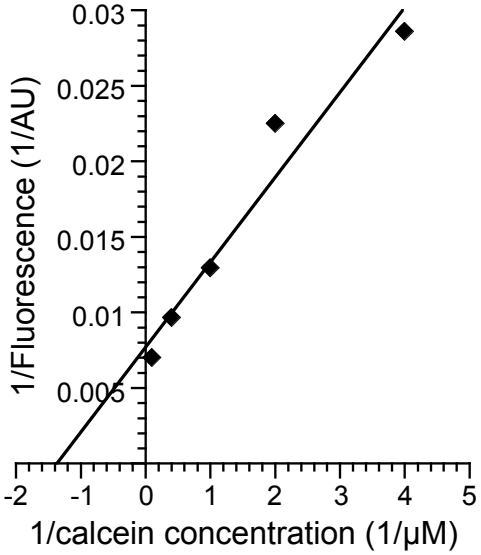

Figure 5.19.: Lineweaver-Burk plot of the DMRP mediated calcein transport

Double reciprocal representation of data depicted on Figure 5.19.

5.5.2.5. Fluo4-AM and fluo3 transport

Fluorescent intensity by FACS was measured at 37˚C in the presence of 4 mM MgATP or MgAMP for 20 min at 2.5 µM of fluo-4 AM (Figure 5.20.) in the presence or absence of 30µM MK571. ATP-dependent fluorescent intensity values of the inside out vesicles were prominent in case MRP1, MRP2 and DMRP as compared to intensity values detected in case of ß-galactosidase control membranes. The fluorescent intensity of the Sf9 vesicles was efficiently reduced in the presence of 30 µM MK571.

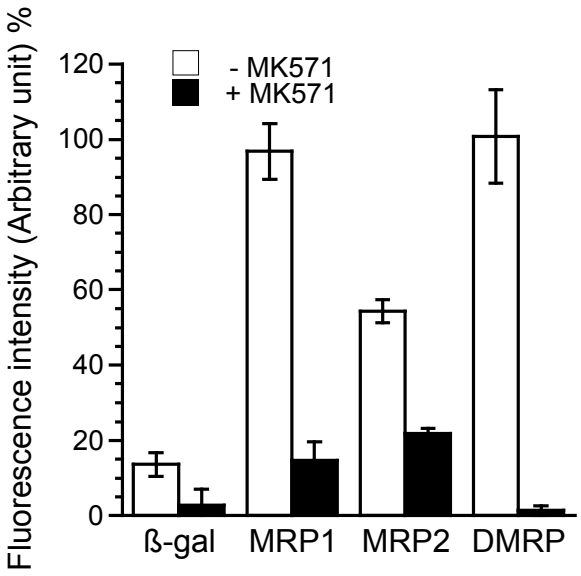

Figure 5.20.: ATP-dependent uptake of inside-out Sf9 membrane vesicles in the presence of Fluo-AM

Geometric mean values of the ATP dependent fluorescent intensity of Sf9 membrane vesicles expressing ß-galactosidase, hMRP1, hMRP2 or DMRP incubated for 20 minutes at 37˚C in the presence of 2.5 µM Fluo-4-AM in the presence or in the absence of 30 µM MK571. Data is normalised to fluorescence intensity values measured for DMRP in the absence of MK571.

To characterise the kinetics of fluo4-AM transport we studied fluorescence intensity as a function of incubation time. Surprisingly, we detected sigmoid curves for the time course for the DMRP, hMRP1 and the hMRP2 expressing inside out vesicles (Figure 5.21.). The curve for DMRP shows evident sigmoid characteristics, while this feature is not obvious for hMRP1 and hMRP2 on the presented figure, however, higher magnification of the data of short incubation times clearly reveals the same phenomenon (data not shown).

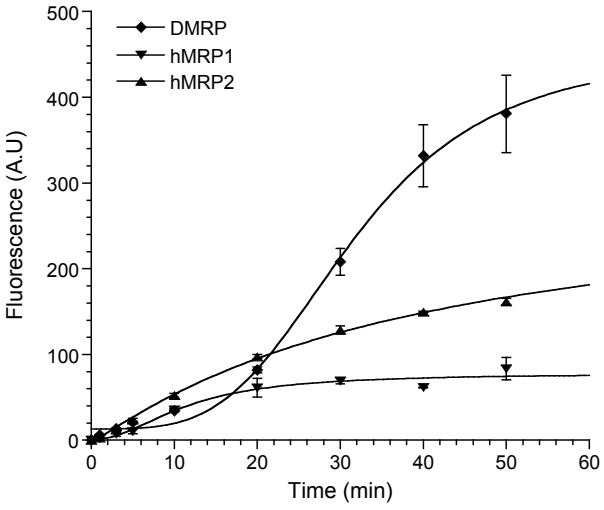

Figure 5.21.: ATP-dependent uptake of inside-out Sf9 membrane vesicles in the presence of Fluo4-AM *hMRP1, hMRP2 or DMRP dependent geometric mean values of the ATP dependent fluorescent intensities as a function of incubation time at 37˚C in the presence of 2.5 µM Fluo-4-AM.*

The sigmoid characteristics of the time course might reflect a delayed phase in the uptake mechanism of the hydrophobic compound, e.g., the investigated MRPs transport their substrates as a so called "vacuum pump" from the lipid bilayer, and incorporation of the tracer into the bilayer is a time consuming step causing a delay of transport. Another possibility is that fluo4-AM is transformed to free fluo4, via membrane-associated esterases potentially present in the Sf9 membrane, and the generated fluo4 is subsequently transported by the above transporters. This process might also cause the delayed phenomenon detected in time-course experiments. As the interaction of Fluo4-AM to the investigated transporters seemed to be complex, we decided to measure transport activity of the free form of a close derivative dye, fluo3. As it is illustrated by the representative histograms depicted on Figure 5.22., the ATP-dependent fluo3 uptake of the ß-galactosidase control membranes at 1µM fluo3 concentration at 37˚C showed negligible background transport activity as compared to the high level ATP dependent activity of DMRP. The specific inhibitor MK571 effectively inhibited the accumulation of 1µM fluo3 in DMRP over-expressing Sf9 vesicles at a concentration of 30 µM. We detected significant MK571 sensitive ATP-dependent activity for hMRP2 overexpressing vesicles as well,

while there was no significant transport activity detected for hMRP1 (data not shown).

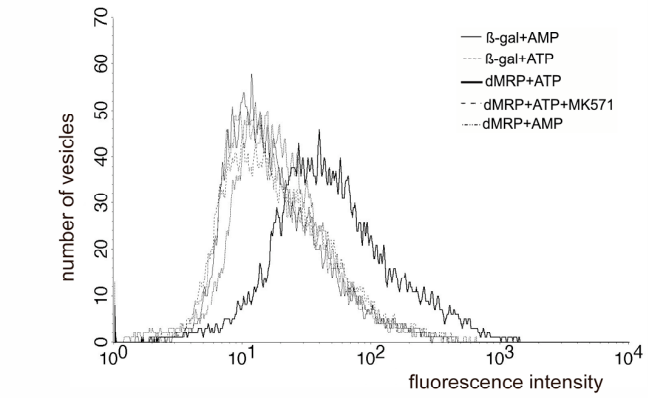

Figure 5.22.: ATP-dependent uptake of fluo3 into inside-out Sf9 vesicles

Histograms representing fluo3 accumulation of 10,000 Sf9 inside–out vesicles expressing ß-galactosidase, or DMRP incubated in the presence of 0.5 µM fluo3 at 37˚C for 10 minutes in the presence of 6 mM MgAMP and 6 mM MgATP or 6 mM MgATP + 30 µM MK571 as indicated.

Time-course for fluo3 depicted a simple saturation curve, and showed approximate linearity up to 0.5 and 1 minute for DMRP and hMRP2 at 37˚C, respectively (Figure 5.23).

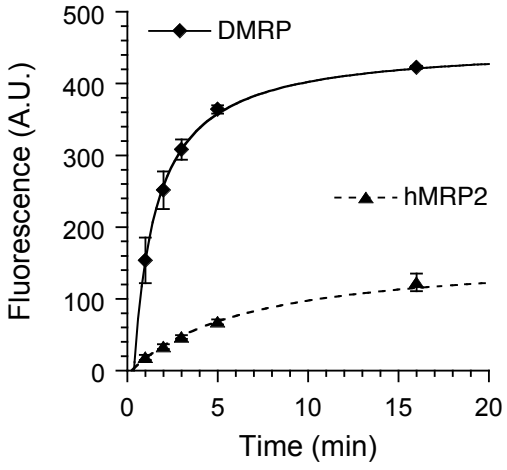

Figure 5.23.: Time-course of the DMRP and hMRP2 mediated fluo3 uptake

Geometric mean values of fluorescence intensity of 10,000 inside-out Sf9 vesicles as a function of incubation time measured at 37˚C at 0.5 µM of fluo3 concentration.

Therefore, the above conditions were used to study concentration dependence of fluo3 for DMRP and hMRP2. Fluo3 transport was saturated in the applied concentration range for both proteins (Figure 5.24).

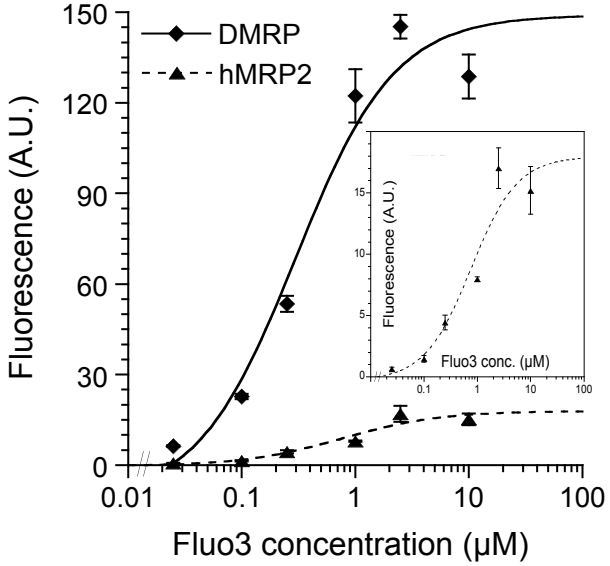

Figure 5.24.: Concentration dependence of DMRP and hMRP2 mediated fluo3 uptake *ATP dependent geometric mean values of the fluorescence intensities of 10,000 Sf9 membrane vesicles as a function of fluo3 concentration incubated at 37˚C for 0.5 minutes for DMRP and 1 minute for MRP2. Fluorescent intensity values were corrected for incubation time. The inset is the re-plot of the MRP2-dependent transport activity in a different scale.*

Fluorescent intensity data were depicted on Lineweaver-Burk plots (Figure 5.25), and the apparent kinetic parameters were determined. The apparent Km values were 0.37 ± 0.13 μM for DMRP and 0.81± 0.40 μM for MRP2. Since we had no calibration for the determination of the amount of dye accumulated in the isolated vesicles in FACS measurements the apparent V_{max} values were only arbitrary units. Since we transport activities of the proteins were measured in the same experiments, these arbitrary data reflected differences of the initial rates of the investigated transporters. We detected 8.4 times higher turnover for DMRP than for MRP2, while quantification of Coomassie stained gels revealed that the

vesicles investigated in FACS measurements all contained similar amounts of over-expressed proteins (data not shown).

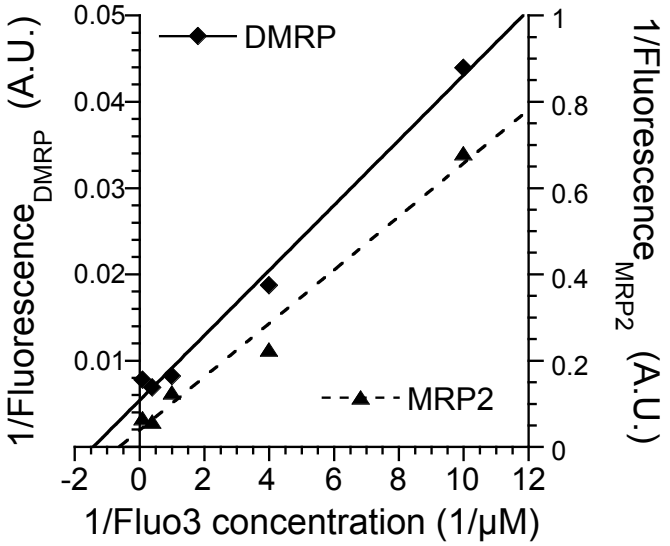

Figure 5.25.: Lineweaver-Burk plot of the DMRP and hMRP2 mediated fluo3 transport *Double reciprocal representation of data depicted on Figure 5.24.*

5.5.2.6. Carboxydichlorofluorescein (CDCF) transport

As illustrated by the representative histograms depicted in Figure 5.26., the ATP-dependent CDCF uptake of the ß-galactosidase control membranes at 37˚C and 1µM CDCF concentration showed negligible background transport activity as compared to the high level ATP dependent activity detected for DMRP. The presence of 30 µM MK571 effectively inhibited the accumulation of CDCF in DMRP over-expressing Sf9 vesicles. In comprehensive CDCF transport experiments the DMRP-dependent dye accumulation was found to be prominent, while a moderate activity was detected for MRP2 and a threshold level of transport activity for MRP1. Therefore we only investigated the activity of the aforementioned two transporters.

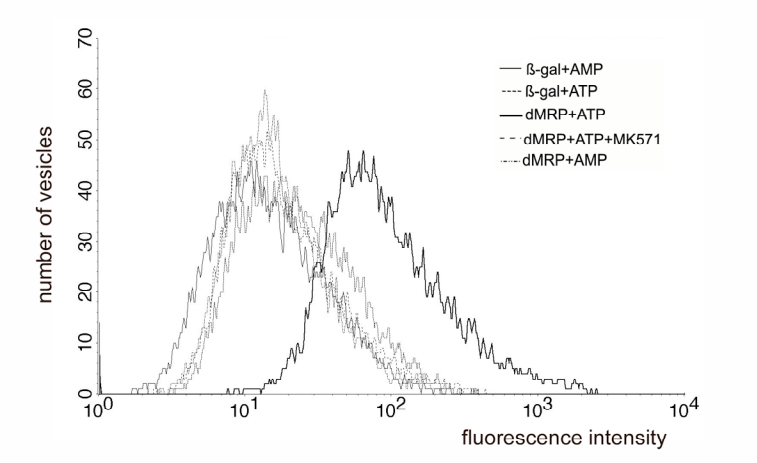

Figure 5.26: ATP-dependent uptake of CDCF into inside-out Sf9 vesicles

Histograms representing CDCF accumulation of 10,000 Sf9 inside–out vesicles expressing ß-galactosidase, or DMRP incubated in the presence of 1 µM CDCF at 37˚C for 20 minutes in the presence of 6 mM MgAMP and 6 mM MgATP or 6 mM MgATP + 30 µM MK571 as indicated.

We investigated the CDCF transport activity at 37˚C as a function of the incubation time. We detected approximate linearity of the CDCF transport up to 0.5 and 1 minute for DMRP and MRP2, respectively (Figure 5.27.).

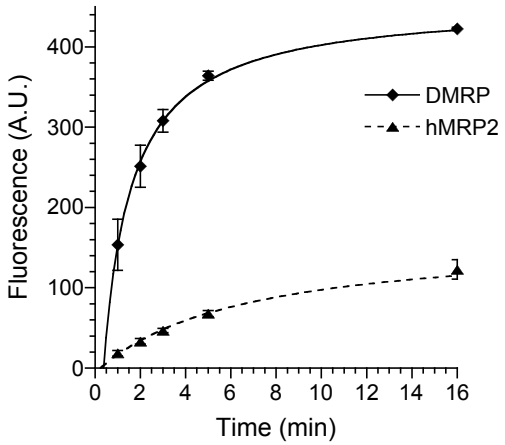

Figure 5.27: Time-course of the DMRP and hMRP2 mediated CDCF uptake

Geometric mean values of fluorescence intensity of 10,000 inside-out Sf9 vesicles as a function of incubation time measured at 37˚C at 2.5 of CDCF concentration.

Applying the above conditions we measured transport activity as a function of CDCF concentration (Figure 5.28.). Since we detected an unspecific ATP independent effect of CDCF on the transport assay above 50µM CDCF concentration, we only used and presented data up to 25µM CDCF concentration. This interval included the whole effective concentration range of CDCF for DMRP but not for MRP2.

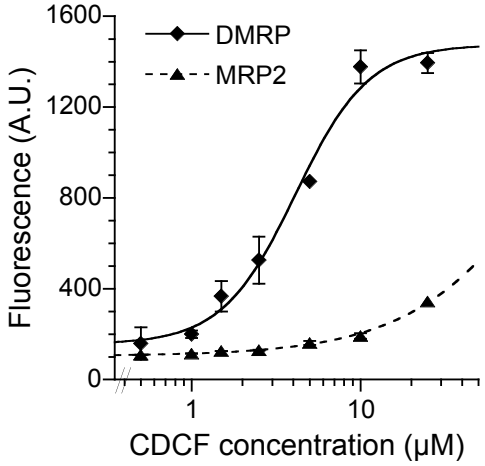

Figure 5.28: Concentration dependence of DMRP and hMRP2 mediated CDCF uptake *ATP dependent geometric mean values of the fluorescence intensities of 10,000 Sf9 membrane vesicles as a function of CDCF concentration incubated at 37˚C for 0.5 minutes for DMRP and 1 minute for MRP2. Fluorescent intensity values were corrected for incubation time.*

Depicting data on Lineweaver-Burk plots we determined the apparent K_m value of the DMRP dependent CDCF transport as 4.1 ± 0.6 µM CDCF (Figure 5.29). Since saturation of hMRP2 by the administered CDCF concentration was not achieved, we could not determine the transport kinetic values for hMRP2, and thus we a comparison of turnover rates of the transporters could not be made.

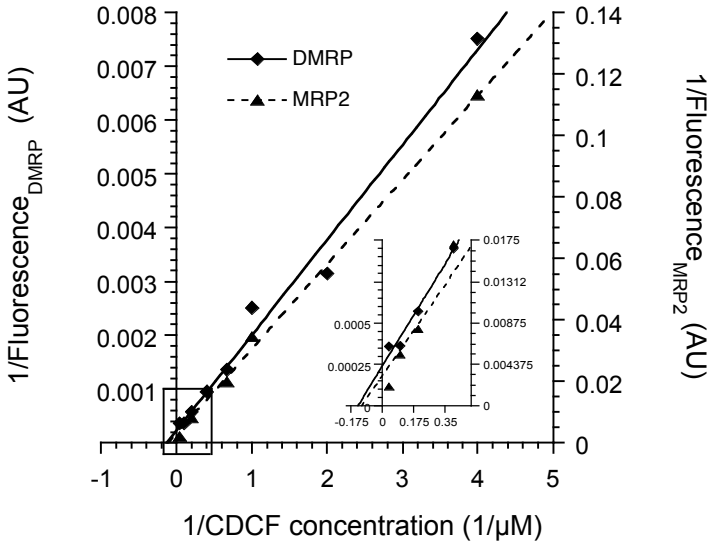

Figure 5.29: Lineweaver-Burk plot of the DMRP and hMRP2 mediated CDCF transport *Double reciprocal representation of the data depicted in Figure 5.28. The inset shows magnification of the data in the rectangle.*

5.5.3. Transport inhibition experiments

5.5.3.1. "Cross-inhibition" of LTC_4 and $E_2$17ßD-glucuronide transport

We tested the impact of each of the above transported substrates, LTC_4 and $E_2$17ßD-glucuronide, on the transport activity of the other substrate. We detected the initial velocity of the transport of the isotope labelled substrates at concentrations far below the K_m determined previously for the tracer. The other substrate was present at saturating (or highest applicable) concentrations (Figure 5.30.). We detected cross-inhibitory effect of LTC_4 and $E_2$17ßD-glucuronide on the transport of the other substrate. 400 nM LTC_4 caused 36.5% inhibition of the $E_2$17ßD-glucuronide transport, in the meanwhile 200µM $E_2$17ßD-glucuronide caused 66.8% inhibition of the LTC_4 transport activity. While in the presence of 5mM NEM-GS the remaining $E_2$17ßD-glucuronide activity was only 7.8%.

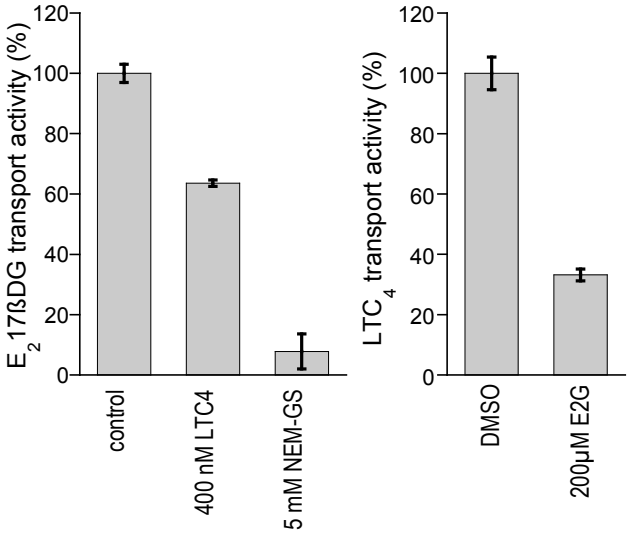

Figure 5.30: Cross-inhibitory effect of LTC_4 and $E_2$17ßD-glucuronide on the transport of the other substrate

$E_2$17ßDG transport activity measured at 10 µM of $E_2$17ßDG concentration at 37˚C for 0.5 min in the presence or absence of 400nM LTC_4 or 5mM NEM-GS, normalised for $E_2$17ßDG transport activity of the control ***(Panel A.)***.

LTC_4 transport of reduced expression vesicles was measured at 10 nM of LTC_4 concentration at 0˚C for 0.5 min in the presence or absence of 200µM $E_2$17ßDG, normalised for LTC_4 transport activity of the control ***(Panel B.)***.

5.5.3.2. Transport inhibition by 20-OH-ecdysone

We investigated the effect of 20-OH-ecdysone, the most effective insect moulting hormone, on the DMRP dependent vesicular transport of [^{3}H]$E_2$17ßD glucuronide and [^{3}H]leukotriene C_4. We found that 20-OH-ecdysone did not influence DMRP dependent uptake of the above substrates at the investigated concentration range of 1nM-10µM (data not shown).

5.5.3.3. Transport inhibition by pesticides

In vitro and *in vivo* pesticide resistance of various organism mediated by ABC transporters, mostly MDR1 and MRP1 homologues, were previously documented (Bain and LeBlanc, 1996; Shabbir et al., 2005; Smital et al., 2000; Sreeramulu et al., 2007) and (Dupuy et al., 2006; Tribull et al., 2003) (Lespine et al., 2006), respectively. To investigate the effect of some commercially available pesticides on DMRP function we studied the effect of fenitrothion, bioalletrin, aldicarb and dichlorodiphenyl trichloroethane (DDT) on the DMRP dependent vesicular transport of [^{3}H]$E_2$17ßD glucuronide and [^{3}H]leukotriene C_4. We measured the uptake of [^{3}H]$E_2$17ßD glucuronide as the function of the pesticide concentration at 37˚C for 0.5 min at 10 µM [^{3}H]$E_2$17ßD glucuronide concentration (Figure 5.31.).

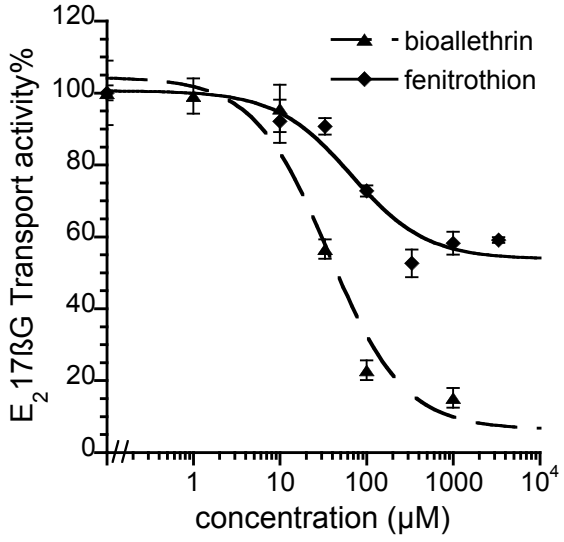

Figure 5.31.: Influence of pesticides on the $E_2$17ßD glucuronide transport activity of DMRP. *DMRP dependent $E_2$17ßD glucuronide transport activity as a function of pesticide concentration measured at 37˚C for 0.5 min at 10 µM of [^{3}H]$E_2$17ßD glucuronide concentration, normalised for DMRP basal ATPase activity.*

Bioallethrin inhibited the [^{3}H]$E_2$17ßD glucuronide transport effectively with IC_{50} value of 36µM, while the inhibition of fenitrothion was less effective and

showed a IC_{50} value of 62µM. DDT slightly inhibited both the ATP dependent and independent labelling of the Sf9 vesicles in a concentration dependent manner, reflecting a possibly unspecific interaction of the compound with the transport inhibition assay (data not shown). Aldicarb did not have any affect on the [^{3}H]$E_2$17ßD glucuronide transport. In case of pesticides giving negative results in [^{3}H]$E_2$17ßD glucuronide transport experiments [^{3}H]leukotriene C_4 transport inhibition experiments were also performed. The initial rate of the leukotriene C_4 transport was measured at 10nM LTC_4 concentration as a function of the pesticides. Neither aldicarb nor DDT altered the [^{3}H]leukotriene C_4 transport at the investigated pesticide concentration ranges from 1µM to 1mM (data not shown).

5.5.4. Vanadate-sensitive ATPase activity of DMRP

5.5.4.1. Basal and NEM-GS stimulated ATPase activity

It is a common feature of ABC transporters that transport of the substrates is highly coupled to ATP hydrolysis. As a consequence, transported substrates influence ATPase activity most commonly by increasing the rate of ATP hydrolysis (substrate-stimulated ATPase activity). Vanadate specifically inhibits ATP hydrolysis of ABC transporters. Therefore, the ABC transporter specific ATP hydrolysis can be discriminated from the ATPase activity of other types of proteins by its sensitivity for vanadate (vanadate-sensitive ATPase activity). In our experiments we determined the ATP dependent vanadate-sensitive ATPase activity, and we refer to it as ATPase activity in the following. We found that the hMRP substrate gluthatione conjugated N-ethylmaleimide (NEM-GS) stimulated the basal ATPase activity of DMRP about two fold at the concentration of 5 mM. Therefore we characterised the ATPase activity of DMRP in the absence (basal activity) or in the presence of 5mM NEM-GS (stimulated activity). We determined the linear phase of the time-course for the basal and NEM-GS stimulated ATPase activity (Figure 5.32. panel A.). The vanadate-sensitive basal and the NEM-GS stimulated ATPase activities of

DMRP were found to show approximate linearity up to 5 minutes at 37˚C and 3.3 mM Mg^{2+}ATP concentration. We determined the basal and NEM-GS stimulated ATPase activities as a function of the Mg^{2+}ATP concentration, as well. As depicted in panel B. of Figure 5.32., both vanadate-sensitive basal and NEM-GS stimulated activities were saturated above 2 mM Mg^{2+}ATP concentration.

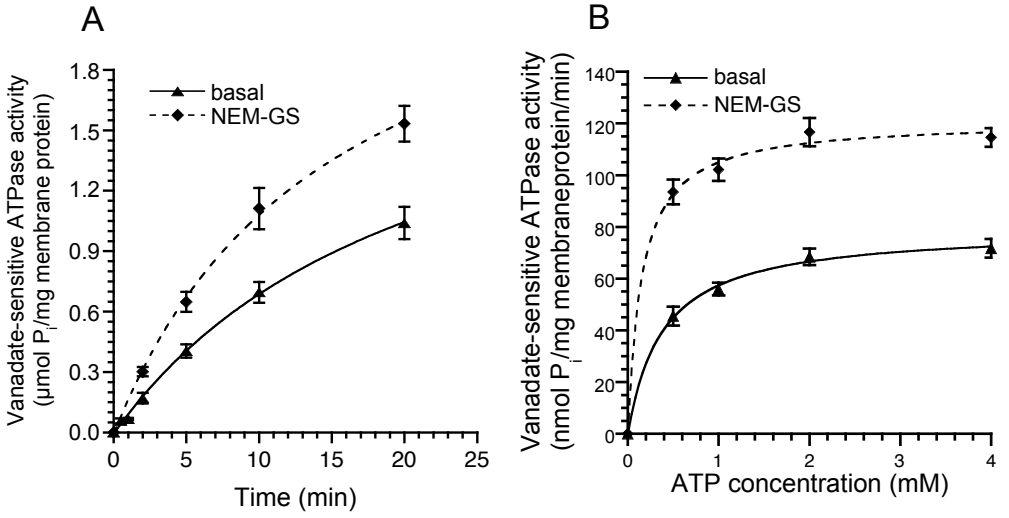

Figure 5.32.: Time-course and Mg2+ATP dependence of the basal and NEM-GS stimulated ATPase activity of DMRP *DMRP dependent vanadate–sensitive ATPase activity in the presence or absence of 5 mM NEM-GS measured 37˚C in the presence of 3.3 mM Mg^{2+}ATP or 3.3 mM Mg^{2+}AM* ***(Panel A.).*** *The DMRP dependent vanadate–sensitive ATPase activity was measured as a function of Mg2+ATP concentration at 37˚C for 5 minutes in the presence or absence of 5 mM NEM-GS* ***(Panel B.).***

5.5.4.2. Effect of modulators on the ATPase activity of DMRP

To further characterise the ATPase activity of the transporter we investigated its vanadate-sensitive ATPase activity in response to NEM-GS, probenecid, LTC_4, $E_2$17ßDG and calcein (Figure 5.33.). Experiments were performed at 37˚C for 5 minutes incubation time in the presence of 3.3 mM Mg^{2+}ATP on samples containing 30µg total membrane protein. Control membranes from cells

expressing ß-galactosidase had a low level basal ATPase activity (5-8 nmol P_i/mg of membrane protein/min) independent of the presence of the tested compounds (data not shown). The basal vanadate-sensitive ATPase activity of DMRP in the absence of any substrates was unusually high (68-75 nmol P_i/mg of membrane protein/min) compared to that of human MRP1 (6-8 nmol P_i/mg of membrane protein/min) (Bakos et al., 2000; Bodo et al., 2003b). This basal activity could be stimulated by 1.9 fold in the presence of the NEM-GS at the concentration of 2.5 mM, and 1.8 fold in the presence of probenecid at the concentration of 1mM (Figure 5.33.) The EC_{50} values of these interactions were 599µM and 117µM for NEM-GS and probenecid, respectively. Surprisingly, though substrates usually increase the rate of ATP hydrolysis, the investigated DMRP substrates LTC_4, calcein, and $E_2$17ßDG all inhibited the basal ATPase activity of DMRP significally. The inhibition of the DMRP dependent basal vanadate-sensitive ATPase activity was found to be 54% for LTC_4, 23% for calcein and 87.5% for $E_2$17ßDG, at the concentration of 600nM, 100µM and 1mM, respectively (Figure 5.33.). The applicable concentrations of LTC_4, calcein and $E_2$17ßDG did not involve the whole effective concentration range of the above compounds on the basal ATPase activity of DMRP therefore the absolute IC_{50} values for LTC_4, calcein and $E_2$17ßDG inhibition could not be determined. It is important to note that these inhibitory concentration ranges of ATPase activity measurements correlated with the apparent K_m values determined in the transport experiments. MK571, the specific MRP inhibitor, effectively inhibited both the NEM-GS stimulated and the basal ATPase activity of DMRP in a concentration dependent manner with IC_{50} values of 1.05 and 2.05µM, respectively (Figure 5.34).

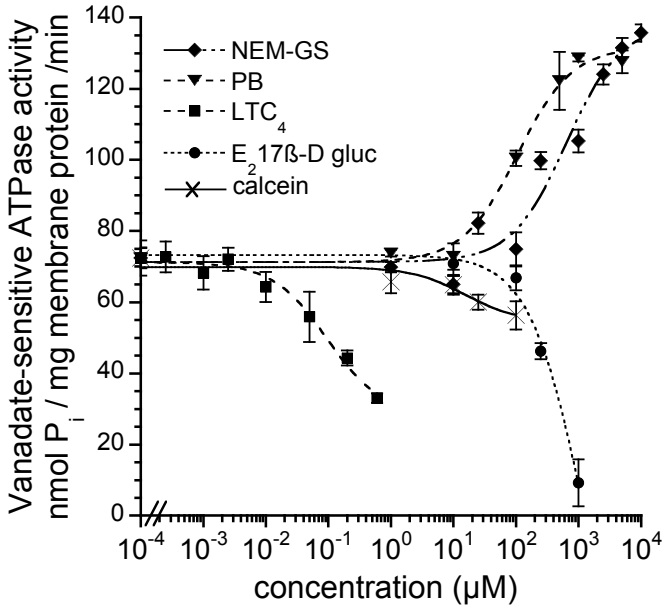

Figure 5.33.: Effect of modulators on the vanadate-sensitive ATPase activity of DMRP. *DMRP dependent vanadate–sensitive ATPase activity was determined as a function of concentration of the following compounds: NEM-GS (diamond), probenecid (triangle), LTC_4 (square), $E_2$17ßDG (circle) and calcein (star). Experiments were performed at 37˚C for 5 min incubation at 3.3 mM of Mg^{2+}ATP concentration.*

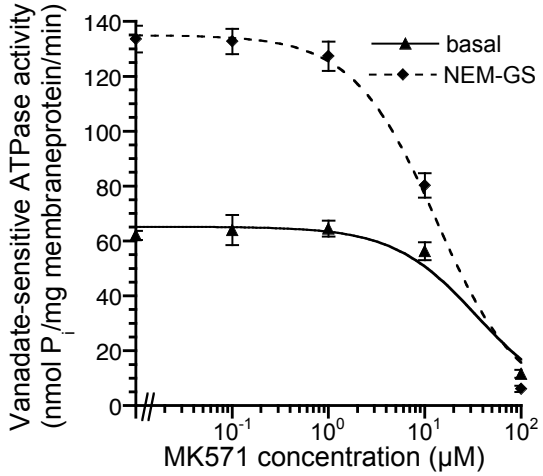

Figure 5.34.: Effect of MK571 on the basal and NEM-GS stimulated ATPase activity of DMRP *DMRP dependent vanadate–sensitive ATPase activity was determined as a function of MK571 concentration in the absence (triangle) or in the presence (diamond) of 5 mM NEM-GS. Experiments were performed at 37˚C for 5 min incubation at 3.3 mM of Mg^{2+}ATP concentration.*

5.5.4.3. Effect of pesticides and 20-OH ecdysone on the ATPase activity of DMRP

We found that the pesticides, bioallethrin and fenitrothion effectively inhibited the DMRP dependent $E_2$17ßDG transport, suggesting that these compounds are potential substrates for DMRP, while we found no evidence for the specific interaction of aldicarb and DDT with the transporter in transport inhibition experiments. To investigate the interaction of the pesticides on the ATPase activity of DMRP, we measured DMRP dependent ATPase activity as a function of pesticide concentration, for fenitrothion, bioalletrin, aldicarb and DDT. Among the above pesticides fenitrothion, bioalletrin, and DDT have effectively inhibited the ATPase activity of DMRP in a concentration dependent manner (Figure 5.35.).

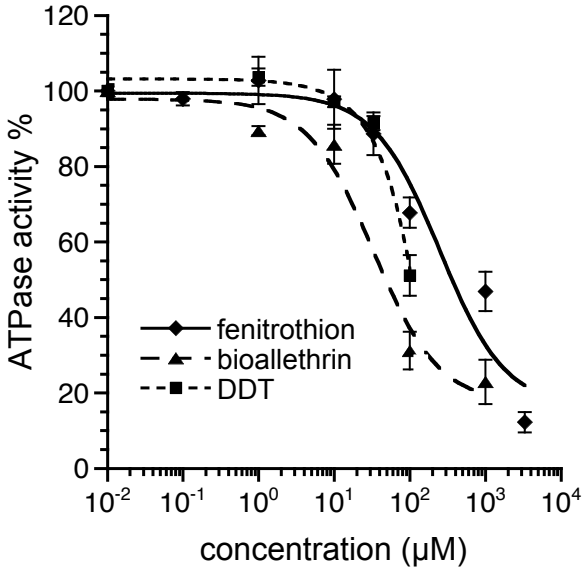

Figure 5.35: Effect of pesticides on the DMRP dependent basal ATPase activity

DMRP mediated vanadate–sensitive ATPase activity was depicted as a function of pesticide concentration. Experiments were performed at 37˚C for 5 min incubation at 3.3 mM of Mg^{2+}ATP concentration, and normalised for basal activity.

The IC_{50} values for fenitrothion, bioalletrin and DDT were found to be 251µM, 32.9µM and 15.2µM, respectively. Fenitrothion and bioalletrin did not have any significant effect on neither the vanadate insensitive ATPase activity of the DMRP expressing membranes, nor the ATPase activity of the ß-galactosidase control membranes, thus supporting the conclusion that the interaction of DMRP and the above pesticides was specific. However, though DDT had a 56% inhibitory effect on the vanadate-sensitive ATPase activity, DDT inhibited the vanadate-insensitive ATPase activity as well in a similar concentration dependent manner (data not shown). Moreover, side scattering measurements suggested micelle formation of DTT above ~ 50µM. These facts suggest that DDT might interfere with the ATPase activity measurement assay. We therefore concluded that ATPase activity measurements are not suitable for investigating the interaction of DDT and DMRP. The other pesticide, aldicarb did not have any effect on the DMRP dependent ATPase activity at the concentration range of 1µM to 1mM.

We investigated the effect of the insect moulting hormone, 20-OH ecdysone, on the vanadate-sensitive ATPase activity of DMRP and found that 20-OH-ecdysone did not influence the basal ATPase activity of DMRP at the investigated concentration range of 1nM-10µM (data not shown).

5.5.5. Transition-state thermodynamics of DMRP

5.5.5.1. Determination of thermodynamic parameters of the transition state of ATP hydrolysis of DMRP

Due to the unusually high turnover rate of DMRP in the functional assays, the correlation between temperature and enzyme activity of DMRP could be investigated in the Sf9 system. From such data the thermodynamic parameters of the transition-state of the ATP hydrolysis of DMRP could be determined. Due to the low turnover rate of other MRP-type ABC transporters, no such investigation

has yet been done for any of these proteins. Therefore, studies of the evolutionarily and functionally related *Drosophila* MRP possessing unusually high basal activity might serve as a useful model for the human MRP orthologues. We investigated the temperature dependence of the vanadate-sensitive ATPase activity in the absence (basal activity) or in the presence of substrates (600 nM LTC_4 or 5 mM NEM-GS) at 4-centigrade intervals from 17 to 37˚C (in experiments not documented here we found evidence for DMRP being capable of transporting the isotope labelled compound NEM-GS). First, the time-course of the ATPase activity was determined for each temperature (data not shown), and incubation times showing linear relationship (corresponding to the initial velocity of the reaction) were used to obtain data for the temperature dependence (Figure 5.36.).

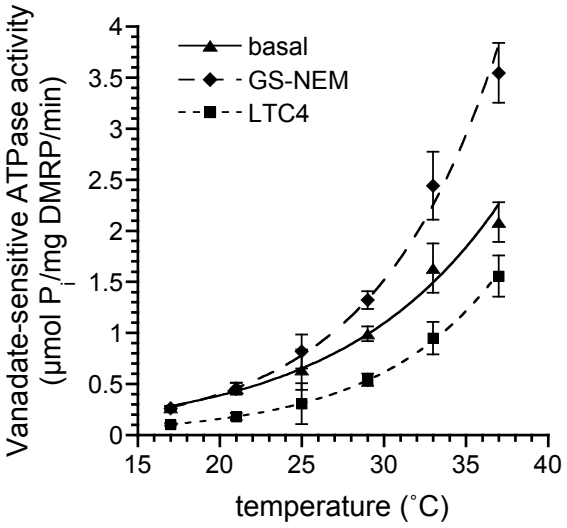

Figure 5.36.: Effect of temperature on the vanadate-sensitive ATPase activity

Initial rates of DMRP dependent vanadate–sensitive ATPase activity as the function of temperature. ATPase activities in the absence of any modulators (triangles) or in the presence of 5 mM NEM-GS (diamonds), or at the presence of 600 nM LTC4 (squares).

Data obtained in ATPase activity measurements were corrected for DMRP content of the Sf9 membrane preparations. Densitometric analysis of Coomassie

stained gels revealed that DMRP makes up ~3.3% of total membrane protein content, this data was used for the above correction. As shown in Figure 5.36, an exponential function was detected for both the basal and the modulated ATPase activities. For the transition-state analysis of these temperature dependence data sets, the logarithm of ATPase activity values divided by the absolute temperature was plotted against the reciprocal of absolute temperature according to the Eyring equation (see Methods for details) and lines were fitted to data sets applying linear regression. Linear Eyring relationships were detected for the basal, the NEM–GS stimulated, as well as the LTC4 inhibited ATPase activities (Figure 5.37). The linearity of these plots indicated that single overall rate-limiting steps were detected for all enzymatic reactions.

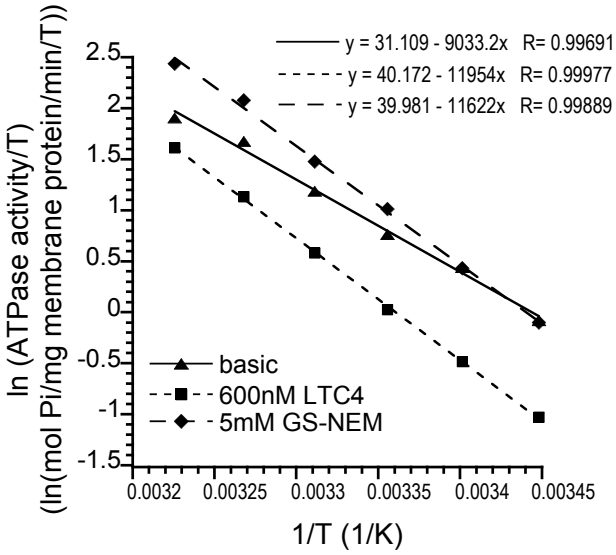

Figure 5.37.: Eyring plot of basal and modulated ATPase activity of DMRP

Eyring plot showing ln (vanadate-sensitive ATPase activity/T) of DMRP as a function of 1/T, in the absence of any modulators (triangles) or in the presence of 5 mM NEM-GS (diamonds), or at the presence of 600 nM LTC_4 (squares). ***The equations of the fitted lines are depicted.***

The slope and y-intercept values of the fitted lines were found to be similar for the ATPase activity modulated by NEM-GS and LTC_4, while these parameters were different for the basal activity (Figure 5.37. equations, Table 5.1.).

Employing standard thermodynamic equations (see Experimental for details) we have calculated the thermodynamic parameters (the enthalpic, entropic, and free energy terms, and the activation energy) for the rate limiting transition-states for 37˚C (see Table 5.1). The activation enthalpy (ΔH‡) was found to be 75.11 ± 2.96 kJ/mol, the activation entropy ΔS‡ = 95.11 ± 3.64 J/mol/˚K and the calculated Gibbs free energy ΔG‡ = 46.62 ± 4.09 kJ/mol (310˚K) for the transition-state detected in the absence of exogenous modulators. The presence of exogenous modulators, LTC_4 or NEM-GS, resulted in a different picture concerning the transition-state thermodynamics. Both the activation enthalpy and the activation entropy were significantly higher in the presence of these exogenous modulators, ΔH‡ = 96.63 ± 2.29 kJ/mol and ΔS‡ = 168.87 ± 3.88 J/mol/˚K for NEM-GS, and ΔH‡ = 99.39 ± 1.05 kJ/mol and ΔS‡ = 170.46 ± 1.79 J/mol/˚K for LTC_4. The Gibbs free energy calculated from these two thermodynamic parameters resulted in similar values for all three enzymatic reactions, namely 46.62 ± 4.09 kJ/mol, 44.28 ± 3.49 kJ/mol and 46.55 ± 1.60 kJ/mol for basal, NEM-GS stimulated and LTC_4 inhibited activities, respectively. A one-way ANOVA analysis revealed no significant differences among the three $\Delta G^{\ddagger}$ values (p value = 0.846). Also, we found no statistically significant differences when the three $\Delta G^{\ddagger}$ values were compared in pairs with Student's t-test at 95% probability level.

Table 5.1.: Transition-state thermodynamic parameters of the ATP-hydrolysis

Activation enthalpy ($\Delta H^{\ddagger}$), activation energy (E_a), activation entropy ($\Delta S^{\ddagger}$), and Gibbs free energy ($\Delta G^{\ddagger}$) values calculated from the fitted lines obtained from basal and modulated activities depicted in Figure 5.37.

	slope	y-intercept	$\Delta H^{\#}$ (kJ/mol)	E_a (kJ/mol)	$T^*\Delta S^{\#}$ (kJ/mol)	$\Delta G^{\#}$ (kJ/mol)
basal	-9033 ± 355	31.11±1.19	75.11 ±2.96	75.42 ±2.97	29.49 ±1.13	46.62 ±4.09
NEM-GS	-11622 ± 275	39.98±0.92	96.63 ±2.29	96.95 ±2.30	52.35 ±1.20	44.28 ±3.49
LTC_4	-11954 ± 127	40.17±0.42	99.39 ±1.05	99.71 ±1.06	52.85 ±0.55	46.55 ±1.60

5.5.5.2. Linear free energy relationship (LFER) analysis

In our previous experiments we detected a high level basal ATPase activity of DMRP. However, most of the investigated substrates, LTC_4, calcein and $E_2$17ßDG, inhibited the basal activity, in contrast to the commonly detected substrate-stimulation of the basal ATPase activity of ABC transporters. Moreover, thermodynamics analysis of the transition state formation of DMRP revealed that these thermodynamic parameters are markedly different in the absence or in the presence of external modifiers, NEM-GS and LTC_4.

Based on this reasoning we raised the possibility that an endogenous modifier of the DMRP function may be present in the Sf9 membranes. This modifier could either be an endogenous substrate or an endogenous allosteric activator triggering the intrinsic ATPase activity of DMRP (for further explanation of the above hypothesis see Discussion section).

To further investigate the nature of the endogenous modifier, we performed linear free energy relationship experiments. We detected the ATPase activities of the same samples at two different temperatures, namely at 25 and 37˚C, in the presence or in the absence of different concentrations of LTC_4 and $E_2$17ßDG. First we plotted the ATPase activities measured in the presence of LTC_4 and $E_2$17ßDG at 37˚C as a function of the corresponding activities measured at 25˚C (Figure 5. 38.). We fitted straight lines by nonlinear regression to the datasets of LTC_4 and $E_2$17ßDG.

Statistical analysis revealed no significant differences between the slope and intercept parameters of these lines, showing the same linear free energy relationships of the two datasets. Therefore, in the following these two datasets were merged, and was being referred as substrate transport coupled (or coupled) ATPase activity. To find out whether ATPase activity measured in the absence of any external substrate fits to this line, the basal activity values were plotted on the plot as well (Figure 5.39).

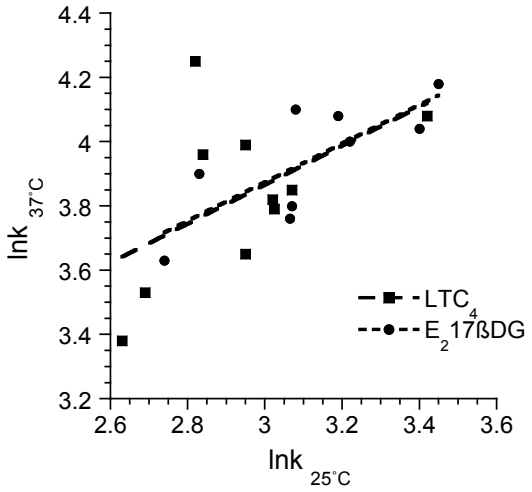

Figure 5.38.: Linear free energy relationships for coupled ATPase activities

Log turnover numbers of ATPase activities measured at 37˚C in the presence of 100, 200, 400 nM of LTC_4 and 100, 200, 400 µM of $E_2$17ßDG as a function of the corresponding data for log turnover numbers at 25˚C. The dashed lines show the linear regression of the values in the presence of LTC_4 and $E_2$17ßDG.

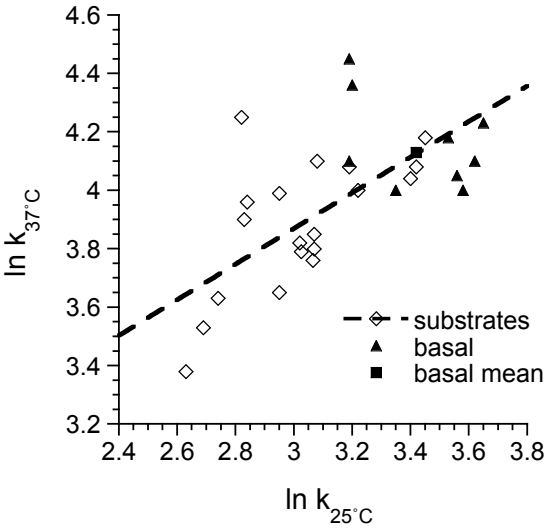

Figure 5.39.: Linear free energy relationships for coupled and basal ATPase activities

Log turnover numbers of ATPase activities measured at 37˚C in the presence of 100, 200, 400 nM of LTC_4 or 100, 200, 400 µM of $E_2$17ßDG (substrates, open diamond) or in the absence of external substrates (basal, black triangles) as a function of the corresponding data for log turnover numbers at 25˚C. Mean value of basal activity is represented by a black square. The dashed lines show the linear regression of the coupled ATPase activity values measured in the presence of LTC_4 and $E_2$17ßDG.

Theoretically, the dataset in the absence of exogenous substrates refers to a single point on this plot and therefore, the mean value of this basal activity was plotted on Figure 5.39 (black square).

Statistical analysis revealed that the mean value of the basal activity with its standard error interval lies within the error (confidence) interval of the straight line which was fitted to the merged data set of the coupled activity, meaning that there is no statistical evidence against the assumption that the basal activities fits together with the coupled activities.

5.5.6. Effect of cyclodextrins on the basal and stimulated ATPase activity of DMRP

Cyclodextrins (CD) are cyclic oligosaccharide complexes, with defined 3D structure, forming toroids of hydrophobic inner and hydrophilic outer surfaces exposed to the solvent. Due to these characteristics, cyclodextrins of different chemical modulations are suitable pharmaceutical vectors for the solvation and penetration of a wide range of hydrophobic compounds. As a consequence of these characteristics, empty cyclodextrins are capable of destructing components of membranes as well, therefore via application of “empty” cyclodextrins the membrane composition of the biological membranes can be modified.

As we suspected the presence of a modifying membrane component of the basal ATPase activity of DMRP, we were seeking for cyclodextrins that cause inhibition of the basal ATPase activity of DMRP, without influencing the stimulated activity. If we succeeded with such perturbation of the membrane composition of the vesicles, we would be able to determine the linear free energy relationship for such perturbed membranes and thus elucidate the presence of an endogenous modifier.

Therefore, we investigated the basal and NEM-GS stimulated ATPase activity of Sf9 membrane vesicles treated with different empty cyclodextrins of 10mM

concentration (for details see Methods). Basal and NEM-GS stimulated ATPase activities of the samples treated with different CD species normalised to the control sample are depicted in Figure 5.40. From the tested CD species only 2298 and 2285 caused significant inhibition of the basal activity. The CD species 2285 eliminated the NEM-GS stimulated ATPase activity as well, thus showing a potential inhibitory effect of DMRP function. In contrast, CD 2298 did not influence NEM-GS stimulated ATPase activity, reflecting a specific interaction of this CD on the basal ATPase activity of DMRP (Figure 5.41.).

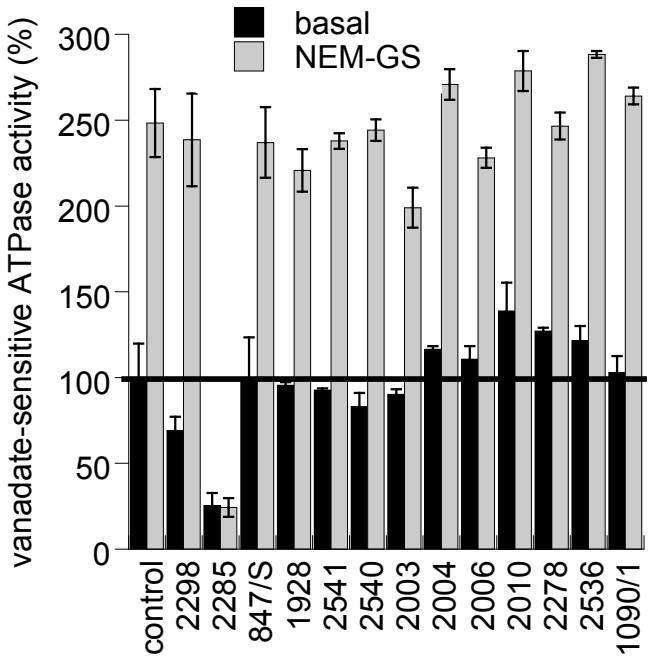

Figure 5.40.: Effect of cyclodextrin treatment on the basal and stimulated ATPase activity of DMRP *Vanadate–sensitive ATPase activity of cyclodextrin treated and control Sf9 membrane vesicles overexpressing DMRP in the absence or in the presence of 5 mM NEM-GS. Experiments were performed at 37˚C for 5 min incubation at 3.3 mM of Mg^{2+}ATP concentration, and normalised for basal activity of the control. Error bars depict the standard deviation of the estimate of mean value.*

Treatment of vesicles with CD 847/S as a control did not influence either the basal or the NEM-GS stimulated ATPase activity (data not shown).

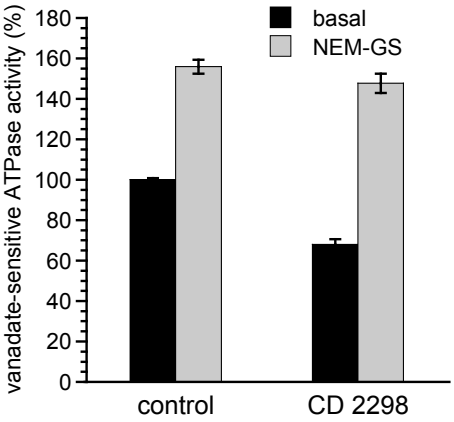

Figure 5.41.: Effect of cyclodextrin 2298 treatment on the basal and stimulated ATPase activity of DMRP *Vanadate–sensitive ATPase activity of cyclodextrin treated and control Sf9 membrane vesicles overexpressing DMRP in the absence or in the presence of 5 mM NEM-GS. Experiments were performed at 37˚C for 5 min incubation at 3.3 mM of Mg^{2+}ATP concentration, and normalised for basal activity of the control. The standard error of the estimate of mean value (S.E.M.) is depicted.*

The basal activity of DMRP with CD 2298 treatment was inhibited by 32%, and we could not succeed to obtain higher inhibition effect by applying different treatment conditions. Therefore, we concluded that this treatment is not applicable in LFER analysis, since due to the low modulatory effect of CD 2298 on the ATPase activity of DMRP LFER plots would still not be conclusive. However, experiments with empty cyclodextrins provided further indirect evidence for the presence of an endogenous modifier in the Sf9 vesicles.

6. Discussion

To resolve the evolutionary relationship between the human and *Drosophila* ABCC proteins we have subjected the entire protein sequences to a phylogenetic analysis. Our analysis revealed close relationship of DMRP to the long human MRPs, identifying DMRP as the *Drosophila melanogaster* orthologue of human MRP1, 2, 3 and 6. Comparison of the sequence of DMRP to that of hMRP1, with experimentally proven membrane topology, revealed that DMRP shows the canonical 5+6+6 long MRP membrane topology in contrast to the previously published predicted membrane arrangement.

At the beginning of our investigations, the function of DMRP was completely unknown, data were only available of the gene and the mRNA level. To characterise DMRP function, we expressed the protein in the Sf9 baculovirus heterologous expression system, previously shown in our laboratory to be suitable for the characterisation of the human MRPs. Our preliminary experiments indicated that DMRP harboured outstanding activity in *in vitro* assays, consequently we assumed that the *Drosophila* orthologue of long human MRPs might be a suitable MRP model protein. Therefore, we systematically investigated DMRP function in comparative *in vitro* assays to analyse the characteristics of DMRP in the light of its human orthologues. We determined the ability of DMRP to transport numerous human MRP substrates in vesicular transport experiments, we tested an array of human MRP inhibitors on DMRP function and characterised its ATPase cycle by measuring nucleotide binding, trapping and vanadate-sensitive ATPase activity.

Using isolated inside-out Sf9 membrane vesicles we characterised the transport activity of the protein with seven different human MRP substrates ([^{3}H]ß-estradiol 17-ß-D-glucuronide, [^{3}H]leukotriene C_4, and [^{3}H]cyclic AMP, calcein, Fluo4-AM, Fluo3, and carboxydichlorofluorescein)

Ability of the human long MRPs, MRP1 (Jedlitschky et al., 1996; Loe et al., 1996), MRP2 (Cui et al., 1999), MRP3 (Zelcer et al., 2001; Zeng et al., 2000), and MRP7 (Chen et al., 2003) to transport $E_2$17ßDG, the major metabolic derivative of estradiol, had been shown previously, the only exception being MRP6, which was found to be unable of transporting this compound at a measurable rate (Belinsky et al., 2002). The majority of these proteins showed modest capacity and high K_m value for $E_2$17ßDG transport (apparent K_m of 10-70 μM) with the exception of MRP2, which possessed high apparent K_m value, but showed the highest capacity for this substrate among human long MRPs (Bodo et al., 2003a). Our comparative analysis revealed that DMRP possessed a 50 ± 25 nmol/mg of membrane protein/min transport activity, that was 4.6 times higher turnover for this substrate than that of hMRP2, and taking the expression levels in consideration reflect about 18 times higher turnover for DMRP than that of hMRP2. However, similarly to hMRP2, the determined apparent K_m value for DMRP dependent $E_2$17ßDG transport was found to be high (344 ± 182 μM). Therefore we considered DMRP as a unique high capacity transporter for $E_2$17ßDG, resembling the properties of MRP2, as both transporters show high K_m and transport rate values.

Since the inflammatory mediator leukotriene C_4 (LTC_4) is an established MRP substrate due to the fact that all long MRPs are capable of transporting LTC_4 (Chen et al., 2003; Cui et al., 1999; Ilias et al., 2002; Leier et al., 1994; Zeng et al., 2000), we investigated the LTC_4 transport properties of DMRP, as well. Unexpectedly, we found that DMRP is able to transport LTC_4 at a remarkable high turnover at even 0˚C. We determined the transport kinetic parameters of this activity on ice. To be able to directly compare transport activity data of DMRP to that of hMRP1 we applied a different approach and measured transport activities at 23˚C with dramatically reduced vesicle content in case of DMRP. We found that the maximal transport rate of DMRP for LTC_4 was approximately 40 times higher than that of the physiologically relevant hMRP1 (3038±666 and 73± 15 pmol/mg of membrane protein/min for DMRP and MRP1, respectively), while DMRP possessed slightly higher apparent K_m value

for LTC_4 than MRP1 (231 ± 60 nM and 187 ± 47 nM for DMRP and MRP1, respectively). The V_{max} value of LTC_4 transport determined at 23˚C with reduced vesicle content was in line with the V_{max} value estimated from measurements performed at 0˚C, while at 0˚C we determined a lower apparent K_m value (58 ± 11nM) for the DMRP dependent LTC_4 transport activity. The two different approaches for determining transport kinetic values revealed that the rate limiting factor of the LTC_4 transport activity at high temperatures was not the too high inner concentration of the accumulated tracer in the inside-out vesicles, but some other factor, most probably the amount of LTC_4 available in the reaction buffer. This hypothesis could not be investigated in details, due to the low maximal applicable concentration of LTC_4 (as a result of the methanol content of the LTC_4 stock solution).

For the short MRP substrate, cyclic AMP (Chen et al., 2001; Jedlitschky et al., 2000), we could not detect any DMRP dependent transport activity.

Previously, hMRP1 dependent calcein (Feller et al., 1995), hMRP1 and hMRP2 dependent fluo3 (Keppler et al., 1999; Kyle-Cezar F, 2007; Nies et al., 1998) and hMRP2 and hMRP5 dependent carboxydichlorofluorescein (CDCF) transport (Pratt et al., 2006) has been described. We investigated the ability of DMRP to transport these fluorescent substrates in vesicular transport experiments and determined transport kinetic parameters. In our experiments using flow cytometry, the apparent K_m values could be determined, whereas the determined maximal transport activity values were only arbitrary units, due to the lack of calibration. Therefore turnover rates could only be compelled if activities of the different transporters were measured in the very same experiments, revealing relative turnover ratio differences of the investigated transporters.

We determined the apparent K_m values for three fluorescent substrates, calcein, fluo3 and carboxydichlorofluorescein (CDCF). The determined apparent K_m values were found to be 1.15 ± 0.17 μM, 0.37 ± 0.13 μM and 4.1 ± 0.6 μM for calcein, fluo3 and CDCF, respectively in case of DMRP and 0.81± 0.40 μM for fluo3 in case of MRP2. We detected a high apparent turnover rate for DMRP for

all the above fluorescent substrates, while hMRP2 investigated in parallel showed only moderate transport activity for fluo3 and CDCF. Based on considerations described above, we could only determine the relative turnover ratio for fluo3 transport for DMRP and hMRP2. We detected 8.4 times higher turnover rate for DMRP than for hMRP2 for this substrate. The hMRP1 dependent transport activities were not possible to investigate in our FACS measurements, possibly due to the limits of the sensitivity of our assay and the relatively low turnover of hMRP1 for these substrates.

In transport inhibition experiments we detected cross-inhibitory effect of LTC_4 and $E_2$17ßDG raising the possibility that the binding sites of these substrates are overlapping in case of DMRP, similarly to the case of hMRP1 (Loe et al., 1996).

We investigated the inhibitor profile of DMRP and found that the organic anions, probenecid, benzbromarone, indomethacin, and the leukotriene receptor antagonist MK571 exhibited potent inhibitory effects on DMRP function at relevant concentration ranges, that negatively impact the function of the human orthologues, as well (Bakos et al., 2000; Bakos et al., 1998; Bodo et al., 2003a; Bodo et al., 2003b; Ilias et al., 2002).

Taken together, our transport measurements demonstrated that DMRP harboured overlapping combined substrate specificity for the human long MRP substrates, moreover, DMRP possessed unusually high transport turnover rates. In addition, DMRP exhibited an inhibitor profile similar to that of the human MRPs.

Detecting such high transport activity rates for DMRP made us curious about its ATP hydrolytic cycle, since it seemed very likely that this transporter harboured an unusually high ATPase turnover coupled to such an intensive substrate transport activity.

To analyse the ATP hydrolytic cycle, we first investigated the ability of DMRP to bind the isotope labelled azido-ATP analogue, Mg-8-N_3-[α-^{32}P]ATP, and to form the trapped nucleotide transition state complex in the presence of trapping

anions, fluoroaluminate and vanadate. We have shown similar functionality of DMRP in these assays to the function of hMRP1. The presence of substrates did not influence DMRP dependent trapping of azido-ATP significantly, possibly due to the relatively low influence of these compounds on the turnover of the ATP hydrolytic cycle.

To further characterise the ATP hydrolytic characteristics of DMRP, we performed vanadate-sensitive ATPase activity measurements. These measurements, conducted in the absence of any external modulators, revealed that DMRP has the highest vanadate-sensitive basal ATPase activity (68-75 nmol P_i/mg membrane protein/min) of any MRP studied to date (Bakos et al., 2000; Bodo et al., 2003b; Deeley et al., 2006). This high level basal ATPase activity, though being unique in the MRP subfamily, does not stand alone among ABC transporters, as e.g., MDR1 and ABCG2 possess similar high level basal ATPase activities (Ozvegy et al., 2002; Sarkadi et al., 1992).

The high basal activity of DMRP could be the consequence of several different factors. On one hand, DMRP might possess such a high basal ATPase activity due to its inherent characteristics. The fact that *dMRP* was shown to be expressed in *Drosophila melanogaster* in all investigated life stages (Tarnay et al., 2004), and that DMRP was detected in adult wild type fly and membrane preparations of S2 cells (this work) suggested that DMRP is expressed ubiquitously. Taking into consideration this prevalence and the high basal ATPase activity of DMRP, we considered this possibility to be unlikely, since the presence of such an active protein hydrolysing high amounts of ATP uncoupled from any useful transport function seems to be not feasible. Though the possibility of selective and potent regulation of DMRP function *in vivo* cannot be excluded.

On the other hand, Sf9 membranes might contain an endogenous compound that positively modulates DMRP activity either by allosteric modulation or by being transported as a substrate. (Alternatively, Sf9 membranes may lack a putative negative regulator, which being present in *Drosophila* could inhibit or regulate the high ATP hydrolysing activity of DMRP *in vivo*.)

Finally, it is also possible that the high activity of DMRP detected in our *in vitro* experiments arose from the fact that it is an insect protein expressed in an insect cell providing optimal conditions (e.g. suitable membrane composition, post transcriptional modification etc.) for the protein function, in the absence of any hypothetical endogenous modifier. It is accepted that the function of human ABC proteins in the Sf9 cells sometimes might be impaired, so that the detected difference in the turnover rates of human and *Drosophila* proteins might have reflected the effects of the applied expression system.

Due to the fact that ATP hydrolysis and substrate transport are highly coupled mechanisms orchestrated by the communication of the different domains of the ABC transporters, substrates influence ATP hydrolysis most commonly via stimulating basal ATPase activity of the protein.

The basal ATPase activity of DMRP could be further stimulated approximately two fold in the presence of NEM-GS and probenecid, showing that DMRP is not fully activated in the absence of exogenous stimulators. However, the investigated DMRP transport substrates LTC_4, calcein, and $E_2$17ßDG inhibited the basal ATPase activity significantly.

The fact that these transported substrates inhibit ATPase activity, together with the high-level of basal activity of DMRP compared to human MRPs, underscores the possibility that there is an endogenous modifier (an endogenous substrate or an endogenous allosteric activator) present in the Sf9 cell membrane preparation. The presence of such an endogenous modifier might stimulate the intrinsic ATPase activity to the measured level (here referred to as basal ATPase activity) keeping the transporter in a partially activated state. This partial activation would imply that the transporter effectively hydrolyses ATP in the absence of any exogenous substrates. The administered exogenous substrates might successfully compete with the hypothetical endogenous modulator, potentially causing a substrate dependent apparent inhibition of the vanadate-sensitive ATPase activity. The above endogenous modifier hypothesis could explain the presented odd characteristics of the DMRP ATPase reaction. Experiments with

cyclodextrin 2298 are also consistent with this hypothesis, since this cyclodextrin species significantly reduced the basal ATPase activity while did not alter NEM-GS stimulated ATPase activity. The possible explanation of this fact is that cyclodextrin 2298 specifically modified the membrane composition of the Sf9 membrane vesicles, potentially by extracting the endogenous modifier from the membrane, thus causing apparent inhibition of the basal ATPase activity. The fact that the NEM-GS stimulated activity remained the same was in line with this theory, and supported the idea of the DMRP function remaining intact despite of the treatment with cyclodextrin 2298.

We aimed to further analyse the endogenous modifier hypothesis discussed above, in order to see weather basal activity is the consequence of the presence of an endogenous substrate or endogenous activator. To clarify the nature of the endogenous modifier linear free energy relationship (LFER) experiments were performed. We determined the initial velocity of the ATP hydrolysis at 25 and 37˚C in the absence (basal activity) or in the presence of external substrates (substrate coupled activity), and plotted the log turnover numbers determined at 37˚C as a function of the log turnover numbers determined at 25˚C. We determined the regression line representing substrate coupled ATPase activities, in the presence of various concentrations of $E_2$17ßDG and LTC_4, and the point representing the basal ATPase activity on the LFER plot. The mean value of the basal ATPase activity fitted to the line corresponding to the substrate transport coupled ATPase activities.

If the point representing the basal ATPase activity did not fit significantly to the regression line determined for substrate coupled ATPase activities, one could conclude that the basal activity reflects a different mechanism (other than substrate coupled activity) characterised by a distinct rate-limiting step. Such a result would support the presence of an endogenous allosteric activator molecule in the Sf9 membrane rather than the presence of an endogenous substrate. The lack of such an endogenous substrate using LFER analysis was previously shown for MDR1 by al Shawi et al. (Al-Shawi et al., 2003).

The fact that the mean value representing the basal activity fitted to the regression line of the substrate coupled activity on the LFER plot allowed for the following alternative interpretations.

On one hand, basal activity could be an endogenous substrate coupled activity, with the same rate-limiting step for ATP hydrolysis detected for $E_2$17ßDG and LTC_4 transport coupled ATPase activities, thus fitting to the determined regression line.

On the other hand, basal activity could be the consequence of an endogenous allosteric activator (allosteric activity). In such a case ATP hydrolysis likely harbours a different rate-limiting step in contrast to the substrate coupled activity, therefore this allosteric activity is likely characterised by a different regression line. If so, than there is a probability that the regression lines of the substrate coupled and the allosteric activities cross each other on the LFER plot. If so, than the determined point of the basal ATPase activity (here interpreted as allosteric activity) might be located on the the regression line of the coupled activity just due to a coincidence, being present at the crossing points of the two distinct regression lines.

Based on the above considerations, the question concerning the presence of an endogenous allosteric activator or an endogenous substrate could not be answered.

In our experiments we demonstrated that the close relative high turnover DMRP is an applicable MRP model protein sharing functional characteristics with the human MRPs. Studies concerning the steady state thermodynamics of the catalytic cycle of ABC transporters require highly active proteins. The thermodynamics of two human ABC transporters, MDR1 (Al-Shawi et al., 2003; Sauna et al., 2006) and CFTR (Csanady et al., 2006) have been studied in detail so far. Such investigations have previously not been possible for any MRP due to their low turnover rate.

We aimed to apply DMRP as a model in such investigations to reveal characteristics of the catalytic cycle of MRP-type proteins. Therefore we investigated the vanadate-sensitive ATPase activity as a function of temperature, over a 20-centigrade temperature range, in the absence or in the presence of the substrates LTC_4 and NEM-GS, at saturating concentrations. We obtained linear Eyring relationships for the basal, the NEM-GS stimulated, and the LTC_4 inhibited ATPase activities. The linearity of these plots indicated that single overall rate-limiting steps were detected for the above three enzymatic reactions. Employing thermodynamic calculations based on the linearised Eyring equation we have determined the apparent thermodynamic parameters, the enthalpic, entropic, and Gibbs free energy terms, for the rate limiting transition-states at 37˚C. The determined Gibbs free energy of the transition-state was not significantly different for the basal, the stimulated, and the inhibited reactions. Despite of the similar Gibbs free energy values, the composition of this term was quite different for the basal and the modified ATPase activity reactions. Interestingly, in the case of the activated and the inhibited reactions we found the same phenomenon: the activation enthalpy was elevated approximately 1.3 times compared to the value detected for basal activity, while this energetically unfavourable change was compensated for by the dramatic elevation of the activation entropy. The phenomenon that the presence of a transported substrate elevates the activation enthalpy (and its related parameter, the activation energy) seems to be odd, but similar effects have been reported previously for MDR1 (Al-Shawi et al., 2003). The large changes detected in activation entropy represent substantial changes in the degree of freedom during formation of the transition-state. In light of our experiments it is very likely that large conformational rearrangements happen during catalysis in the presence of exogenous modulators as compared to the externally not modified reaction cycle. These changes in entropy might reflect the crosstalk between the ATP hydrolysis and drug transport. In the absence of exogenous modulators, the same change in the Gibbs free energy has been achieved by a distinct way. Relatively low activation energy had to be overcome, but there was a lot smaller positive entropic contribution to this energetics.

In conclusion we observed two distinct rate-limiting steps for the catalytic mechanism of DMRP, one in the absence and another in the presence of exogenous substrates. The question, whether the detected thermodynamic characteristics of the transition state in the absence of exogenous modulators is the consequence of the presence of an endogenous allosteric activator or an endogenous substrate, requires further investigations.

Previous analysis of the catalytic cycle of MDR1 revealed two distinct rate limiting steps for the formation of the transition-state intermediates of ATP-hydrolysis, one coupled and one uncoupled to drug transport (Al-Shawi et al., 2003). It is important to note that in case of the MDR-type ABC transporters the two NBDs are functionally equivalent (Beaudet and Gros, 1995) and ATP hydrolysis is an alternating process (Sauna and Ambudkar, 2000). However MRP1-type proteins harbour two functionally asymmetric NBDs and their catalytic mechanism is presumably different from that of MDR-type proteins (Deeley et al., 2006).

Importantly, our results suggest that the transition state formation of the catalytic intermediates shares common characteristics for MDR and MRP-type proteins, in respect to their steady-state thermodynamic characteristics.

To provide data for the understanding of the physiological role of DMRP we aimed to study the localisation of the endogenous protein in *Drosophila melanogaster* S2 cells by confocal microscopy, but unfortunately the only available antibody for DMRP was found to be not applicable in such experiments. However, in membrane preparations of S2 cells we were able to detect the presence of DMRP by Western blotting. We could also detect the presence of DMRP in adult flies, both in separated heads and bodies, using Western blot technique. Our data complemented the previously published data concerning mRNA levels of *dMRP* suggesting ubiquitous expression of *dMRP* gene.

We investigated the effect of the insect moulting hormone 20-OH ecdysone on the endogenous levels of DMRP in S2 cells using Western blot technique. We did not find any effect of the hormone in the applied concentrations and detected time points. We did not find any interaction of the hormone with DMRP *in vitro* neither in ATPase or transport activity, nor in trapping experiments. This was in line with the unpublished results of our collaborator, Robinow et al. Their experiments, applying northern blot technique, revealed that *dMRP* gene is not inducible by 20-OH ecdysone, neither in adult nor in larval tissues.

ABC transporters were found to be involved in the resistance of various organisms against pesticides. *In vitro* and *in vivo* studies of MDR1 have shown interaction of pesticides with the protein (Bain and LeBlanc, 1996; Shabbir et al., 2005; Smital et al., 2000; Sreeramulu et al., 2007), while the role of MRPs in pesticide resistance has only recently been taken under investigation. *In vivo* studies on *MRP1* deficient mice suggested that MRP1 may be responsible for protecting the seminiferous tubules from methoxychlor-induced damage (Dupuy et al., 2006; Tribull et al., 2003), and *in vitro* experiments have shown the anti-parasitic drugs ivermectin and moxidectin to be substrates of MRP1 (Lespine et al., 2006).

We investigated the possibility that DMRP is able to transport the commercially available pesticides, bioalletrin, fenitrothion, DDT and aldicarb potentially providing chemo-immunity against these potent pesticides. We showed specific interaction of bioalletrin and fenitrothion with DMRP both in ATPase activity and $E_2$17ßD glucuronide transport inhibition experiments. Therefore we concluded that these pesticides are candidate substrates for the investigated DMRP isoform. DDT showed interaction with DMRP in ATPase activity experiments but the specificity of this interaction was questionable. Since DDT did not alter the $E_2$17ßD glucuronide and the [^{3}H]leukotriene C_4 transport, we interpreted these data as DDT probably not having any specific interaction with DMRP. We detected no interactions of DMRP with aldicarb neither in transport nor in ATPase activity experiments. In conclusion we considered that aldicarb and DDT were likely not substrates for the investigated DMRP isoform.

However, our collaborators at Hawaii investigated the effect of these pesticides on the survival of wild type (wt) and *dMRP-/-* flies in direct contact toxicity assays (Robinow et al., unpublished data). They have observed that *dMRP*-/- flies, lacking all potential DMRP isoforms, were sensitive to DDT and aldicarb in comparison to wt flies, while there was no difference between survivals of wt and *dMRP*-/- animals for fenitrothion and bioallethrin.

Taking into consideration the various DMRP isoforms present in *Drosophila* and the potential complex compartmentalisation and metabolism of the above pesticides *in vivo* in contrast to our *in vitro* experiments conducted with overexpressed protein and unmodified drugs in simplified assay systems we consider that these *in vitro* and *in vivo* data are not inconsistent.

7. Conclusions

We have shown that the Drosophila Multidrug Resistance-associated Protein (DMRP) is the fruit fly orthologue of the long human MRPs, MRP1, 2, 3 and 6. Instead of the domain arrangement previously published by Grailles et al, based on *in silico* analysis, we proposed a new membrane topology model for DMRP.

We expressed the protein in Sf9 cells, using the baculovirus expression system established and extensively used in our laboratory previously for the characterisation of human MRPs. Since our preliminary experiments indicated that DMRP harboured outstanding turnover among MRPs studied so far, we decided to investigate its characteristics in systematic comparative functional assays. To reveal whether DMRP could be a useful model protein for its human orthologues we have investigated its substrate and inhibitor profile and its ATP hydrolytic cycle.

We have studied the transport activity of DMRP for established human MRP substrates, such as leukotriene C4, ß-estradiol 17-ß-D-glucuronide, calcein, fluo3, and carboxydichlorofluorescein to determine the related transport kinetic parameters. We found that DMRP was able to transport these human long MRP substrates and showed a combined substrate specificity of its human orthologues. Moreover, DMRP possessed the highest turnover rate for all the above human MRP substrates ever detected. Similarly, to the combined substrate specificity, we detected an overlapping inhibitory profile for DMRP resembling the characteristics of human MRPs.

In conclusion, we demonstrated that DMRP was a functional orthologue of the human long MRPs. We considered DMRP as a suitable model protein of human long MRPs, harbouring similar substrate specificity, inhibitor profile and kinetics, whereas possessing outstanding transport capacity.

Moreover, we detected unusually high vanadate-sensitive basal ATPase activity for DMRP, which was inducible by NEM-GS and probenecide. However, as a surprise, established substrates inhibited this activity significantly. Taking the high level of basal activity and the inhibitory character of the transported

substrates in consideration, we hypothesised the presence of an endogenous modifier in the Sf9 cell membrane preparations. This endogenous modifier either could be an endogenous substrate or an endogenous allosteric activator.

To further analyse the nature of the endogenous modifier we applied linear free energy relationship (LFER) analysis. Since the mean value of the basal activity fitted to the regression line of the substrate coupled activities in the LFER analysis, we could not conclusively discriminate between the presence of an endogenous substrate or an endogenous allosteric activator. Therefore further investigations are necessary to characterise the nature of this endogenous modifier.

Taking advantage of the remarkably high vanadate-sensitive basal ATPase activity of DMRP we determined the transition-state thermodynamic parameters of the ATPase cycle. Our transition state thermodynamic analysis revealed two distinct rate-limiting steps, one for the basal and another for the modulated (both stimulatory and inhibitory) activity, resulting in the same overall change in the activation free energy. Since such investigations require highly active transporters, and human MRPs show only modest ATPase activity, here we are the first to present data concerning the thermodynamics of an MRP-type ABC-transporter. Our data suggest that independently of the previously published differences between the catalytic cycle of MDR and MRP-type proteins, the steady-state formation of the catalytic intermediates of these proteins might be similar in respect to their thermodynamic features.

Studying the endogenous expression of DMRP we provided supporting evidence for the idea that products of the *dMRP* gene are ubiquitously present in Drosophila flies and embryonic cells.

In addition we have found two pesticides, bioallethrin and fenitrothion, as potential candidate substrates for DMRP.

8. Summary

ATP Binding Cassette transporters are ubiquitous integral membrane proteins transporting ligands across biological membranes, a process critical for most aspects of cell physiology. Some of them are clinically important with their dysfunction underlying human genetic diseases, such as cystic fibrosis, while others, e.g. MDR1 and MRP1, are capable of extruding wide range of cytotoxic agents resulting in multidrug resistance phenotype of cancer cells.

The human long MRPs, MRP1, 2, 3 and 6, have only one fruit fly orthologue, Drosophila MRP (DMRP). We have expressed this protein in Sf9 cells, and investigated its activity in comparative functional assays. We demonstrated that DMRP is a useful model protein of human long MRPs, harbouring combined substrate specificity, similar inhibitory profile, and kinetics to its human orthologues. However, DMRP possesses outstanding turnover for the investigated established human MRP substrates, LTC_4, $E_2$17ßD-glucuronide, calcein, fluo3 and CDCF. Moreover, DMRP has a high-level NEM-GS and probenecid inducible vanadate-sensitive basal ATPase activity. As a surprise, this activity is inhibited by the established substrates. As an explanation for this odd feature we hypothesised the presence of an endogenous modifier. Our results derived from linear free energy relationship analysis were not conclusive to further characterise the nature of this modifier. The question weather this endogenous modifier is an endogenous substrate or an allosteric activator remains unsolved. However, taking advantage of the remarkable activity of DMRP, we determined the transition-state thermodynamic parameters of the ATPase cycle. Our analysis revealed two distinct rate-limiting steps for basal and for modulated ATPase activities, resulting in the same change of activation free energy. Since the modest ATPase activity of human MRPs did not allow such investigations we are the first to present data concerning thermodynamics of an MRP-type transporter. Our data suggests similarities of the steady-state thermodynamics of the catalytic cycle of MDR and MRP-type proteins. In addition, we provided data for the expression of endogenous DMRP and identified two potential pesticide substrates.

9. Összefoglalás

Az ABC transzporterek az élővilágban széleskörűen elterjedt integráns membránfehérjék. Tevékenységük, a membránokon keresztüli aktív transzport élettanilag több szempontból is kiemelt fontosságú. A humán genom 48 ABC génje közül többen állnak öröklődő betegségek (például a cisztikus fibrosis) hátterében, míg mások (például az MDR1 és az MRP1) a tumorok multidrog rezisztenciájának kialakításáért felelősek. A Drosophila MRP (DMRP) az emberi ”hosszú” MRP-k egyetlen ecetmuslica ortológja. Ezt a fehérjét Sf9 sejtekben fejeztük ki és aktivitását összehasonlító vizsgálatokban jellemeztük. Kimutattuk, hogy a DMRP az emberi homológok jó modellje, mivel azokkal átfedő szubsztrát specificitással, inhibítor profillal és kinetikai jellemzőkkel bír, ugyanakkor kiemelkedően magas transzport kapacitás jellemzi fontos modellértékű humán szubsztrátok (LTC_4, ösztradiol-glükuronid, calcein, fluo3 and CDCF) tekintetében. Megállapítottuk, hogy a DMRP kiugróan magas vanadát-szenzitív alap ATP-áz aktivitással rendelkezik, amely NEM-GS és probenecid jelenlétében fokozható, ugyanakkor meglepő módon a transzportált szubsztrátok ezt az aktivitást gátolták. Ezen eredményeink alapján feltételeztük, hogy a jelenség hátterében egy az Sf9 sejtekben endogén módon jelenlévő ismeretlen DMRP szubsztrát vagy allosztérikus aktivátor áll. A DMRP kiemelkedő aktivitását alapul véve termodinamikai szempontból jellemeztük a fehérje ATP-áz ciklusának átmenti állapotát. Kísérleteinkben jól elkülöníthetően különöző sebességmeghatározó lépést tapasztaltunk az alapaktivitás illetve a modulált aktivitások esetében, ugyanakkor mindkét esetben azonos aktivációs szabadenergia változást határoztunk meg. Mivel az emberi MRP-k alacsony aktivitása hasonló vizsgálatokat nem tesz lehetővé, kísérleteink a modellértékű ecetmuslica DMRP fehérjén az elsők az MRP-típusú ABC-transzporterek körében. Eredményeink jelentősége, hogy vizsgálataink alapján az MDR és MRP-típusú transzporterek katalitikus ciklusának átmeneti állapota termodinamikai szempontból hasonló, bár a két fehérje katalitikus ciklusa eltérő. Kísérleteinkben ezen kívül vizsgáltuk a fehérje endogén expresszióját valamint azonosítottuk két potenciális peszticid szubsztrátját.

10. Bibliography

Adachi, Y., Suzuki, H., Schinkel, A. H., and Sugiyama, Y. (2005). Role of breast cancer resistance protein (Bcrp1/Abcg2) in the extrusion of glucuronide and sulfate conjugates from enterocytes to intestinal lumen. Mol Pharmacol *67*, 923-928.

Adams, M. D., Celniker, S. E., Holt, R. A., Evans, C. A., Gocayne, J. D., Amanatides, P. G., Scherer, S. E., Li, P. W., Hoskins, R. A., Galle, R. F.*, et al.* (2000). The genome sequence of Drosophila melanogaster. Science *287*, 2185-2195.

Akasaka, T., Klinedinst, S., Ocorr, K., Bustamante, E. L., Kim, S. K., and Bodmer, R. (2006). The ATP-sensitive potassium (KATP) channel-encoded dSUR gene is required for Drosophila heart function and is regulated by tinman. Proc Natl Acad Sci U S A *103*, 11999-12004.

Al-Shawi, M. K., Polar, M. K., Omote, H., and Figler, R. A. (2003). Transition state analysis of the coupling of drug transport to ATP hydrolysis by P-glycoprotein. J Biol Chem *278*, 52629-52640.

Allikmets, R., Singh, N., Sun, H., Shroyer, N. F., Hutchinson, A., Chidambaram, A., Gerrard, B., Baird, L., Stauffer, D., Peiffer, A.*, et al.* (1997). A photoreceptor cell-specific ATP-binding transporter gene (ABCR) is mutated in recessive Stargardt macular dystrophy. Nat Genet *15*, 236-246.

Anaka, M., MacDonald, C. D., Barkova, E., Simon, K., Rostom, R., Godoy, R. A., Haigh, A. J., Meinertzhagen, I. A., and Lloyd, V. (2008). The white gene of Drosophila melanogaster encodes a protein with a role in courtship behavior. J Neurogenet *22*, 243-276.

Bain, L. J., and LeBlanc, G. A. (1996). Interaction of structurally diverse pesticides with the human MDR1 gene product P-glycoprotein. Toxicol Appl Pharmacol *141*, 288-298.

Bakos, E., Evers, R., Sinko, E., Varadi, A., Borst, P., and Sarkadi, B. (2000). Interactions of the human multidrug resistance proteins MRP1 and MRP2 with organic anions. Mol Pharmacol *57*, 760-768.

Bakos, E., Evers, R., Szakacs, G., Tusnady, G. E., Welker, E., Szabo, K., de Haas, M., van Deemter, L., Borst, P., Varadi, A., and Sarkadi, B. (1998). Functional multidrug resistance protein (MRP1) lacking the N-terminal transmembrane domain. J Biol Chem *273*, 32167-32175.

Bakos, E., Hegedus, T., Hollo, Z., Welker, E., Tusnady, G. E., Zaman, G. J., Flens, M. J., Varadi, A., and Sarkadi, B. (1996). Membrane topology and glycosylation of the human multidrug resistance-associated protein. J Biol Chem *271*, 12322-12326.

Beaudet, L., and Gros, P. (1995). Functional dissection of P-glycoprotein nucleotide-binding domains in chimeric and mutant proteins. Modulation of drug resistance profiles. J Biol Chem *270*, 17159-17170.

Belinsky, M. G., Chen, Z. S., Shchaveleva, I., Zeng, H., and Kruh, G. D. (2002). Characterization of the drug resistance and transport properties of multidrug resistance protein 6 (MRP6, ABCC6). Cancer Res *62*, 6172-6177.

Bensadoun, A., and Weinstein, D. (1976). Assay of proteins in the presence of interfering materials. Anal Biochem *70*, 241-250.

Bera, T. K., Iavarone, C., Kumar, V., Lee, S., Lee, B., and Pastan, I. (2002). MRP9, an unusual truncated member of the ABC transporter superfamily, is highly expressed in breast cancer. Proc Natl Acad Sci U S A *99*, 6997-7002.

Berge, K. E., von Bergmann, K., Lutjohann, D., Guerra, R., Grundy, S. M., Hobbs, H. H., and Cohen, J. C. (2002). Heritability of plasma noncholesterol sterols and relationship to DNA sequence polymorphism in ABCG5 and ABCG8. J Lipid Res *43*, 486-494.

Bodo, A., Bakos, E., Szeri, F., Varadi, A., and Sarkadi, B. (2003a). Differential modulation of the human liver conjugate transporters MRP2 and MRP3 by bile acids and organic anions. J Biol Chem *278*, 23529-23537.

Bodo, A., Bakos, E., Szeri, F., Varadi, A., and Sarkadi, B. (2003b). The role of multidrug transporters in drug availability, metabolism and toxicity. Toxicol Lett *140-141*, 133-143.

Borst, P., de Wolf, C., and van de Wetering, K. (2007). Multidrug resistance-associated proteins 3, 4, and 5. Pflugers Arch *453*, 661-673.

Borycz, J., Borycz, J. A., Kubow, A., Lloyd, V., and Meinertzhagen, I. A. (2008). Drosophila ABC transporter mutants white, brown and scarlet have altered contents and distribution of biogenic amines in the brain. J Exp Biol *211*, 3454-3466.

Brooks-Wilson, A., Marcil, M., Clee, S. M., Zhang, L. H., Roomp, K., van Dam, M., Yu, L., Brewer, C., Collins, J. A., Molhuizen, H. O*., et al.* (1999). Mutations in ABC1 in Tangier disease and familial high-density lipoprotein deficiency. Nat Genet *22*, 336-345.

Chen, C. J., Chin, J. E., Ueda, K., Clark, D. P., Pastan, I., Gottesman, M. M., and Roninson, I. B. (1986). Internal duplication and homology with bacterial transport proteins in the mdr1 (P-glycoprotein) gene from multidrug-resistant human cells. Cell *47*, 381-389.

Chen, Z. S., Guo, Y., Belinsky, M. G., Kotova, E., and Kruh, G. D. (2005). Transport of bile acids, sulfated steroids, estradiol 17-beta-D-glucuronide, and leukotriene C4 by human multidrug resistance protein 8 (ABCC11). Mol Pharmacol *67*, 545-557.

Chen, Z. S., Hopper-Borge, E., Belinsky, M. G., Shchaveleva, I., Kotova, E., and Kruh, G. D. (2003). Characterization of the transport properties of human multidrug resistance protein 7 (MRP7, ABCC10). Mol Pharmacol *63*, 351-358.

Chen, Z. S., Lee, K., and Kruh, G. D. (2001). Transport of cyclic nucleotides and estradiol 17-beta-D-glucuronide by multidrug resistance protein 4. Resistance to 6-mercaptopurine and 6-thioguanine. J Biol Chem *276*, 33747-33754.

Cheng, S. H., Rich, D. P., Marshall, J., Gregory, R. J., Welsh, M. J., and Smith, A. E. (1991). Phosphorylation of the R domain by cAMP-dependent protein kinase regulates the CFTR chloride channel. Cell *66*, 1027-1036.

Cole, S. P., Bhardwaj, G., Gerlach, J. H., Mackie, J. E., Grant, C. E., Almquist, K. C., Stewart, A. J., Kurz, E. U., Duncan, A. M., and Deeley, R. G. (1992). Overexpression of

a transporter gene in a multidrug-resistant human lung cancer cell line. Science *258*, 1650-1654.

Cole, S. P., Sparks, K. E., Fraser, K., Loe, D. W., Grant, C. E., Wilson, G. M., and Deeley, R. G. (1994). Pharmacological characterization of multidrug resistant MRP-transfected human tumor cells. Cancer Res *54*, 5902-5910.

Cooray, H. C., Blackmore, C. G., Maskell, L., and Barrand, M. A. (2002). Localisation of breast cancer resistance protein in microvessel endothelium of human brain. Neuroreport *13*, 2059-2063.

Csanady, L., Chan, K. W., Seto-Young, D., Kopsco, D. C., Nairn, A. C., and Gadsby, D. C. (2000). Severed channels probe regulation of gating of cystic fibrosis transmembrane conductance regulator by its cytoplasmic domains. J Gen Physiol *116*, 477-500.

Csanady, L., Nairn, A. C., and Gadsby, D. C. (2006). Thermodynamics of CFTR channel gating: a spreading conformational change initiates an irreversible gating cycle. J Gen Physiol *128*, 523-533.

Csanady, L., Seto-Young, D., Chan, K. W., Cenciarelli, C., Angel, B. B., Qin, J., McLachlin, D. T., Krutchinsky, A. N., Chait, B. T., Nairn, A. C., and Gadsby, D. C. (2005). Preferential phosphorylation of R-domain Serine 768 dampens activation of CFTR channels by PKA. J Gen Physiol *125*, 171-186.

Cui, Y., Konig, J., Buchholz, J. K., Spring, H., Leier, I., and Keppler, D. (1999). Drug resistance and ATP-dependent conjugate transport mediated by the apical multidrug resistance protein, MRP2, permanently expressed in human and canine cells. Mol Pharmacol *55*, 929-937.

Daleke, D. L. (2003). Regulation of transbilayer plasma membrane phospholipid asymmetry. J Lipid Res *44*, 233-242.

Dawson, R. J., and Locher, K. P. (2006). Structure of a bacterial multidrug ABC transporter. Nature *443*, 180-185.

Dawson, R. J., and Locher, K. P. (2007). Structure of the multidrug ABC transporter Sav1866 from Staphylococcus aureus in complex with AMP-PNP. FEBS Lett *581*, 935-938.

Dazert, P., Meissner, K., Vogelgesang, S., Heydrich, B., Eckel, L., Bohm, M., Warzok, R., Kerb, R., Brinkmann, U., Schaeffeler, E*., et al.* (2003). Expression and localization of the multidrug resistance protein 5 (MRP5/ABCC5), a cellular export pump for cyclic nucleotides, in human heart. Am J Pathol *163*, 1567-1577.

De Vree, J. M., Ottenhoff, R., Bosma, P. J., Smith, A. J., Aten, J., and Oude Elferink, R. P. (2000). Correction of liver disease by hepatocyte transplantation in a mouse model of progressive familial intrahepatic cholestasis. Gastroenterology *119*, 1720-1730.

Dean, M., and Allikmets, R. (2001). Complete characterization of the human ABC gene family. J Bioenerg Biomembr *33*, 475-479.

Dean, M., and Annilo, T. (2005). Evolution of the ATP-binding cassette (ABC) transporter superfamily in vertebrates. Annu Rev Genomics Hum Genet *6*, 123-142.

Dean M, A. R., Rando Allikmets (2003). Human and Drosophila ABC Proteins (London: Academic Press, Elsevier).

Dean, M., Rzhetsky, A., and Allikmets, R. (2001). The human ATP-binding cassette (ABC) transporter superfamily. Genome Res *11*, 1156-1166.

Deeley, R. G., Westlake, C., and Cole, S. P. (2006). Transmembrane transport of endo- and xenobiotics by mammalian ATP-binding cassette multidrug resistance proteins. Physiol Rev *86*, 849-899.

DeGorter, M. K., Conseil, G., Deeley, R. G., Campbell, R. L., and Cole, S. P. (2008). Molecular modeling of the human multidrug resistance protein 1 (MRP1/ABCC1). Biochem Biophys Res Commun *365*, 29-34.

Demirel, O., Waibler, Z., Kalinke, U., Grunebach, F., Appel, S., Brossart, P., Hasilik, A., Tampe, R., and Abele, R. (2007). Identification of a lysosomal peptide transport system induced during dendritic cell development. J Biol Chem *282*, 37836-37843.

Donner, M. G., and Keppler, D. (2001). Up-regulation of basolateral multidrug resistance protein 3 (Mrp3) in cholestatic rat liver. Hepatology *34*, 351-359.

Dreesen, T. D., Johnson, D. H., and Henikoff, S. (1988). The brown protein of Drosophila melanogaster is similar to the white protein and to components of active transport complexes. Mol Cell Biol *8*, 5206-5215.

Dupuy, J., Lespine, A., Sutra, J. F., and Alvinerie, M. (2006). Fumagillin, a new P-glycoprotein-interfering agent able to modulate moxidectin efflux in rat hepatocytes. J Vet Pharmacol Ther *29*, 489-494.

Ellard, S., Flanagan, S. E., Girard, C. A., Patch, A. M., Harries, L. W., Parrish, A., Edghill, E. L., Mackay, D. J., Proks, P., Shimomura, K.*, et al.* (2007). Permanent neonatal diabetes caused by dominant, recessive, or compound heterozygous SUR1 mutations with opposite functional effects. Am J Hum Genet *81*, 375-382.

Elliott, A. M., and Al-Hajj, M. A. (2009). ABCB8 mediates doxorubicin resistance in melanoma cells by protecting the mitochondrial genome. Mol Cancer Res *7*, 79-87.

Ewart, G. D., Cannell, D., Cox, G. B., and Howells, A. J. (1994). Mutational analysis of the traffic ATPase (ABC) transporters involved in uptake of eye pigment precursors in Drosophila melanogaster. Implications for structure-function relationships. J Biol Chem *269*, 10370-10377.

Eyring, H. (1935). The Activated Complex in Chemical Reactions. The Journal of Chemical Physics *3*, 107-115.

Feller, N., Broxterman, H. J., Wahrer, D. C., and Pinedo, H. M. (1995). ATP-dependent efflux of calcein by the multidrug resistance protein (MRP): no inhibition by intracellular glutathione depletion. FEBS Lett *368*, 385-388.

Flens, M. J., Zaman, G. J., van der Valk, P., Izquierdo, M. A., Schroeijers, A. B., Scheffer, G. L., van der Groep, P., de Haas, M., Meijer, C. J., and Scheper, R. J. (1996). Tissue distribution of the multidrug resistance protein. Am J Pathol *148*, 1237-1247.

Fulop, K., Barna, L., Symmons, O., Zavodszky, P., and Varadi, A. (2009). Clustering of disease-causing mutations on the domain-domain interfaces of ABCC6. Biochem Biophys Res Commun *379*, 706-709.

Gadsby, D. C., Vergani, P., and Csanady, L. (2006). The ABC protein turned chloride channel whose failure causes cystic fibrosis. Nature *440*, 477-483.

Gerrard, B., Stewart, C., and Dean, M. (1993). Analysis of Mdr50: a Drosophila P-glycoprotein/multidrug resistance gene homolog. Genomics *17*, 83-88.

Graf, G. A., Yu, L., Li, W. P., Gerard, R., Tuma, P. L., Cohen, J. C., and Hobbs, H. H. (2003). ABCG5 and ABCG8 are obligate heterodimers for protein trafficking and biliary cholesterol excretion. J Biol Chem *278*, 48275-48282.

Grailles, M., Brey, P. T., and Roth, C. W. (2003). The Drosophila melanogaster multidrug-resistance protein 1 (MRP1) homolog has a novel gene structure containing two variable internal exons. Gene *307*, 41-50.

Gros, P., Croop, J., and Housman, D. (1986). Mammalian multidrug resistance gene: complete cDNA sequence indicates strong homology to bacterial transport proteins. Cell *47*, 371-380.

Guo, Y., Kotova, E., Chen, Z. S., Lee, K., Hopper-Borge, E., Belinsky, M. G., and Kruh, G. D. (2003). MRP8, ATP-binding cassette C11 (ABCC11), is a cyclic nucleotide efflux pump and a resistance factor for fluoropyrimidines 2',3'-dideoxycytidine and 9'-(2'-phosphonylmethoxyethyl)adenine. J Biol Chem *278*, 29509-29514.

Higgins, C. F., Hiles, I. D., Salmond, G. P., Gill, D. R., Downie, J. A., Evans, I. J., Holland, I. B., Gray, L., Buckel, S. D., Bell, A. W., and et al. (1986). A family of related ATP-binding subunits coupled to many distinct biological processes in bacteria. Nature *323*, 448-450.

Hipfner, D. R., Almquist, K. C., Leslie, E. M., Gerlach, J. H., Grant, C. E., Deeley, R. G., and Cole, S. P. (1997). Membrane topology of the multidrug resistance protein (MRP). A study of glycosylation-site mutants reveals an extracytosolic NH2 terminus. J Biol Chem *272*, 23623-23630.

Hipfner, D. R., Gauldie, S. D., Deeley, R. G., and Cole, S. P. (1994). Detection of the M(r) 190,000 multidrug resistance protein, MRP, with monoclonal antibodies. Cancer Res *54*, 5788-5792.

Hirrlinger, J., Konig, J., and Dringen, R. (2002). Expression of mRNAs of multidrug resistance proteins (Mrps) in cultured rat astrocytes, oligodendrocytes, microglial cells and neurones. J Neurochem *82*, 716-719.

Holland, I. B., and Blight, M. A. (1999). ABC-ATPases, adaptable energy generators fuelling transmembrane movement of a variety of molecules in organisms from bacteria to humans. J Mol Biol *293*, 381-399.

Hollenstein, K., Dawson, R. J., and Locher, K. P. (2007a). Structure and mechanism of ABC transporter proteins. Curr Opin Struct Biol *17*, 412-418.

Hollenstein, K., Frei, D. C., and Locher, K. P. (2007b). Structure of an ABC transporter in complex with its binding protein. Nature *446*, 213-216.

Hopfner, K. P., Karcher, A., Shin, D. S., Craig, L., Arthur, L. M., Carney, J. P., and Tainer, J. A. (2000). Structural biology of Rad50 ATPase: ATP-driven conformational control in DNA double-strand break repair and the ABC-ATPase superfamily. Cell *101*, 789-800.

Hopper, E., Belinsky, M. G., Zeng, H., Tosolini, A., Testa, J. R., and Kruh, G. D. (2001). Analysis of the structure and expression pattern of MRP7 (ABCC10), a new member of the MRP subfamily. Cancer Lett *162*, 181-191.

Hopper-Borge, E., Xu, X., Shen, T., Shi, Z., Chen, Z. S., and Kruh, G. D. (2009). Human multidrug resistance protein 7 (ABCC10) is a resistance factor for nucleoside analogues and epothilone B. Cancer Res *69*, 178-184.

Hyde, S. C., Emsley, P., Hartshorn, M. J., Mimmack, M. M., Gileadi, U., Pearce, S. R., Gallagher, M. P., Gill, D. R., Hubbard, R. E., and Higgins, C. F. (1990). Structural model of ATP-binding proteins associated with cystic fibrosis, multidrug resistance and bacterial transport. Nature *346*, 362-365.

Ilias, A., Urban, Z., Seidl, T. L., Le Saux, O., Sinko, E., Boyd, C. D., Sarkadi, B., and Varadi, A. (2002). Loss of ATP-dependent transport activity in pseudoxanthoma elasticum-associated mutants of human ABCC6 (MRP6). J Biol Chem *277*, 16860-16867.

Jedlitschky, G., Burchell, B., and Keppler, D. (2000). The multidrug resistance protein 5 functions as an ATP-dependent export pump for cyclic nucleotides. J Biol Chem *275*, 30069-30074.

Jedlitschky, G., Leier, I., Buchholz, U., Barnouin, K., Kurz, G., and Keppler, D. (1996). Transport of glutathione, glucuronate, and sulfate conjugates by the MRP gene-encoded conjugate export pump. Cancer Res *56*, 988-994.

Jonker, J. W., Merino, G., Musters, S., van Herwaarden, A. E., Bolscher, E., Wagenaar, E., Mesman, E., Dale, T. C., and Schinkel, A. H. (2005). The breast cancer resistance protein BCRP (ABCG2) concentrates drugs and carcinogenic xenotoxins into milk. Nat Med *11*, 127-129.

Kaminski, W. E., Orso, E., Diederich, W., Klucken, J., Drobnik, W., and Schmitz, G. (2000). Identification of a novel human sterol-sensitive ATP-binding cassette transporter (ABCA7). Biochem Biophys Res Commun *273*, 532-538.

Kao, H. H., Huang, J. D., and Chang, M. S. (2002). cDNA cloning and genomic organization of the murine MRP7, a new ATP-binding cassette transporter. Gene *286*, 299-306.

Kast, C., and Gros, P. (1997). Topology mapping of the amino-terminal half of multidrug resistance-associated protein by epitope insertion and immunofluorescence. J Biol Chem *272*, 26479-26487.

Kelly, A., Powis, S. H., Kerr, L. A., Mockridge, I., Elliott, T., Bastin, J., Uchanska-Ziegler, B., Ziegler, A., Trowsdale, J., and Townsend, A. (1992). Assembly and function of the two ABC transporter proteins encoded in the human major histocompatibility complex. Nature *355*, 641-644.

Kelsell, D. P., Norgett, E. E., Unsworth, H., Teh, M. T., Cullup, T., Mein, C. A., Dopping-Hepenstal, P. J., Dale, B. A., Tadini, G., Fleckman, P*., et al.* (2005). Mutations in ABCA12 underlie the severe congenital skin disease harlequin ichthyosis. Am J Hum Genet *76*, 794-803.

Keppler, D., Cui, Y., Konig, J., Leier, I., and Nies, A. (1999). Export pumps for anionic conjugates encoded by MRP genes. Adv Enzyme Regul *39*, 237-246.

Kerem, B., Rommens, J. M., Buchanan, J. A., Markiewicz, D., Cox, T. K., Chakravarti, A., Buchwald, M., and Tsui, L. C. (1989). Identification of the cystic fibrosis gene: genetic analysis. Science *245*, 1073-1080.

Kielar, D., Kaminski, W. E., Liebisch, G., Piehler, A., Wenzel, J. J., Mohle, C., Heimerl, S., Langmann, T., Friedrich, S. O., Bottcher, A*., et al.* (2003). Adenosine triphosphate binding cassette (ABC) transporters are expressed and regulated during terminal keratinocyte differentiation: a potential role for ABCA7 in epidermal lipid reorganization. J Invest Dermatol *121*, 465-474.

Kim, S. K., and Rulifson, E. J. (2004). Conserved mechanisms of glucose sensing and regulation by Drosophila corpora cardiaca cells. Nature *431*, 316-320.

Klein, I., Sarkadi, B., and Varadi, A. (1999). An inventory of the human ABC proteins. Biochim Biophys Acta *1461*, 237-262.

Kuwana, H., Shimizu-Nishikawa, K., Iwahana, H., and Yamamoto, D. (1996). Molecular cloning and characterization of the ABC transporter expressed in Trachea (ATET) gene from Drosophila melanogaster. Biochim Biophys Acta *1309*, 47-52.

Kyle-Cezar F, E.-L. J., dos Santos Goldenberg RC, Rumjanek VM. (2007). Expression of c-kit and Sca-1 and their relationship with multidrug resistance

protein 1 in mouse bone marrow mononuclear cells. Immunology *121*, 122-128.

Lamers, M. H., Perrakis, A., Enzlin, J. H., Winterwerp, H. H., de Wind, N., and Sixma, T. K. (2000). The crystal structure of DNA mismatch repair protein MutS binding to a G x T mismatch. Nature *407*, 711-717.

Lee, J. Y., and Parks, J. S. (2005). ATP-binding cassette transporter AI and its role in HDL formation. Curr Opin Lipidol *16*, 19-25.

Lee, K., Belinsky, M. G., Bell, D. W., Testa, J. R., and Kruh, G. D. (1998). Isolation of MOAT-B, a widely expressed multidrug resistance-associated protein/canalicular multispecific organic anion transporter-related transporter. Cancer Res *58*, 2741-2747.

Leggas, M., Adachi, M., Scheffer, G. L., Sun, D., Wielinga, P., Du, G., Mercer, K. E., Zhuang, Y., Panetta, J. C., Johnston, B*., et al.* (2004). Mrp4 confers resistance to topotecan and protects the brain from chemotherapy. Mol Cell Biol *24*, 7612-7621.

Leier, I., Jedlitschky, G., Buchholz, U., Center, M., Cole, S. P., Deeley, R. G., and Keppler, D. (1996). ATP-dependent glutathione disulphide transport mediated by the MRP gene-encoded conjugate export pump. Biochem J *314 (Pt 2)*, 433-437.

Leier, I., Jedlitschky, G., Buchholz, U., Cole, S. P., Deeley, R. G., and Keppler, D. (1994). The MRP gene encodes an ATP-dependent export pump for leukotriene C4 and structurally related conjugates. J Biol Chem *269*, 27807-27810.

Lespine, A., Dupuy, J., Orlowski, S., Nagy, T., Glavinas, H., Krajcsi, P., and Alvinerie, M. (2006). Interaction of ivermectin with multidrug resistance proteins (MRP1, 2 and 3). Chem Biol Interact *159*, 169-179.

Lewis, H. A., Zhao, X., Wang, C., Sauder, J. M., Rooney, I., Noland, B. W., Lorimer, D., Kearins, M. C., Conners, K., Condon, B.*, et al.* (2005). Impact of the deltaF508 mutation in first nucleotide-binding domain of human cystic fibrosis transmembrane conductance regulator on domain folding and structure. J Biol Chem *280*, 1346-1353.

Linsel-Nitschke, P., Jehle, A. W., Shan, J., Cao, G., Bacic, D., Lan, D., Wang, N., and Tall, A. R. (2005). Potential role of ABCA7 in cellular lipid efflux to apoA-I. J Lipid Res *46*, 86-92.

Locher, K. P., Lee, A. T., and Rees, D. C. (2002). The E. coli BtuCD structure: a framework for ABC transporter architecture and mechanism. Science *296*, 1091-1098.

Loe, D. W., Almquist, K. C., Cole, S. P., and Deeley, R. G. (1996). ATP-dependent 17 beta-estradiol 17-(beta-D-glucuronide) transport by multidrug resistance protein (MRP). Inhibition by cholestatic steroids. J Biol Chem *271*, 9683-9689.

Mackenzie, S. M., Brooker, M. R., Gill, T. R., Cox, G. B., Howells, A. J., and Ewart, G. D. (1999). Mutations in the white gene of Drosophila melanogaster affecting ABC transporters that determine eye colouration. Biochim Biophys Acta *1419*, 173-185.

Madon, J., Hagenbuch, B., Landmann, L., Meier, P. J., and Stieger, B. (2000). Transport function and hepatocellular localization of mrp6 in rat liver. Mol Pharmacol *57*, 634-641.

Merino, G., Alvarez, A. I., Pulido, M. M., Molina, A. J., Schinkel, A. H., and Prieto, J. G. (2006). Breast cancer resistance protein (BCRP/ABCG2) transports fluoroquinolone antibiotics and affects their oral availability, pharmacokinetics, and milk secretion. Drug Metab Dispos *34*, 690-695.

Mornon, J. P., Lehn, P., and Callebaut, I. (2008). Atomic model of human cystic fibrosis transmembrane conductance regulator: membrane-spanning domains and coupling interfaces. Cell Mol Life Sci *65*, 2594-2612.

Muller, M., Klein, I., Kopacsi, S., Remaley, A. T., Rajnavolgyi, E., Sarkadi, B., and Varadi, A. (2006). Co-expression of human ABCG5 and ABCG8 in insect cells generates an androstan stimulated membrane ATPase activity. FEBS Lett *580*, 6139-6144.

Myers, E. W., Sutton, G. G., Delcher, A. L., Dew, I. M., Fasulo, D. P., Flanigan, M. J., Kravitz, S. A., Mobarry, C. M., Reinert, K. H., Remington, K. A.*, et al.* (2000). A whole-genome assembly of Drosophila. Science *287*, 2196-2204.

Nagata, K., Yamamoto, A., Ban, N., Tanaka, A. R., Matsuo, M., Kioka, N., Inagaki, N., and Ueda, K. (2004). Human ABCA3, a product of a responsible gene for abca3 for fatal surfactant deficiency in newborns, exhibits unique ATP hydrolysis activity and generates intracellular multilamellar vesicles. Biochem Biophys Res Commun *324*, 262-268.

Nasonkin, I., Alikasifoglu, A., Ambrose, C., Cahill, P., Cheng, M., Sarniak, A., Egan, M., and Thomas, P. M. (1999). A novel sulfonylurea receptor family member expressed

in the embryonic Drosophila dorsal vessel and tracheal system. J Biol Chem *274*, 29420-29425.

Neldner, K. H. (1988). Pseudoxanthoma elasticum. Clin Dermatol *6*, 1-159.

Nichols, C. G. (2006). KATP channels as molecular sensors of cellular metabolism. Nature *440*, 470-476.

Nies, A. T., Cantz, T., Brom, M., Leier, I., and Keppler, D. (1998). Expression of the apical conjugate export pump, Mrp2, in the polarized hepatoma cell line, WIF-B. Hepatology *28*, 1332-1340.

Nies, A. T., and Keppler, D. (2007). The apical conjugate efflux pump ABCC2 (MRP2). Pflugers Arch *453*, 643-659.

Obmolova, G., Ban, C., Hsieh, P., and Yang, W. (2000). Crystal structures of mismatch repair protein MutS and its complex with a substrate DNA. Nature *407*, 703-710.

Ocorr, K., Perrin, L., Lim, H. Y., Qian, L., Wu, X., and Bodmer, R. (2007). Genetic control of heart function and aging in Drosophila. Trends Cardiovasc Med *17*, 177-182.

Olson, D. P., Scadden, D. T., D'Aquila, R. T., and De Pasquale, M. P. (2002). The protease inhibitor ritonavir inhibits the functional activity of the multidrug resistance related-protein 1 (MRP-1). Aids *16*, 1743-1747.

Ozvegy, C., Varadi, A., and Sarkadi, B. (2002). Characterization of drug transport, ATP hydrolysis, and nucleotide trapping by the human ABCG2 multidrug transporter. Modulation of substrate specificity by a point mutation. J Biol Chem *277*, 47980-47990.

Pinkett, H. W., Lee, A. T., Lum, P., Locher, K. P., and Rees, D. C. (2007). An inward-facing conformation of a putative metal-chelate-type ABC transporter. Science *315*, 373-377.

Pratt, S., Chen, V., Perry, W. I., 3rd, Starling, J. J., and Dantzig, A. H. (2006). Kinetic validation of the use of carboxydichlorofluorescein as a drug surrogate for MRP5-mediated transport. Eur J Pharm Sci *27*, 524-532.

Qian, Y. M., Song, W. C., Cui, H., Cole, S. P., and Deeley, R. G. (2001). Glutathione stimulates sulfated estrogen transport by multidrug resistance protein 1. J Biol Chem *276*, 6404-6411.

Reid, G., Wielinga, P., Zelcer, N., van der Heijden, I., Kuil, A., de Haas, M., Wijnholds, J., and Borst, P. (2003). The human multidrug resistance protein MRP4 functions as a prostaglandin efflux transporter and is inhibited by nonsteroidal antiinflammatory drugs. Proc Natl Acad Sci U S A *100*, 9244-9249.

Riordan, J. R., Rommens, J. M., Kerem, B., Alon, N., Rozmahel, R., Grzelczak, Z., Zielenski, J., Lok, S., Plavsic, N., Chou, J. L., and et al. (1989). Identification of the cystic fibrosis gene: cloning and characterization of complementary DNA. Science *245*, 1066-1073.

Robbiani, D. F., Finch, R. A., Jager, D., Muller, W. A., Sartorelli, A. C., and Randolph, G. J. (2000). The leukotriene C(4) transporter MRP1 regulates CCL19 (MIP-3beta, ELC)-dependent mobilization of dendritic cells to lymph nodes. Cell *103*, 757-768.

Rommens, J. M., Iannuzzi, M. C., Kerem, B., Drumm, M. L., Melmer, G., Dean, M., Rozmahel, R., Cole, J. L., Kennedy, D., Hidaka, N., and et al. (1989). Identification of the cystic fibrosis gene: chromosome walking and jumping. Science *245*, 1059-1065.

Roth, C. W., Holm, I., Graille, M., Dehoux, P., Rzhetsky, A., Wincker, P., Weissenbach, J., and Brey, P. T. (2003). Identification of the Anopheles gambiae ATP-binding cassette transporter superfamily genes. Mol Cells *15*, 150-158.

Sager, G. (2004). Cyclic GMP transporters. Neurochem Int *45*, 865-873.

Sarkadi, B., Homolya, L., Szakacs, G., and Varadi, A. (2006). Human multidrug resistance ABCB and ABCG transporters: participation in a chemoimmunity defense system. Physiol Rev *86*, 1179-1236.

Sarkadi, B., Price, E. M., Boucher, R. C., Germann, U. A., and Scarborough, G. A. (1992). Expression of the human multidrug resistance cDNA in insect cells generates a high activity drug-stimulated membrane ATPase. J Biol Chem *267*, 4854-4858.

Sauna, Z. E., and Ambudkar, S. V. (2000). Evidence for a requirement for ATP hydrolysis at two distinct steps during a single turnover of the catalytic cycle of human P-glycoprotein. Proc Natl Acad Sci U S A *97*, 2515-2520.

Sauna, Z. E., Nandigama, K., and Ambudkar, S. V. (2006). Exploiting reaction intermediates of the ATPase reaction to elucidate the mechanism of transport by P-glycoprotein (ABCB1). J Biol Chem *281*, 26501-26511.

Schinkel, A. H., and Jonker, J. W. (2003). Mammalian drug efflux transporters of the ATP binding cassette (ABC) family: an overview. Adv Drug Deliv Rev *55*, 3-29.

Schrodt, S., Koch, J., and Tampe, R. (2006). Membrane topology of the transporter associated with antigen processing (TAP1) within an assembled functional peptide-loading complex. J Biol Chem *281*, 6455-6462.

Shabbir, A., DiStasio, S., Zhao, J., Cardozo, C. P., Wolff, M. S., and Caplan, A. J. (2005). Differential effects of the organochlorine pesticide DDT and its metabolite p,p'-DDE on p-glycoprotein activity and expression. Toxicol Appl Pharmacol *203*, 91-98.

Shirihai, O. S., Gregory, T., Yu, C., Orkin, S. H., and Weiss, M. J. (2000). ABC-me: a novel mitochondrial transporter induced by GATA-1 during erythroid differentiation. Embo J *19*, 2492-2502.

Shyng, S., and Nichols, C. G. (1997). Octameric stoichiometry of the KATP channel complex. J Gen Physiol *110*, 655-664.

Smeets, P. H., van Aubel, R. A., Wouterse, A. C., van den Heuvel, J. J., and Russel, F. G. (2004). Contribution of multidrug resistance protein 2 (MRP2/ABCC2) to the renal excretion of p-aminohippurate (PAH) and identification of MRP4 (ABCC4) as a novel PAH transporter. J Am Soc Nephrol *15*, 2828-2835.

Smital, T., Sauerborn, R., Pivcevic, B., Krca, S., and Kurelec, B. (2000). Interspecies differences in P-glycoprotein mediated activity of multixenobiotic resistance mechanism in several marine and freshwater invertebrates. Comp Biochem Physiol C Toxicol Pharmacol *126*, 175-186.

Smith, A. J., Timmermans-Hereijgers, J. L., Roelofsen, B., Wirtz, K. W., van Blitterswijk, W. J., Smit, J. J., Schinkel, A. H., and Borst, P. (1994). The human MDR3 P-glycoprotein promotes translocation of phosphatidylcholine through the plasma membrane of fibroblasts from transgenic mice. FEBS Lett *354*, 263-266.

Smith, P. C., Karpowich, N., Millen, L., Moody, J. E., Rosen, J., Thomas, P. J., and Hunt, J. F. (2002). ATP binding to the motor domain from an ABC transporter drives formation of a nucleotide sandwich dimer. Mol Cell *10*, 139-149.

Sreeramulu, K., Liu, R., and Sharom, F. J. (2007). Interaction of insecticides with mammalian P-glycoprotein and their effect on its transport function. Biochim Biophys Acta *1768*, 1750-1757.

Strautnieks, S. S., Bull, L. N., Knisely, A. S., Kocoshis, S. A., Dahl, N., Arnell, H., Sokal, E., Dahan, K., Childs, S., Ling, V.*, et al.* (1998). A gene encoding a liver-specific ABC transporter is mutated in progressive familial intrahepatic cholestasis. Nat Genet *20*, 233-238.

Szabo, K., Welker, E., Bakos, Muller, M., Roninson, I., Varadi, A., and Sarkadi, B. (1998). Drug-stimulated nucleotide trapping in the human multidrug transporter MDR1. Cooperation of the nucleotide binding domains. J Biol Chem *273*, 10132-10138.

Szakacs, G., Ozvegy, C., Bakos, E., Sarkadi, B., and Varadi, A. (2001). Role of glycine-534 and glycine-1179 of human multidrug resistance protein (MDR1) in drug-mediated control of ATP hydrolysis. Biochem J *356*, 71-75.

Szakacs, G., Varadi, A., Ozvegy-Laczka, C., and Sarkadi, B. (2008). The role of ABC transporters in drug absorption, distribution, metabolism, excretion and toxicity (ADME-Tox). Drug Discov Today *13*, 379-393.

Tapadia, M. G., and Lakhotia, S. C. (2005). Expression of mdr49 and mdr65 multidrug resistance genes in larval tissues of Drosophila melanogaster under normal and stress conditions. Cell Stress Chaperones *10*, 7-11.

Tarnay, J. N., Szeri, F., Ilias, A., Annilo, T., Sung, C., Le Saux, O., Varadi, A., Dean, M., Boyd, C. D., and Robinow, S. (2004). The dMRP/CG6214 gene of Drosophila is evolutionarily and functionally related to the human multidrug resistance-associated protein family. Insect Mol Biol *13*, 539-548.

Tearle, R. G., Belote, J. M., McKeown, M., Baker, B. S., and Howells, A. J. (1989). Cloning and characterization of the scarlet gene of Drosophila melanogaster. Genetics *122*, 595-606.

Trauner, M., Arrese, M., Soroka, C. J., Ananthanarayanan, M., Koeppel, T. A., Schlosser, S. F., Suchy, F. J., Keppler, D., and Boyer, J. L. (1997). The rat canalicular conjugate export pump (Mrp2) is down-regulated in intrahepatic and obstructive cholestasis. Gastroenterology *113*, 255-264.

Tribull, T. E., Bruner, R. H., and Bain, L. J. (2003). The multidrug resistance-associated protein 1 transports methoxychlor and protects the seminiferous epithelium from injury. Toxicol Lett *142*, 61-70.

Tsuchida, M., Emi, Y., Kida, Y., and Sakaguchi, M. (2008). Human ABC transporter isoform B6 (ABCB6) localizes primarily in the Golgi apparatus. Biochem Biophys Res Commun *369*, 369-375.

Tusnady, G. E., Bakos, E., Varadi, A., and Sarkadi, B. (1997). Membrane topology distinguishes a subfamily of the ATP-binding cassette (ABC) transporters. FEBS Lett *402*, 1-3.

Tusnady, G. E., and Simon, I. (1998). Principles governing amino acid composition of integral membrane proteins: application to topology prediction. J Mol Biol *283*, 489-506.

Uitto, J., Pulkkinen, L., and Ringpfeil, F. (2001). Molecular genetics of pseudoxanthoma elasticum: a metabolic disorder at the environment-genome interface? Trends Mol Med *7*, 13-17.

Urbatsch, I. L., Sankaran, B., Weber, J., and Senior, A. E. (1995). P-glycoprotein is stably inhibited by vanadate-induced trapping of nucleotide at a single catalytic site. J Biol Chem *270*, 19383-19390.

van Aubel, R. A., Smeets, P. H., Peters, J. G., Bindels, R. J., and Russel, F. G. (2002). The MRP4/ABCC4 gene encodes a novel apical organic anion transporter in human kidney proximal tubules: putative efflux pump for urinary cAMP and cGMP. J Am Soc Nephrol *13*, 595-603.

van de Wetering, K., Zelcer, N., Kuil, A., Feddema, W., Hillebrand, M., Vlaming, M. L., Schinkel, A. H., Beijnen, J. H., and Borst, P. (2007). Multidrug resistance proteins 2 and 3 provide alternative routes for hepatic excretion of morphine-glucuronides. Mol Pharmacol *72*, 387-394.

Van Eck, M., Pennings, M., Hoekstra, M., Out, R., and Van Berkel, T. J. (2005). Scavenger receptor BI and ATP-binding cassette transporter A1 in reverse cholesterol transport and atherosclerosis. Curr Opin Lipidol *16*, 307-315.

Walker, J. E., Saraste, M., Runswick, M. J., and Gay, N. J. (1982). Distantly related sequences in the alpha- and beta-subunits of ATP synthase, myosin, kinases and other ATP-requiring enzymes and a common nucleotide binding fold. Embo J *1*, 945-951.

Wijnholds, J., Evers, R., van Leusden, M. R., Mol, C. A., Zaman, G. J., Mayer, U., Beijnen, J. H., van der Valk, M., Krimpenfort, P., and Borst, P. (1997). Increased sensitivity to anticancer drugs and decreased inflammatory response in mice lacking the multidrug resistance-associated protein. Nat Med *3*, 1275-1279.

Wijnholds, J., Mol, C. A., van Deemter, L., de Haas, M., Scheffer, G. L., Baas, F., Beijnen, J. H., Scheper, R. J., Hatse, S., De Clercq, E.*, et al.* (2000). Multidrug-resistance protein 5 is a multispecific organic anion transporter able to transport nucleotide analogs. Proc Natl Acad Sci U S A *97*, 7476-7481.

Wolters, J. C., Abele, R., and Tampe, R. (2005). Selective and ATP-dependent translocation of peptides by the homodimeric ATP binding cassette transporter TAP-like (ABCB9). J Biol Chem *280*, 23631-23636.

Wu, C. T., Budding, M., Griffin, M. S., and Croop, J. M. (1991). Isolation and characterization of Drosophila multidrug resistance gene homologs. Mol Cell Biol *11*, 3940-3948.

Xie, L. H., John, S. A., Ribalet, B., and Weiss, J. N. (2007). Activation of inwardly rectifying potassium (Kir) channels by phosphatidylinosital-4,5-bisphosphate (PIP2): interaction with other regulatory ligands. Prog Biophys Mol Biol *94*, 320-335.

Zelcer, N., Saeki, T., Reid, G., Beijnen, J. H., and Borst, P. (2001). Characterization of drug transport by the human multidrug resistance protein 3 (ABCC3). J Biol Chem *276*, 46400-46407.

Zeng, H., Liu, G., Rea, P. A., and Kruh, G. D. (2000). Transport of amphipathic anions by human multidrug resistance protein 3. Cancer Res *60*, 4779-4784.

Zhou, S., Morris, J. J., Barnes, Y., Lan, L., Schuetz, J. D., and Sorrentino, B. P. (2002). Bcrp1 gene expression is required for normal numbers of side population stem cells in mice, and confers relative protection to mitoxantrone in hematopoietic cells in vivo. Proc Natl Acad Sci U S A *99*, 12339-12344.

Zolnerciks, J. K., Wooding, C., and Linton, K. J. (2007). Evidence for a Sav1866-like architecture for the human multidrug transporter P-glycoprotein. Faseb J *21*, 3937-3948.

11. Bibliography of the candidate's publications

Publications related to dissertation:

1. Tarnay J.N, **Szeri F,** Iliás A, Annilo T, Sung T.C, Le Saux O, Váradi A, Dean M, Boyd C.D, Robinow S. (2004) The *dMRP/CG6214* gene of *Drosophila* is evolutionarily and functionally related to the human multidrug resistance-associated protein family. *Insect Mol. Biol.* **13**(5):539-548
2. **Szeri F,** Iliás A, Pomozi V, Robinow S, Bakos É, Váradi A. (2009) The high turnover Drosophila multidrug resistance-associated protein shares the biochemical features of its human orthologues *Biochimica et Biophysica Acta-Biomembranes,* **1788:** 402-409

Publications not related to dissertation:

1. Klein I, Ésik O, Homolya V, **Szeri F**, Váradi A. (2001) Molecular genetic diagnostic program of multiple endocrine neoplasia type 2A and familial medullary thyroid carcinoma syndromes in Hungary. *J Endocrinol.*, **170**: 661-666
2. Bodó A, Bakos É, **Szeri F,** Váradi A, Sarkadi B. (2003) The role of multidrug transporters in drug availability, metabolism and toxicity. *Toxicol Lett.,* **140**:133-143.
3. Bodó A, Bakos É, **Szeri F,** Váradi A, Sarkadi B. (2003) Differential modulation of the human liver conjugate transporters MRP2 and MRP3 by bile acids and organic anions. *J Biol Chem,* **278**:23529-37.

12. Acknowledgements

First of all, I am deeply indebted to my tutors, András Váradi and Balázs Sarkadi, who, being remarkable scientists and outstanding personalities at the same time, kindly provided me with a critical and supportive scientific background.

I am grateful to Károly Liliom for many valuable discussions and his help in statistical analysis, interpretation of the thermodynamic experiments, and HPLC experiments not documented here. His critical reading of my manuscript is greatly appreciated.

I feel grateful to Attila Iliás for introducing me to the basic laboratory protocols, computer programs, and for his help in the expression of DMRP. His reliable and supportive attitude will never be forgotten.

I am grateful to Éva Bakos, my first tutor being a graduent student, to further keep an eye on my work, providing me with her valuable advices.

I feel grateful to Gergely Szakács for his devotion to all scientific questions. His critical reading of my manuscript is highly appreciated.

I thank László Homolya for his help in confocal experiments, Viola Pomozi for making me familiar with FACS measurements and Zalán Szabó for the thorough reading of my manuscript. The professional assistance of Györgyi Demeter, and Judit Kis is greatly acknowledged.

I feel grateful to the whole Váradi and Sarkadi groups for providing intimate and motivating scientific atmosphere in the laboratory.

Last but not least I am deeply indebted to my parents for providing persistent background support for me, and my little daughter for adding her special spice of personality to my life.